



**Escola Tècnica Superior d'Enginyeria
de Telecomunicació de Barcelona**

UNIVERSITAT POLITÈCNICA DE CATALUNYA

PROJECTE FI DE CARRERA

NEW METHODS FOR MEASURING AND MONITORING CHROMATIC DISPERSION IN OPTICAL COMMUNICATION SYSTEMS

Autor: Cristhian A. Obando Velazco

Directora: María C. Santos Blanco

Data: 15 de Febrer de 2010

Table of contents

1. INTRODUCTION	6
1.1. Objectives.....	6
1.2. Project Organization	8
2. BASIC CONCEPTS.....	9
2.1 Dispersion Theory	9
2.1.1 Intermodal dispersion	9
2.1.2 Chromatic Dispersion	9
2.2 RF tone-based chromatic dispersion measurement techniques	12
2.2.1 Mach-Zehnder Modulator	12
2.2.1.1 Configurations.....	13
2.2.1.2 Transfer Function	14
2.2.2 Mach-Zehnder (push pull) + DUT + Detector Mathematical Analysis without considering amplitude distortions	16
2.2.3 Mach-Zehnder (asymmetric) + DUT + Detector Mathematical Analysis without considering amplitude distortions.....	17
2.2.4 Mach-Zehnder (push pull) + DUT + Detector Mathematical Analysis considering amplitude distortions	18
2.2.5 Mach-Zehnder (asymmetric) + DUT + Detector Mathematical Analysis considering amplitude distortions	19
2.2.6 Modulation Phase Shift Method (MPSM).....	21
2.2.7 Peucheret`s Method.....	23
2.3 Dispersion Compensating Elements	24
2.3. 1 Dispersion Compensating Fiber.....	24
2.3.2 Chirped Fiber Bragg Grating.....	25
2.4 VPI Simulation Tool.....	26
2.4.1 Signal Representation	26
2.4.3 Restrictions on Global Parameters	27
2.4.4 Module Parameters.....	27
2.4.5 Sweep Configuration	28
2.4.6 Simulation example.....	28
3. ASYMMETRIC-MODULATION BIAS CONTROLLED METHOD (ABCM)	33
3.1 Description and Mathematical Analysis	33

3.2 VPI simulations	35
3.2.1 Analysis of the dispersion inserted by the DUT.....	36
3.2.2.1 RF Frequency Sweep.....	42
3.2.2.2 RF Amplitude sweep.....	44
3.2.2.3 Nominal Dispersion Sweep	46
3.3 Experiments.....	48
3.3.1 Laboratory Equipment.....	48
3.3.1.1 Optical and Electrical Sources	48
3.3.1.1.1 Laser New Focus 6427.....	48
3.3.1.1.2 Programmable DC Source PROMAX FA-851	49
3.3.1.2 Optical devices	50
3.3.1.2.1 Modulator FUJITSU FTM7921ER/052 H74M-5208-062	50
3.3.1.2.2 Polarization Controller.....	51
3.3.1.3 Passive Devices	52
3.3.1.3.1 Bias-tee.....	52
3.3.1.3.2 Optical detector Agère.....	52
3.3.1.4 Devices under test (DUTs).....	53
3.3.1.4.1 Fiber Brag Grating PIRELLI CDC-04074	53
3.3.1.4.2 Chromatic Dispersion Compensating Fiber	54
3.3.1.5 Measurement Devices	55
3.3.1.5.1 Network Analyzer HP 8753D	55
3.3.1.5.2 Optical Multimeter HP 8153A	57
3.3.2 Experimental Transfer Function	58
3.3.2.1 Setup	58
3.3.2.2 Transfer Function for FUJITSU Modulator.....	59
3.3.3 ABCM Experiment	60
3.3.3.1 General description	60
3.3.3.2 Setup characterization.....	62
3.3.3.3 Results	65
3.3.3.3.1 Results obtained with the FBG	65
3.3.3.3.2 Results obtained with the DCF	66
4. ASYMMETRIC MODULATION BIAS-CONTROLLED METHOD - SUPPRESSED CARRIER (PROOF OF CONCEPT).....	67
4.1 Description and Mathematical Analysis	67

4.2 VPI simulations	71
4.2.1 Analysis of the dispersion inserted by the DUT.....	75
4.2.2 Analysis of the effect caused by the setup's parameters.....	77
4.2.2.1 RF Frequency Sweep.....	78
4.2.2.2 RF Amplitude Sweep	80
4.2.2.3 Nominal Dispersion Sweep	84
4.2.2.4 Coupling factor Sweep.....	86
4.3 Experiments.....	87
4.3.1 Laboratory Equipment.....	87
4.3.1.1 Optical Coupler	87
4.3.1.2 Laser HP 83424A.....	88
4.3.1.3 Agilent Spectrum Analyzer.....	89
4.3.2 General description of the experiment.....	90
4.3.3 Setup characterization.....	90
4.3.4 Carrier Suppression Experiment.....	91
4.3.5 Dispersion Measurement Experiment	93
5. CONCLUSIONS AND FUTURE LINES	97
6. ANNEX.....	100
7. INDEX OF TABLES	121
8. INDEX OF FIGURES	122
9. BIBLIOGRAPHIC REFERENCES.....	125

1. INTRODUCTION

With the progressive increase of data flow to travel through communication networks all around the world, high-capacity low-loss physical media are an urgent and important need. In this purpose, optical fiber appears as an outstanding choice due to its large bandwidth and low attenuation features.

In the path towards next-generation optical networks with increased bit rates and complexity, compensation of fiber optic transmission impairments turns into a critical issue. Small variations due to temperature, stress, aging or dynamic path reconfiguration, may have a tremendous impact in performance and therefore adaptive compensation based on high-precision real-time on-line monitoring is essential [1].

Chromatic dispersion (CD) stands out as one of the most limiting impairments. Great research efforts have been devoted to find cost-effective and accurate techniques for its real-time on-line monitoring. In this regard, the use of radiofrequency (RF) pilot tones added at the emitter is advantageous because it offers good sensitivity, high dynamic range and reconfigurability, it also simplifies the receiver and allows monitoring at any given point in the network without the need to recover the data, and finally because the tones are useful for other network management issues such as channel identification. [1].

1.1. Objectives

This PFC main goal is to introduce new approaches on the chromatic dispersion measurement field, based on the big range of possibilities the setup of a general standard RF-tone modulation chromatic modulation method provides, and to show its good performance pointing towards a real-time on-line monitoring system for optical communication networks. The project's objectives are defined considering two well-delimited stages.

First, we will study some standard RF-tone-addition techniques for measuring chromatic dispersion, specifically the Modulation Phase Shift Method (MPSM) [2] and the Peucheret's Method [3]. We will analyze their operating principles, recognize all the variables involved in their basic configurations and evaluate their performances under different measurement conditions.

We will also study the implications of real-time on-line monitoring of chromatic dispersion in optical networks. We have to consider that the test signal has to travel together with the data; therefore, it is a priority to keep the optical carrier unaltered in the transmission and reception procedures.

This background will help us to identify the main drawbacks of both methods which motivate the proposal of a new improved technique based on a similar mathematical basis but with better performance in terms of accuracy and cost trade-off.

The general features of this new approach will be exposed on a basic setup designed for a laboratory environment, so that we can contrast it with the conventional techniques. This method dubbed Asymmetric Modulation Bias-Controlled Method (ABCM) will focus on RF

modulated signal amplitude and will take advantage of its direct relation with chromatic dispersion.

One of the basic building blocks of these standard methods is the device that imposes the RF pure-tone modulation to the optical signal, namely the Mach-Zehnder interferometric modulator usually in the conventional push-pull configuration and biased at the quadrature point. In the context of the new improved CD measurement methods, we will observe how the Mach-Zehnder modulator Bias Voltage concept gains relevance; becoming the main variable to be handled by the use of a dual drive Mach-Zehnder modulator in asymmetric configuration.

Finally, we will analyze this ABCM method performance while some fixed parameters (RF Frequency, Nominal Dispersion, V_b resolution) take different values in order to find out the optimum operating conditions.

The problem when trying to apply the ABCM to the real-time on-line monitoring of optical networks is that it relies in the eventual cancellation of the optical carrier which in a network monitoring application is shared with the data and it is essential for a proper data recovery. We must find an alternative where this optical carrier cancellation is not essential for the monitoring function and that would be the ABCM-SC (SC for suppressed carrier)

Therefore, on a second stage, we will focus on giving this new perspective about dispersion measurement a direct application in optical communications field. We will restructure the ABCM into a practical dispersion monitoring system for optical communication networks. This improved monitoring technique will be based on a proof-of-concept study (no real data transmission considered) to evaluate the method's performance in terms of accuracy, robustness and adaptability, building the basis for data transmission experiments in future projects.

An important aspect to take into account will be the way we carry out the RF tone addition procedure without altering the optical carrier (transmitted data). To accomplish this requirement we will use a Bessel function analysis to achieve a carrier-suppressed modulation of the RF tone, which introduces another important handling parameter: the RF Tone Amplitude.

We will also be concerned about isolating the emitter part (where data is transmitted) from the monitoring point (where dispersion is measured), but at the same time complementing each other to operate in a real-time situation.

Finally, we will study the requirement of including the second RF harmonic detection together with the first harmonic as it adjusts better to a real-time monitoring system and increases the accuracy level in chromatic dispersion measurement.

1.2. Project Organization

This PFC is divided in five chapters which follow a general-to-particular subject matter where each chapter makes reference to the previous one.

Chapter 2 Basic Concepts: provides a complete explanation of the theoretical knowledge that supports this PFC's proposals and makes a general description of the main devices and tools used.

Chapter 3 ABC Technique: presents the structured study of this new method for measuring chromatic dispersion including mathematical analysis, VPI simulations, and experimental verification; and it also proposes different operating situations.

Chapter 4 ABC – SC Technique: aims at redefine the technique exposed in the previous chapter to develop a new system capable to satisfy real –time dispersion monitoring requirements. It follows the same method of study used in the previous chapter.

Chapter 5 Conclusions: evaluates the performance of the two techniques proposed in this PFC by making use of the results obtained in charts and graphics, and verifies the achievement of the objectives.

2. BASIC CONCEPTS

2.1 Dispersion Theory

Dispersion is a typical phenomenon in optical media which yields the time spread of a transmitted pulse. It is caused by the different delays suffered by each of the optical signal's components, so that at the detector, these components are recovered at different arrival times, generating a distorted signal with respect to the transmitted one.

There are two well-defined types of dispersion:

2.1.1 Intermodal dispersion

Intermodal dispersion is characteristic of multimode fibers where the optical signal propagates in many "modes", each one following a different trajectory inside the fiber's core in the rays theory analogy. Therefore, all the modes from a determined pulse experience different delays, generating the pulse spread explained above.

2.1.2 Chromatic Dispersion

Chromatic dispersion is present in all types of fibers but in the multimode fiber the more relevant effect comes from intermodal dispersion. In this work, we will be mainly concerned with single-mode fiber where no intermodal dispersion occurs, and therefore we will only study chromatic dispersion. The physical phenomenon behind chromatic dispersion is explained below:

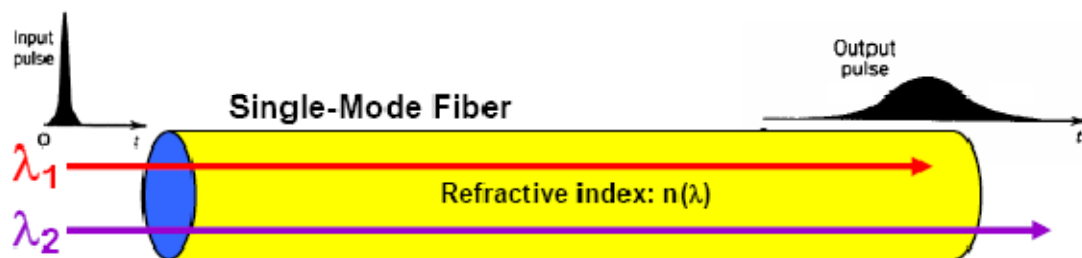


Figure 2.1 Chromatic dispersion basic schema

A generic optical pulse with carrier frequency ω_0 transmitted through a single-mode fiber under ideal conditions (non-lossy transmission line with no deformation of the fundamental mode), can be represented like this:

$$E_{(r,t)} = A(t)e^{j\omega_0 t}e^{-j\beta(\omega)z} \quad (1)$$

where the $A(t)$ is a slowly varying function of time as compared to the second term $e^{j\omega_0 t}$, and the last term $e^{-j\beta(\omega)z}$ reflects phase constant dependence with frequency (minus sign indicates the signal propagates on the 'z' axis positive direction).

Expression (1) illustrates very well the dispersion effect as a relation between β and ω . If this relation is linear, such as on an ideal transmission line: $\beta(\omega) = \frac{\omega}{V_{prop}}$, where V_{prop} is the wave propagation velocity, the resulting wave form will not change but it will suffer an overall time delay proportional to z distance. Thus, at the detector we will have:

$$E_{(r,t)} = A \left(t - \frac{z}{V_{prop}} \right) e^{j\omega_0 \left(t - \frac{z}{V_{prop}} \right)} \quad (2)$$

In a real case, where the dispersion relation is not linear an exact solution for the detected signal could be difficult to treat analytically. Nevertheless, if we consider that the phase constant changes slowly while the operating frequency gets further from ω_0 , we can use a Taylor Polynomial to express $\beta(\omega)$ in a valid way, as follows:

$$\begin{aligned} \beta(\omega) &= \beta(\omega_0) + (\omega - \omega_0) \left. \frac{\partial \beta}{\partial \omega} \right|_{\omega_0} + \frac{1}{2} (\omega - \omega_0)^2 \left. \frac{\partial^2 \beta}{\partial \omega^2} \right|_{\omega_0} + \dots = \\ \beta(\omega) &= \beta_0 + (\omega - \omega_0) \beta_1 + \frac{1}{2} (\omega - \omega_0)^2 \beta_2 \end{aligned} \quad (3)$$

Now, we will explain the relations between the three β parameters defined above: β_0 , β_1 and β_2 , and the physical concepts they refer to.

The first term, β_0 , causes no effect over the envelope; however, it yields a certain phase shift on the optical carrier. It can be stated that the carrier travels with a determined velocity established by β_0 called “*phase velocity*”, while the envelope does not move.

β_0 is formally expressed as:

$$\begin{aligned} \beta_0(\omega) &= \left. \frac{2\pi}{\lambda} \right|_{\omega_0} = \left. \frac{2\pi f}{v_f} \right|_{\omega_0} = \left. \frac{\omega}{v_f} \right|_{\omega_0} = \frac{\omega_0}{v_f} \\ v_f &= \frac{n}{n(\omega)} = \frac{\omega_0}{\beta_0} \end{aligned} \quad (4)$$

where the phase velocity v_f represents the propagation velocity of the optical carrier at frequency ω_0 , in other words, it is the velocity needed for an external agent to see the wave’s phase as a constant.

β_1 term generates a time delay on the envelope but without modifying the wave form, so that the information transmitted will be kept unaltered.

In this case, there is not a unique phase velocity for all spectral components; each component along the optical signal spectral width has a different phase velocity. Thus, while the optical carrier propagates with a velocity established by β_0 , the envelope propagates with the resulting velocity of all spectral components, which is called “*group velocity*” v_g and depends on β_1 .

In the same way, there is a time delay suffered by the transmitted signal, called group delay τ_g , which can be defined as the time spent by the signal’s envelope to cover a ‘ z distance’ over a single mode fiber. It is related to β_1 by $\tau_g = \beta_1 z$.

$$\beta_1 = \left. \frac{\partial \beta(\omega)}{\partial \omega} \right|_{\omega_0} = \left. \frac{\partial \left(\frac{\omega}{v_f} \right)}{\partial \omega} \right|_{\omega_0}$$

Replacing equation (4):

$$\begin{aligned} &= \left. \frac{\partial \left(\frac{\omega n(\omega)}{c} \right)}{\partial \omega} \right|_{\omega_0} = \left. \frac{n(\omega) + \omega \frac{\partial n(\omega)}{\partial \omega}}{c} \right|_{\omega_0} \\ &= \frac{1}{c} \left(n(\omega_0) + \omega_0 \left. \frac{\partial n(\omega)}{\partial \omega} \right|_{\omega_0} \right) = \frac{\tau_g}{z} = \frac{1}{v_g} \end{aligned} \quad (5)$$

$$v_g = \frac{c}{n(\omega_0) + \omega_0 \left. \frac{\partial n(\omega)}{\partial \omega} \right|_{\omega_0}} = \frac{c}{N(\omega_0)} \quad (6)$$

The group velocity v_g concept only makes sense when the referred optical signals present different frequencies and phases in a dispersive transmission channel. In any other case, the group velocity will be equal to the phase velocity, as it happens in the vacuum.

In expression (6), we define N as the group refraction index of the channel, in direct analogy with phase velocity.

The last parameter, β_2 , causes both amplitude reduction and spread of the envelope, unlike previous parameters which do not modify the pulse form; however, the signal's energy is kept constant.

β_2 is also responsible for altering the carrier's phase shift causing a chirp effect on it, that is, a kind of acceleration and deceleration in frequency.

The most common parameter to characterize the chromatic dispersion is the chromatic dispersion coefficient D , defined as β_1 variation with respect to the wave length, as it is shown below:

$$\beta_2 = \frac{\partial^2 \beta_0}{\partial \omega^2} = \frac{\partial \beta_1}{\partial \omega} = \frac{\partial \lambda}{\partial \omega} \left(\frac{\partial \beta_1}{\partial \lambda} \right) = \frac{\partial \lambda}{\partial \omega} D = -\frac{2\pi c}{\omega^2} D \quad (7)$$

The dispersion coefficient can also be defined starting from the relation between the spreading suffered by the transmitted pulse $\Delta\tau_g$, and the spectral width $\Delta\omega$:

$$\Delta\tau_g = \frac{\partial \tau_g}{\partial \omega} \Delta\omega$$

Replacing expression (5) we have:

$$\begin{aligned} \frac{\partial}{\partial \omega} \left(\frac{z}{v_g} \right) \Delta\omega &= z \frac{\partial \omega}{\partial \lambda} \frac{\partial \beta_1}{\partial \omega} \frac{\partial \lambda}{\partial \omega} \Delta\omega = z D \Delta\lambda \\ \Rightarrow D &= \frac{\Delta\tau_g}{z \Delta\lambda} \end{aligned} \quad (8)$$

This final expression for the chromatic dispersion coefficient (8) clarifies the relation between pulse spreading and the fiber's dispersion. In addition, it helps us to define the typical units to express the chromatic dispersion: $ps/nm \cdot Km$ (pulse delay in picoseconds, wave length spectral width in nanometers and fiber's length in kilometers).

2.2 RF tone-based chromatic dispersion measurement techniques

This PFC focuses on chromatic dispersion measurement methods which use as a test signal to inject on the DUT a pure RF tone modulated signal. A generic setup is sketched on Figure 2.2.

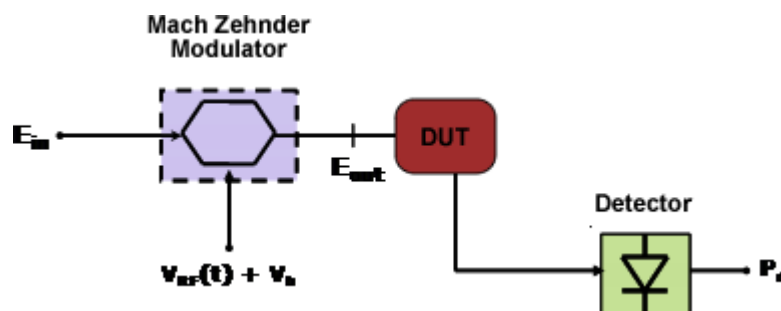


Figure 2.2 Block composed by MZM, DUT and Detector

In Figure 2.2 there is first an optical source, usually a laser which could be tunable. After that, we find an external modulator that modulates the carrier with the RF pure tone modulation. This test signal is input to the DUT and it is recovered at its output by an optical detector that follows a square law characteristic.

We will now review the models and parameters used to describe each of the elements on the basic setup.

2.2.1 Mach-Zehnder Modulator

The Mach-Zehnder Modulator is an interferometric modulator which plays a fundamental role in the setups of most techniques referred above. It provides a large range of potential handling variables and configurations.

Its operation principle is based on the linear electro-optical effect (Pockels effect) where the media's optical refraction index is modified according to the applied electrical field, resulting in a phase modulation of the optical signal. Therefore, at both Mach-Zehnder's branches, the propagated light gets phase-modulated by the electric field applied on the electrodes. By combining again these two signals, we obtain an amplitude modulation at the output.

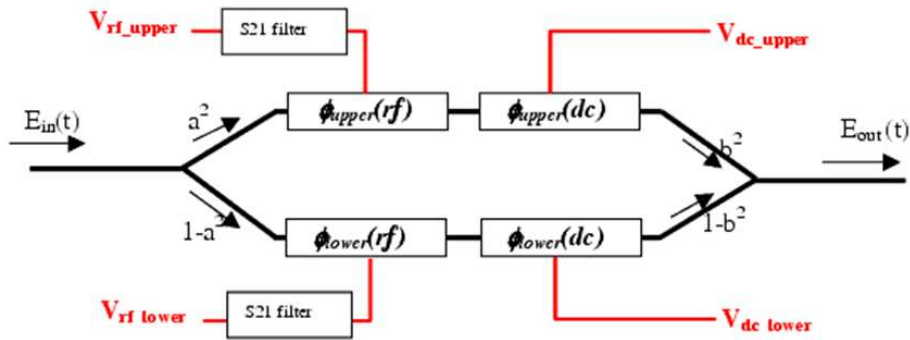


Figure 2.3 Schematic of Mach-Zehnder Modulator

The signals featured in Figure 2.3 are defined by the following expressions:

$$\left. \begin{aligned}
 & \dots \\
 & \dots \\
 & \dots
 \end{aligned} \right\} (9)$$

is the electric field of the coherent light beam emitted by the laser at frequency. is the result of combining both branches' optical signals. and are the phase shifts generated at each Mach-Zehnder's branch through the electro-optic effect. is the bias voltage, i.e. a continuous voltage required to set the modulator at any of its possible operating points. is a reference voltage related to the electrodes' sensitivity. is the modulation index which relates the phase shift with the voltage applied on each branch.

Another important parameter for a MZM is the Extinction Ratio (ER) defined as the relation between the maximum and minimum power levels according to the device's transfer function. It is used to express the efficiency with which the transmitted optical power is modulated over the optical fiber transport. According to this definition, if we have a minimum power equal to "0", represents that we have an infinite extinction ratio, which is impossible to achieve in real devices.

2.2.1.1 Configurations

We will consider here two basic configurations for the Mach-Zehnder Modulator: push pull and asymmetric.

- Push-Pull:

This configuration lets us achieve an amplitude modulation with no chirp effect, because the phase shifts into each of the interferometric have exactly the same magnitude.

$$E_{out} = \frac{A_0}{2} [\cos(\omega_0 + \theta_0 + \theta(t)) + \cos(\omega_0 + \theta_0 - \theta(t))] = A_0 [\cos(\omega_0 + \theta_0) \cos(\theta(t))] \quad (10)$$

- Asymmetric: $\theta_1(t) \neq \theta_2(t)$

Here we have no restriction on choosing each branch's parameters, it just depends on what we want to obtain. It is also possible to use one branch or the other separately.

This PFC's proposal requires the bias voltage to become the fundamental handling parameter within the RF tone based dispersion monitoring technique and this condition is only accomplished by using a single – branch configuration in the setup (this property will be deeply explained in section 2.2.3). By single-branch configuration it is meant that both the RF signal and the polarization bias are applied to only one of the interferometric branches, either the same or to each one of the branches.

Thus, the output expression would be:

$$E_{out} = \frac{A_0}{2} [\cos(\omega_0 + \theta_0 + \theta(t)) + \cos(\omega_0 + \theta_0)]$$

$$= \frac{A_0}{2} [\cos(\omega_0 + \theta_0) + \cos(\omega_0 + \theta_0) \cos(\theta(t)) - \sin(\omega_0 + \theta_0) \sin(\theta(t))] \quad (11)$$

2.2.1.2 Transfer Function

To recover the RF modulating signal after applying an amplitude or phase modulation we use the principle of square law detection, which states that the electrical power at the detector's output is proportional to the received optical power.

In absence of RF modulation (MZM just driven by bias voltage), the generic expression of the signal detected by the square-law detector results as follows:

$$P_{dDC}^{MZ} = \frac{A_0^2}{4} \cos^2\left(\frac{\theta_{b1} - \theta_{b2}}{2}\right) \quad (12)$$

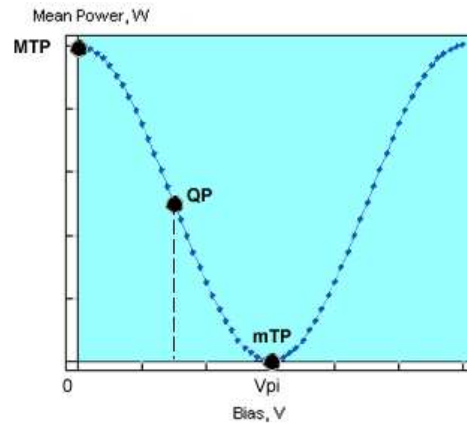


Figure 2.4 Mach-Zehnder's Transfer Function

- Quadrature Point (QP): located at the center of the linear zone, makes possible to obtain the modulator's maximum linearity. A $\frac{V_\pi}{2}$ voltage is required between the branches.
- Minimum Transmission Point (mTP): There is no power at the output (in an ideal situation). There will be a voltage difference between branches equal to V_π (half-wave voltage). In practice the carrier at the modulator's output is not completely cancelled out, because the power split over the two branches will never be exactly the same (see ER definition in section 2.2.1).
- Maximum Transmission Point (MTP): The power at the output is maximum. There is no phase shift between branches (voltage difference equal to 0).

Now we will explain the relation between the V_b required to obtain V_π and the corresponding electrode's sensitivity V_c for each configuration:

a) Push-Pull:

Replacing push-pull condition in expression (12) we have:

$$P_{dDC}^{MZ} = \frac{A_0^2}{4} \cos^2\left(\frac{\theta_b - (-\theta_b)}{2}\right)$$

$$P_{dDC}^{MZ} = \frac{A_0^2}{4} \cos^2(\theta_b) = 0 \Rightarrow \theta_b = \frac{\pi}{2}$$

Therefore, the relation between electrode's sensitivity V_c and V_π is:

$$\theta_b = \frac{V_b}{V_c} \pi = \frac{\pi}{2} \Rightarrow V_b = \frac{V_c}{2} = V_\pi \quad (13)$$

b) Single-branch asymmetric:

Replacing Single-branch asymmetric condition in expression (12) we have:

$$P_{dDC}^{MZ} = \frac{A_0^2}{4} \cos^2\left(\frac{\theta_b - (0)}{2}\right)$$

$$P_{dDC}^{MZ} = \frac{A_0^2}{4} \cos^2\left(\frac{\theta_b}{2}\right) = 0 \Rightarrow \theta_b = \pi$$

Therefore, the relation between electrode's sensitivity V_c and V_π is:

$$\theta_b = \frac{V_b}{V_c} \pi = \pi \Rightarrow V_b = V_c = V_\pi \quad (14)$$

We must emphasize that the electrodes' sensitivity is defined as the voltage needed to generate a 180° phase shift on the optical signal into that particular electrode. Each branch can have a different V_c value, however, we will consider they are the same, in order to simplify the calculations.

Unlike V_c , the half-wave voltage V_π does depend on the Mach-Zehnder's configuration, and it is obtained as follows:

$$V_{\pi} = mTP - MTP \quad (15)$$

It is also important to mention that, experimentally, we verified how the operating point can take a different value from one measurement to other. This phenomenon is known as bias drift [5] and is caused by the Mach-Zehnder dependence with temperature, and also due to environmental conditions, vibrations, etc.

2.2.2 Mach-Zehnder (push pull) + DUT + Detector Mathematical Analysis without considering amplitude distortions

Within a basic setup of a dispersion measurement technique based on RF tone modulation, the study of the block composed by the Mach-Zehnder, the DUT and the detector becomes an essential issue, as it establishes all the possible expressions for the detected signal, including amplitude and phase terms from which the different techniques calculate the dispersion coefficient D .

As it is shown in Figure 2.2, the optical source's output is amplitude modulated by the Mach Zehnder Modulator. In the usual configuration it is a single-drive push pull modulator biased at the quadrature point. After that the modulated signal passes through the DUT. Finally, the optical detector recovers the envelope following a square-law characteristic.

We will analyze both the push-pull and the asymmetrical MZ configurations as they set the basis of the chromatic dispersion measurement methods described in section 2.2.

The mathematical analysis will be developed under some particular conditions which are characteristic of RF tone based dispersion monitoring techniques:

- We will work under a small signal condition, that is, $A_{RF} \ll 1$. Thus, we can use the approximation: $e^{-j\alpha} = 1 - j\alpha$
- The development will be done using "low-pass equivalent" expressions to simplify operations, which means working with a carrier frequency equal to 0.

First, at the modulator's output, in a push-pull configuration typical of standard method MPSM we get:

$$E_{MZ} = \frac{A_0}{2} Re[e^{j\theta_b} e^{j\theta_{RF}} + e^{-j\theta_b} e^{-j\theta_{RF}}]$$

$$E_{MZ} = \frac{A_0}{2} Re[e^{j\theta_b}(1 + j\theta_{RF}) + e^{-j\theta_b}(1 - j\theta_{RF})]$$

$$E_{MZ} = \frac{A_0}{2} Re[e^{j\theta_b} + e^{-j\theta_b} + j\frac{A_m}{2}(e^{j\theta_b} - e^{-j\theta_b})(e^{j\omega_m t} + e^{-j\omega_m t})]$$

Passing E_{MZ} through the DUT, the optical signal suffers different phase shifts at the carrier and the sidebands, as it is shown below:

- Phase shift at the carrier: ϕ_0
- Phase shifts at the sidebands: ϕ^+ and ϕ^-

$$E_{DUT} = \frac{A_0}{2} \text{Re}[(e^{j\theta_b} + e^{-j\theta_b})e^{j\phi_0} + j\frac{A_m}{2}(e^{j\theta_b} - e^{-j\theta_b})(e^{j\omega_m t}e^{j\phi^+} + e^{-j\omega_m t}e^{j\phi^-})]$$

$$E_{DUT} =$$

$$\frac{A_0}{2} \text{Re}[(e^{j\theta_b} + e^{-j\theta_b})e^{j\phi_0} + j\frac{A_m}{2}(e^{j\theta_b} - e^{-j\theta_b})e^{j(\frac{\phi^+ + \phi^-}{2})}(e^{j\omega_m t}e^{j(\frac{\phi^+ - \phi^-}{2})} + e^{-j\omega_m t}e^{-j(\frac{\phi^+ - \phi^-}{2})})]$$

$$E_{DUT} = \frac{A_0}{2} \text{Re}[2 \cos \theta_b e^{j\phi_0} - 2A_m \sin \theta_b e^{j(\frac{\phi^+ + \phi^-}{2})} \cos(\omega_m t + \frac{\phi^+ - \phi^-}{2})]$$

$$E_{DUT} =$$

$$\frac{A_0}{2} \cos \theta_b (e^{j\phi_0} + e^{-j\phi_0}) - \frac{A_0 A_m}{2} \sin \theta_b (e^{j(\frac{\phi^+ + \phi^-}{2})} + e^{-j(\frac{\phi^+ + \phi^-}{2})}) \cos(\omega_m t + \frac{\phi^+ - \phi^-}{2})$$

The optical detector takes charge of recovering RF envelope. It consists on a square-law detector and a low-pass filter. So the detected power results:

If we consider $A_m^2 \ll A_m$, the detected power results:

$$P_d =$$

$$\frac{1}{2} \left(\frac{A_0^2}{2} \cos^2 \theta_b - A_0^2 A_m \cos \theta_b \sin \theta_b \left(\frac{e^{j(\frac{\phi^+ + \phi^-}{2} - \phi_0)} + e^{-j(\frac{\phi^+ + \phi^-}{2} - \phi_0)}}{2} \right) \cos(\omega_m t + \frac{\phi^+ - \phi^-}{2}) \right)$$

$$P_d = \frac{A_0^2}{4} \cos^2 \theta_b - \frac{A_0^2 A_m}{2} \cos \theta_b \sin \theta_b \cos \left(\frac{\phi^+ + \phi^-}{2} - \phi_0 \right) \cos(\omega_m t + \frac{\phi^+ - \phi^-}{2}) \quad (16)$$

In the expression obtained, the first term represents the DC component which has no relevance on the dispersion calculation. The second term is RF fundamental harmonic. We can notice how the sidebands' phase shifts, which are directly related to the chromatic dispersion value, appear in both amplitude and phase expressions, as the semi sum and semi difference respectively. Also we observe the bias voltage presence in the amplitude term but contained in two independent sinusoidal factors.

2.2.3 Mach-Zehnder (asymmetric) + DUT + Detector Mathematical Analysis without considering amplitude distortions

This setup can also be implemented using a Mach-Zehnder in an asymmetric configuration, developing the mathematical analysis in a similar way. Therefore, if we use again the low-pass equivalent expressions we will have:

$$E_{MZ} = \frac{A_0}{2} \text{Re}[1 + e^{j\theta_b} e^{j\theta_{RF}}]$$

$$E_{MZ} = \frac{A_0}{2} \text{Re}[1 + e^{j\theta_b} (1 + j\theta_{RF})]$$

$$E_{MZ} = \frac{A_0}{2} \text{Re}[1 + j\frac{A_m}{2} e^{j\theta_b} (e^{j\omega_m t} + e^{-j\omega_m t})]$$

Passing E_{MZ} through the DUT:

$$E_{DUT} = \frac{A_0}{2} \text{Re}[(1 + e^{j\theta_b})e^{j\phi_0} + j\frac{A_m}{2} e^{j\theta_b} (e^{j\omega_m t} e^{j\phi^+} + e^{-j\omega_m t} e^{j\phi^-})]$$

$$E_{DUT} =$$

$$\frac{A_0}{2} \text{Re}[(1 + e^{j\theta_b})e^{j\phi_0} + j\frac{A_m}{2}e^{j\theta_b}e^{j(\frac{\phi^+ + \phi^-}{2})}(e^{j\omega_m t}e^{j(\frac{\phi^+ - \phi^-}{2})} + e^{-j\omega_m t}e^{-j(\frac{\phi^+ - \phi^-}{2})})]$$

$$E_{DUT} =$$

$$\frac{A_0}{2} \text{Re}[e^{\frac{j\theta_b}{2}}(e^{-\frac{j\theta_b}{2}} + e^{\frac{j\theta_b}{2}})e^{j\phi_0} + j\frac{A_m}{2}e^{j\theta_b}e^{j(\frac{\phi^+ + \phi^-}{2})}(e^{j\omega_m t}e^{j(\frac{\phi^+ - \phi^-}{2})} + e^{-j\omega_m t}e^{-j(\frac{\phi^+ - \phi^-}{2})})]$$

$$E_{DUT} =$$

$$\frac{A_0}{2} (\cos(\frac{\theta_b}{2})(e^{j(\phi_0 + \frac{\theta_b}{2})} + (e^{-j(\phi_0 + \frac{\theta_b}{2})})) - A_m(e^{j(\frac{\phi^+ + \phi^-}{2} + \theta_b)} - e^{-j(\frac{\phi^+ + \phi^-}{2} + \theta_b)}) \cos(\omega_m t + \frac{\phi^+ - \phi^-}{2}))$$

$$E_{DUT} =$$

$$\frac{A_0}{2} \cos(\frac{\theta_b}{2})(e^{j(\phi_0 + \frac{\theta_b}{2})} + (e^{-j(\phi_0 + \frac{\theta_b}{2})})) - \frac{A_0 A_m}{2} (e^{j(\frac{\phi^+ + \phi^-}{2} + \theta_b)} - e^{-j(\frac{\phi^+ + \phi^-}{2} + \theta_b)}) \cos(\omega_m t + \frac{\phi^+ - \phi^-}{2}))$$

Finally, following the same conditions at the optical detector, the detected power results:

$$P_d =$$

$$\frac{1}{2} (\frac{A_0^2}{2} \cos^2(\frac{\theta_b}{2}) - \frac{A_0^2 A_m}{2} \cos(\frac{\theta_b}{2}) (\frac{e^{j(\frac{\phi^+ + \phi^-}{2} - \phi_0 + \frac{\theta_b}{2})} - e^{-j(\frac{\phi^+ + \phi^-}{2} - \phi_0 + \frac{\theta_b}{2})}}{2}) \cos(\omega_m t + \frac{\phi^+ - \phi^-}{2}))$$

$$P_d = \frac{A_0^2}{4} \cos^2(\frac{\theta_b}{2}) - \frac{A_0^2 A_m}{4} \cos(\frac{\theta_b}{2}) \sin(\frac{\phi^+ + \phi^-}{2} - \phi_0 + \frac{\theta_b}{2}) \cos(\omega_m t + \frac{\phi^+ - \phi^-}{2}) \quad (17)$$

If we compare the detected power obtained in this case with that of the push-pull configuration some different features emerge, i.e. the appearance of the bias voltage together with the semi sum of the sidebands' phase shifts inside the sine function argument. The new dispersion measurement approach exposed in this PFC takes advantage of this fact to establish the operating principle.

2.2.4 Mach-Zehnder (push pull) + DUT + Detector Mathematical Analysis considering amplitude distortions

In all previous analysis, we considered a DUT which only alters the optical signal phase with respect to frequency; however, some other devices used in optical communication systems, yield also a certain magnitude attenuation at each frequency component.

Thus, in this context, the mathematical analysis requires the use of additional trigonometric identities to obtain a compact expression for detected power.

First, for a push-pull configuration, the procedure is as follows:

At DUT's input, we receive the same optical signal from the modulator as in previous case:

$$E_{MZ} = \frac{A_0}{2} \text{Re}[e^{j\theta_b} + e^{-j\theta_b} + j\frac{A_m}{2}(e^{j\theta_b} - e^{-j\theta_b})(e^{j\omega_m t} + e^{-j\omega_m t})]$$

But now after it passes through the DUT we have:

$$\begin{aligned}
E_{DUT} &= \\
\frac{A_0}{2} \operatorname{Re}[(e^{j\theta_b} + e^{-j\theta_b})A^0 e^{j\phi^0} + j\frac{A_m}{2}(e^{j\theta_b} - e^{-j\theta_b})(A^+ e^{j\omega_m t} e^{j\phi^+} + A^- e^{-j\omega_m t} e^{j\phi^-})] \\
E_{DUT} &= \\
\frac{A_0}{2} \operatorname{Re}[2A^0 \cos \theta_b e^{j\phi^0} - A_m \sin \theta_b (A^+ e^{j\omega_m t} e^{j\phi^+} + A^- e^{-j\omega_m t} e^{j\phi^-})] \\
E_{DUT} &= \\
\frac{A_0 A^0}{2} \cos \theta_b (e^{j\phi^0} + e^{-j\phi^0}) - \frac{A_0 A_m}{4} \sin \theta_b (A^+ (e^{j\omega_m t} e^{j\phi^+} + e^{-j\omega_m t} e^{-j\phi^+}) + A^- (e^{-j\omega_m t} e^{j\phi^-} + e^{j\omega_m t} e^{-j\phi^-}))
\end{aligned}$$

At the optical detector's output, after applying the square-law and the low-pass filtering, we obtain:

$$\begin{aligned}
P_d &= \\
\frac{1}{2} \left(\frac{A_0^2 A^0^2}{2} \cos^2 \theta_b - \frac{A_0^2 A^0 A_m}{2} \cos \theta_b \sin \theta_b (A^+ \left(\frac{e^{j\omega_m t} e^{j\phi^+} e^{-j\phi^0} + e^{-j\omega_m t} e^{-j\phi^+} e^{j\phi^0}}{2} \right) + \right. \\
\left. A^- \left(\frac{e^{-j\omega_m t} e^{j\phi^-} e^{-j\phi^0} + e^{j\omega_m t} e^{-j\phi^-} e^{j\phi^0}}{2} \right) \right)
\end{aligned}$$

$$\begin{aligned}
P_d &= \\
\frac{A_0^2 A^0^2}{4} \cos^2 \theta_b - \frac{A_0^2 A^0 A_m}{4} \cos \theta_b \sin \theta_b (A^+ \cos(\omega_m t + \phi^+ - \phi^0) + A^- \cos(\omega_m t - \phi^- + \phi^0))
\end{aligned}$$

Finally, if we use the following trigonometric identity:

$$A \cos(w + a) + B \cos(w + b) = \sqrt{A^2 + B^2 + 2AB \cos(b - a)} \cos(w + a + \arctan\left(\frac{\sin(b-a)}{\frac{A}{B} + \cos(b-a)}\right))$$

The detected power results:

$$\begin{aligned}
\frac{A_0^2 A^0^2}{4} \cos^2 \theta_b - \frac{A_0^2 A^0 A_m}{4} \cos \theta_b \sin \theta_b \sqrt{A^{+2} + A^{-2} + 2A^+ A^- \cos(\phi^+ + \phi^- - 2\phi^0)} \cos(\omega_m t + \\
\phi^+ - \phi^0 + \arctan\left(\frac{\sin(\phi^+ + \phi^- - 2\phi^0)}{\frac{A^+}{A^-} + \cos(\phi^+ + \phi^- - 2\phi^0)}\right))
\end{aligned} \tag{18}$$

2.2.5 Mach-Zehnder (asymmetric) + DUT + Detector Mathematical Analysis considering amplitude distortions

Once again, if we repeat this analysis for a Mach Zehnder modulator in asymmetric configuration instead, the procedure is as shown below:

$$\begin{aligned}
E_{DUT} &= \frac{A_0}{2} \operatorname{Re}[(1 + e^{j\theta_b})A^0 e^{j\phi^0} + j\frac{A_m}{2} e^{j\theta_b} (A^+ e^{j\omega_m t} e^{j\phi^+} + A^- e^{-j\omega_m t} e^{j\phi^-})] \\
E_{DUT} &= \frac{A_0}{2} \operatorname{Re}[e^{\frac{j\theta_b}{2}} (e^{-\frac{j\theta_b}{2}} + e^{\frac{j\theta_b}{2}}) A^0 e^{j\phi^0} + j\frac{A_m}{2} e^{j\theta_b} (A^+ e^{j\omega_m t} e^{j\phi^+} + A^- e^{-j\omega_m t} e^{j\phi^-})] \\
E_{DUT} &=
\end{aligned}$$

$$\frac{A_0}{2} (A^0 \cos(\frac{\theta_b}{2}) (e^{j(\phi^0 + \frac{\theta_b}{2})} + (e^{-j(\phi^0 + \frac{\theta_b}{2})})) - \frac{A_m}{2} (A^+ e^{j\omega_m t} e^{j\phi^+} + A^- e^{-j\omega_m t} e^{j\phi^-}))$$

$$E_{DUT} =$$

$$\frac{A_0 A^0}{2} \cos(\frac{\theta_b}{2}) (e^{j(\phi^0 + \frac{\theta_b}{2})} + (e^{-j(\phi^0 + \frac{\theta_b}{2})})) - \frac{A_0 A_m}{4} (A^+ (e^{j\omega_m t} e^{j\phi^+} e^{j\frac{\theta_b}{2}} - e^{-j\omega_m t} e^{-j\phi^+} e^{-j\frac{\theta_b}{2}}) + A^- (e^{-j\omega_m t} e^{j\phi^-} e^{j\frac{\theta_b}{2}} - e^{j\omega_m t} e^{-j\phi^-} e^{-j\frac{\theta_b}{2}}))$$

Therefore, at the Optical Detector's output the detected power results:

$$P_d =$$

$$\frac{1}{2} \left(\frac{A_0^2 A^0{}^2}{2} \cos^2\left(\frac{\theta_b}{2}\right) - \frac{A_0^2 A^0 A_m}{2} \cos\left(\frac{\theta_b}{2}\right) \left(\frac{e^{j(\omega_m t + \phi^+ - \phi^0 + \frac{\theta_b}{2})} - e^{j(\omega_m t + \phi^+ - \phi^0 + \frac{\theta_b}{2})}}{2} + \frac{e^{j(\omega_m t + \phi^+ - \phi^0 + \frac{\theta_b}{2})} - e^{j(\omega_m t + \phi^+ - \phi^0 + \frac{\theta_b}{2})}}{2} \right) \right)$$

$$P_d =$$

$$\frac{A_0^2 A^0{}^2}{4} \cos^2\left(\frac{\theta_b}{2}\right) - \frac{A_0^2 A^0 A_m}{2} \cos\left(\frac{\theta_b}{2}\right) (A^+ \sin(\omega_m t + \phi^+ - \phi^0 + \frac{\theta_b}{2}) + A^- \sin(\omega_m t - \phi^- + \phi^0 - \frac{\theta_b}{2}))$$

Finally, by applying an analogous trigonometric identity:

$$A \sin(w + a) + B \sin(w + b) = \sqrt{A^2 + B^2 + 2AB \cos(b - a)} \sin(w + a + \arctan\left(\frac{\sin(b - a)}{\frac{A}{B} + \cos(b - a)}\right))$$

The detected power here results:

$$P_d =$$

$$\frac{A_0^2 A^0{}^2}{4} \cos^2\left(\frac{\theta_b}{2}\right) - \frac{A_0^2 A^0 A_m}{2} \cos\left(\frac{\theta_b}{2}\right) \sqrt{A^{+2} + A^{-2} - 2A^+ A^- \cos(\phi^+ + \phi^- - 2\phi^0)} \sin(\omega_m t + \phi^+ - \phi^0 + \arctan\left(\frac{\sin(\phi^+ + \phi^- - 2\phi^0)}{-\frac{A^+}{A^-} + \cos(\phi^+ + \phi^- - 2\phi^0)}\right))$$

(19)

From the expression above, it is observed how the RF modulating signal phase recovered is not equal to the semi difference between the two major sidebands phase shifts but a much more complex term, unlike the previous case. This fact represents a huge inconvenience for phase-based measuring techniques like MPSM, because, even though the phase shifts at both sidebands are still contained in the phase term, we cannot consider this term as a good approximation of the optical phase shift inserted by the DUT, and therefore there is no guarantee to obtain a correct chromatic dispersion characterization from it.

Unfortunately, this situation is also a pending task for ABCM, because as we observe from expression (19), the bias voltage and the sum of phases in the amplitude recovered are not within the same sinusoidal (basis of ABCM) and it would be a very complex procedure trying to join both parameters in a well-known expression.

Now, we will describe two of the most popular techniques for dispersion measurement: Modulation Phase-Shift Method (MPSM) and Peucheret's Method, whose operating principles served as inspiration and conceptual basis for the new methods featured in this PFC.

2.2.6 Modulation Phase Shift Method (MPSM)

MPSM obtains the group delay response of a device under test (DUT) by measuring the change in phase of a sinusoidal radio frequency (RF) modulation envelope as the wavelength is changed.

Figure 2.5 shows the basic setup for MPSM [7]. The optical source is a tuneable laser. Modulation is impressed using an external modulator, usually a Mach – Zehnder Modulator in push – pull configuration, and recovered by an optical receiver. Phase data are recovered by ratio detection with respect to a reference RF path.

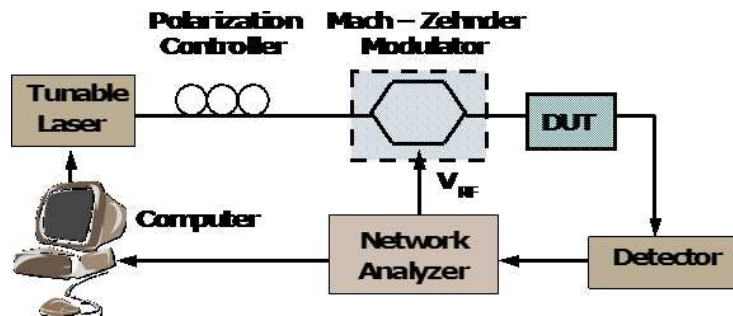


Figure 2.5 MPSM basic setup

As MPSM is included within the techniques which use RF modulation, it applies an amplitude modulation on the optical signal to generate two major sidebands on the carrier (considering small signal condition), where each of them is affected by a phase shift while passing through the DUT, so that, in reception, the network analyzer takes charge of recovering the signal at . The mathematical expression for this signal is obtained from the RF component in (16)

$$P_d = -\frac{A_o^2 A_m}{2} \cos(\theta_B) \sin(\theta_B) \cos\left(\frac{\varphi^+ + \varphi^-}{2} - \varphi_o\right) \cos\left(\omega_m t + \frac{\varphi^+ - \varphi^-}{2}\right) \quad (20)$$

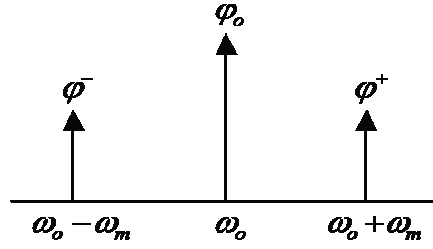


Figure 2.6. Optical phase shifts inserted by the DUT

From the signal above, the network analyzer will recover the electrical phase as the semi difference between the optical phase shifts acquired by the two major sidebands.

$$\Delta\phi = \frac{\phi^+ - \phi^-}{2} \quad (21)$$

After that, we approximate the group delay at the operating wavelength from this electrical phase, as it is explained below:

$$\tau_g = -\frac{d\phi}{d\omega} \approx -\frac{\Delta\phi}{360^\circ} \frac{1}{f_m} \quad (22)$$

where the first factor is defined as the fractional cycle of RF phase shift (expressed in degrees) and the second factor represents the period of the RF sine wave.

Now, by sweeping the optical wavelength with the aid of a tuneable laser, we obtain the complete delay curve for the required bandwidth, and then, chromatic dispersion at the nominal wavelength is calculated by dividing the change of group delay by the wavelength change which stimulates it:

$$D = \frac{d\tau_g}{d\lambda} \approx \frac{\Delta\tau_g}{\Delta\lambda} \quad (23)$$

In order to achieve accurate measures it is important to have a stable wavelength step size, which completely depends on the tuneable laser stability.

In expression (22) we can notice how the group delay and the measured electrical phase present opposite slopes.

The phase of a sinusoidal signal can be interpreted as the argument of this signal when the time variable is equal to zero. For example, if we have $\cos(\omega t + \theta)$, the phase of this signal is $+\theta$. The time delay presented in a sinusoidal signal can be defined as the time value which cancels the argument. For example, the time delay of $\cos(\omega t + \theta)$ is $-\theta/\omega$. Having in mind these concepts, it is of extreme importance to highlight that when the group delay is estimated

based in phase measurements, is necessary to invert the sign of the phase before computing it.

2.2.7 Peucheret's Method

Peucheret's method uses the same setup as MPSM, so, the detected power at RF frequency is also the one of expression (20); however, instead of measuring the signal's phase, it focuses on the amplitude term. As it was explained before, chromatic dispersion is strongly related with the phase shifts at the sidebands, and in this case, we will attempt to calculate it from the semi sum of these phase shifts which is contained into the RF amplitude term.

Nevertheless, due to the channel noise, insertion loss and other signal attenuation factors, it would be necessary to have extremely accurate equipment and a very reliable calibration procedure if we want to measure the exact amplitude value. This is why Peucheret's method operates on the envelope's dips. In order to obtain these dips, Peucheret proposes to carry out a RF Frequency sweep on the setup. The mathematical analysis will be first conducted for the case where no amplitude distortion coming from the DUT is relevant, and then it will be extended to consider a relevant amplitude distortion coming from the DUT.

Once again we start the analysis from expression (20):

$$P_d = -\frac{A_o^2 A_m}{2} \cos(\theta_B) \sin(\theta_B) \cos\left(\frac{\varphi^+ + \varphi^-}{2} - \varphi_o\right) \cos\left(\omega_m t + \frac{\varphi^+ - \varphi^-}{2}\right) \quad (24)$$

To obtain a "zero" in the amplitude term, we have:

$$\begin{aligned} \cos\left(\frac{\phi^+ + \phi^-}{2} - \phi_0\right) &= 0 \\ \frac{\phi^+ + \phi^-}{2} - \phi_0 &= \frac{(2n-1)\pi}{2} \\ \phi^+ + \phi^- - 2\phi_0 &= (2n-1)\pi \end{aligned} \quad (25)$$

As we know from, dispersion theory:

$$\begin{aligned} \sum(\phi) &= \phi^+ + \phi^- = 2\phi_0 + \frac{2\pi D \lambda^2 f_m^2}{c} \\ \phi^+ + \phi^- - 2\phi_0 &= \frac{2\pi D \lambda^2 f_m^2}{c} \end{aligned} \quad (26)$$

Therefore, replacing expression (25) in (26) results:

$$\begin{aligned} \frac{2\pi D \lambda^2 f_n^2}{c} &= (2n-1)\pi \\ D &= \frac{(n-\frac{1}{2})c}{\lambda^2 f_n^2} \end{aligned} \quad (27)$$

Now, we consider characterizing a DUT that inserts different amplitude attenuation levels at each frequency component. The mathematical analysis for this situation was also made in section 2.2.2. Here, we get the RF modulating signal from expression (19):

$$P_d = \frac{A_0^2 A^2}{4} \cos^2\left(\frac{\theta_b}{2}\right) - \frac{A_0^2 A^0 A_m}{2} \cos\left(\frac{\theta_b}{2}\right) \sqrt{A^{+2} + A^{-2} - 2A^+ A^- \cos(\phi^+ + \phi^- - 2\phi^0)} \sin(\omega_m t + \phi^+ - \phi^0 + \arctan\left(\frac{\sin(\phi^+ + \phi^- - 2\phi^0)}{-\frac{A^+}{A^-} + \cos(\phi^+ + \phi^- - 2\phi^0)}\right)) \quad (28)$$

It is inferred that we reach an amplitude dip when the cosine function takes its minimum value (-1), so we have:

$$\begin{aligned} \cos(\phi^+ + \phi^- - 2\phi_0) &= -1 \\ \phi^+ + \phi^- - 2\phi_0 &= (2n - 1)\pi \end{aligned}$$

We notice we are under the same condition than for the non-amplitude degradation DUT and therefore, expression (27) is still valid to calculate chromatic dispersion coefficient. Thus, this analysis confirms Peucheret's method robustness for characterizing this kind of devices, in contrast to MPSM.

Nevertheless, there is an important problem in Peucheret's method, which is the fact that depending on the amount of dispersion introduced by a determined DUT, the RF frequency needed to reach a dip could be too high; therefore, a very large sweep will be required to find it. Moreover, the use of high frequencies on the setup presents two main inconveniences: it may occur that equipment available cannot operate at those frequencies; and also, it is known that increasing the RF Frequency level implies moving the sidebands even further from the carrier losing resolution and accuracy in calculations.

Peucheret tries to solve this problem by including a constant dispersion offset before the DUT in the setup, so the amount of total dispersion to measure increases so that the dip can be reached by using a lower RF frequency, and the level of dispersion desired is now the change in the total dispersion (DUT and offset). However, this procedure relies too much on dispersion offset's stability during the entire process, which is hard to reach in highly dispersive channels.

2.3 Dispersion Compensating Elements

2.3.1 Dispersion Compensating Fiber

The Dispersion Compensating Fiber or DCF is simply a spool of a special type of fiber that has a very large negative dispersion, that is, a group delay spectrum with a negative slope. This amount of dispersion is several times the one of a conventional fiber. Thus, if we place a determined length of DCF after an optical fiber link, we can compensate the dispersion accumulated along the link.

DCF presents some inconveniences. First, 1 Km of DCF with a typical nominal dispersion of -200 ps/nm·km just compensates 10-12 Km of standard SMF (G.652). Also, the attenuation caused by this compensating element at 1550 nm is as large as: three times that in standard fiber. Third, because of its reduced modal diameter, the optical intensity inside the fiber is so high that there is an accentuation of nonlinear effects.

Additionally, although DCFs seem to have a wide wavelength band suitable for WDM applications, their nearly constant dispersion – slope across a large operational optical wavelength band pass does not exactly balance the group delay spectrum of SMFs. Thus, while DCFs neutralize the effect of chromatic dispersion at a single wavelength, a group of wavelengths away from that wavelength will be either under- or overcompensated for dispersion. This effect is known as the “Dispersion-slope mismatch”.

Nowadays, there is work in improving the performance of DCFs. There are new DCFs based in structure of bimodal fiber, reaching a nominal dispersion of approximately $-770 \text{ ps/nm} \cdot \text{km}$ with the same loss as a standard SMF.

2.3.2 Chirped Fiber Bragg Grating

Chirped Fiber Bragg Gratings (CFBG) are considered the best option to cope with chromatic dispersion effects, due to their low-insertion loss and simplicity to be integrated and fabricated.

A FBG consists on a short fiber section which reflects certain wavelengths and transmits the others. This is achieved by changing periodically the media’s refraction index, because, according to Fresnel equations (from which Bragg wavelength λ_B is deduced), the light traveling through a determined media with different refraction indexes could be reflected or refracted. So, the grating period behavior must be such that the wavelength reflected fulfills the relation: $\lambda_B = 2\bar{n}\Delta$.

It is important to mention that FBGs also experience the Dispersion-slope mismatch explained for DCFs.

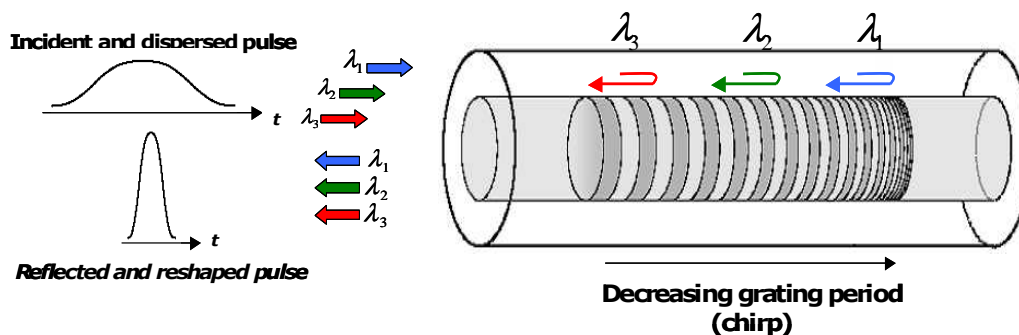


Figure 2.7 Fiber Bragg Grating operating principle

In CFBG (Chirped FBG), unlike UFBG (Unchirped FBG), the induced refraction index does not have a sinusoidal variation with constant period, but the period becomes progressively shorter along the grating length.

Due to the fact that the fiber’s dispersion coefficient in the third window is positive, when the wavelength increases the delay suffered increases too. To compensate this effect, it is necessary to make the larger wavelength travel shorter distances and the opposite way. This procedure makes possible to recover the original wave form at the system’s output.

2.4 VPI Simulation Tool

VPI is a powerful tool which not only lets us verify designs and to evaluate new components but also to investigate and optimize new technologies.

Here we will explain some of the basic concepts and operating principles of this software, in order to clarify some terms used in the development of the present project, and also to understand how the software is structured and how to define certain basic parameters to achieve successful simulations.

2.4.1 Signal Representation

In VPI, data exchange can be organized in two different ways: in blocks or by transmitting individual samples.

The **Block Mode** is the most efficient form of simulation, as modules are only fired when data passes through them, and it is more suitable for system simulation where components are widely – spaced compared with the modeled time, or where the signals flow unidirectionally, from transmitter to receiver. Through this mode, each module generates samples which are packed into a block which, once completed, will be passed to the following module for its respective processing.

The **Sample Mode** is the modality requiring more simulation time; nevertheless, it is also the one allowing more flexibility when designing systems. In this case, each module passes the data to the following one in a sample – by – sample scheme, meaning that different modules may be executing at the same time. This mode is necessary when the delay between the modules is much shorter than a block length, making necessary a fast communication between them in order to fully simulate their joint behavior.

In this project the Block Mode was used since signals flow unidirectionally from transmitter to receiver. Additionally, Block Mode enables the use of the duality between representations in the time and frequency domains which is a very useful tool allowing us to fully understand simulations results. 2.4.2 Global Parameters

Global parameters are common to all modules within a simulation. These values have a big importance for the correct and efficient operation of the simulator. In this section, we will describe the two global parameters with direct influence on simulation performance while working on the Block Mode:

- **TimeWindow:** this value sets the period of real time that is represented as a block of data. Additionally, this time will inevitably fix the spectral resolution of the simulated signals setting, i. e., the resolution of spectral displays.
- **SampleRateDefault:** it specifies the sampling frequency when working in block mode. It is defined as the number of samples taken by second and determines the maximum frequency that can be simulated.

These parameters define the frequency and time resolution respectively; therefore, they will depend on the desired simulation frequencies which will vary depending on the experiment.

2.4.3 Restrictions on Global Parameters

Since VPI works with the FFT algorithm, when working with periodic signals a series of restrictions, which are consequence of making use of this algorithm, have to be considered.

First, the number of samples by Time Window has to be a power of two. This condition sets a limitation when selecting the Time Window and the Sample Rate, since the product of these two variables results in the number of samples, as it appears in expression (29).

$$n^{\circ} \text{ samples} = \text{TimeWindow} \cdot \text{SampleRate} = 2^n \quad (29)$$

Additionally, it has to be considered that the time resolution, given by (30), will determine the maximum allowed simulation frequency which is given by (31).

$$dt = \frac{1}{\text{SampleRateDefault}} \quad (30)$$

$$f_{\max} < \frac{1}{2dt} = \frac{\text{SampleRateDefault}}{2} \quad (31)$$

Finally, the frequency resolution will be given by expression (32). A proper selection of the Time Window is required in order to obtain a correct signal frequency spectrum. At the same time, the Time Window determines the minimum allowed simulation frequency given by expression (33), since the period of the simulated signal always has to be smaller than the Time Window ($T < \text{TimeWindow}$).

$$df = \frac{1}{\text{TimeWindow}} \quad (32)$$

$$f_{\min} > \frac{1}{\text{TimeWindow}} \quad (33)$$

2.4.4 Module Parameters

When a module is placed on a schematic, an instance of the module is created. Each instance can carry unique values for the module's parameters.

The values of the parameters can be edited using the Parameter Editor.

The parameters are grouped in categories and every parameter belongs to a single category. Categories are displayed as folders within the parameter editing panel. In this PFC we have only worked and modified Physical parameters which describe the structure of a device.

For modifying a parameter, it is only necessary to change its value in the corresponding cell and to click the Apply button to make it valid. A Parameter Editor can be kept opened while

running a simulation, but parameter values are only updated at the start of each simulation run.

2.4.5 Sweep Configuration

To detect the influence of specified parameters on the techniques' behavior, VPI offers the possibility of performing parameter sweeps; so we can monitor the system's performance for different parameter settings.

VPI allows the creation of explicit parameter sweeps from the Parameter Editor of the module containing the parameter to be swept. To create this type of sweep it is necessary to just open the Parameter Editor of the module containing the parameter to be swept, to right – click on the desired parameter and to select “Create Sweep Control”.

This will bring about a “Define Control” window where it is possible to define the type and range of the sweep. There are four different control modes: continuous, list, random and expression, but only one of them is used during this project, which is Continuous Mode. In this mode it is necessary to specify the control variable’s name, the upper and lower limits of the sweep as well as the division type (Number of Steps, Step Width, or Percentage of the upper limit minus the lower limit) and the division value (steps that a sweep will increment in).

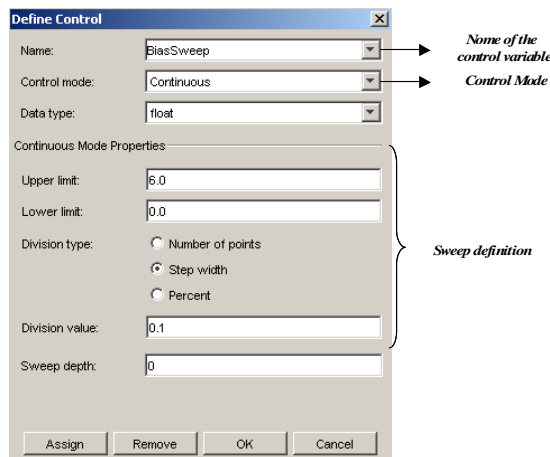


Figure 2.8 Sweep Control Panel

2.4.6 Simulation example

Now, in order to put all the concepts explained above into practice, we will simulate the transfer function of an Asymmetric MZ modulator, which is a fundamental element in this PFC.

- **Setup**

Since we want to obtain the transfer function, we do not insert RF signal into the MZ modulator; meaning that the amplitude of the RF source is set to “zero”. Additionally, it will be necessary to perform a bias sweep. We create a sweep control for the amplitude of the DC source.

The modulator's output is entered into an optic – electric (OE) converter, which, is acting just as a square – law power meter. After that, the OE converter output gets into an “Electrical Power Meter”, which measures the mean power of the DC component.

Additionally, we will use the V_iXY module to plot the mean DC power versus the bias voltage, which is obtained through an “Electrical Power Meter” connected to the output of the DC source.

The setup is shown in Figure 2.9.

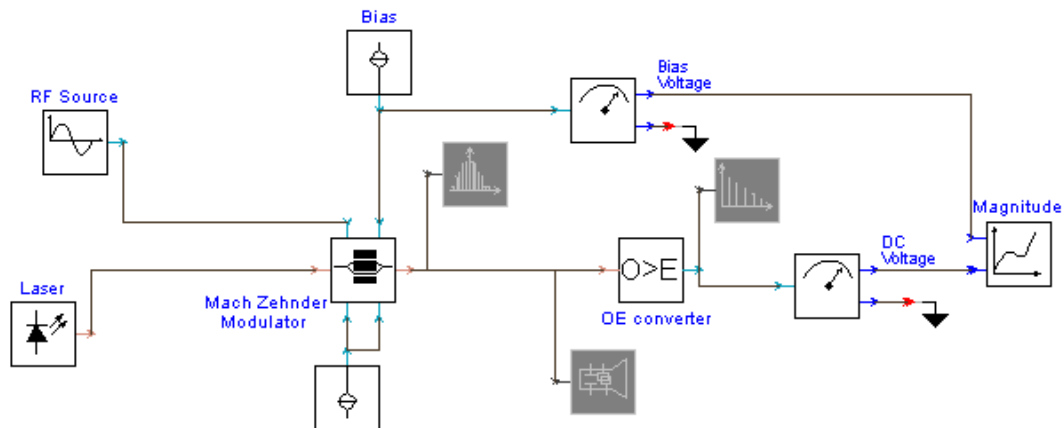


Figure 2.9 VPI simulation setup for measuring the transfer function of a MZM in Asymmetric Configuration

- **Configured Parameters**

For performing this simulation, we need to configure the following parameters:

- Global parameters:

TimeWindow: it is set to 1280 nsec to allow a frequency resolution of 6.25MHz, and a minimum simulation frequency of 6.25 MHz.

SampleRateDefault: it is set to 256e8 Hz allowing RF frequencies until 12.8 GHz.

Selecting these values of time window and sample rate, we are working with 4096 samples by time window.

Name	Value	Unit
Global		
f TimeWindow	160/1e9	s
InBandNoiseBins	OFF	
BoundaryConditions	Periodic	
LogicalInformation	ON	
f SampleModeBandwidth	1280e9	Hz
f SampleModeCenterFrequency	193.1e12	Hz
f SampleRateDefault	256e8	Hz
f BitRateDefault	10e9	bit/s

Figure 2.10 Configured Global Parameters

- General parameters: we have placed as general parameters the emission frequency of the laser (Optical_Freq_Start), which has been set to 192.4 THz (1559.25 nm), and the RF frequency (RF_Frequency), which has been set to 2 GHz (see Figure 2.11).

Name	Value	Unit
General		
f Optical_Freq_Start	192.4e12	Hz
f RF_Frequency	2e9	Hz

Figure 2.11 General Parameters

- Laser: the physical parameters of the laser are shown in
- Figure . The emission frequency was set to the Optical_Freq_Start (192.4 THz), the sample rate was set to the SampleRateDefault (256e8 Hz), and the average power was set to 1 mW.

Name	Value	Unit
Physical		
f EmissionFrequency	Optical_Freq_Start	Hz
f SampleRate	SampleRateDefault	Hz
f AveragePower	1.0e-3	W
f Linewidth	10e6	Hz
f Azimuth	0	deg
f Ellipticity	0	deg
f InitialPhase	0	deg

Figure 2.12 Physical parameters of the Laser

- RF Source: as explained before, the amplitude of the RF signal was set to zero. Even though other parameters as the SampleRate and the Frequency have no physical effect because the amplitude of the signal is zero, it was necessary to specify their values, which have been set to the SampleRateDefault and the RF_Frequency (see
- Figure).

Name	Value	Unit
Physical		
f SampleRate	SampleRateDefault	Hz
f Amplitude	0	a.u.
f Frequency	RF_Frequency	Hz
f Phase	0.0	deg
f Bias	0.0	a.u.

Figure 2.13 Physical parameters of the RF Source

- Modulator: in this module we modified the values of V_{π_DC} and V_{π_RF} which are the DC and RF voltages respectively, required into each particular electrode, to yield a phase change of π in the optical signal. Therefore, these values correspond with the electrode sensitivity (V_c). Consequently, to mimic the modulator used in the laboratory, we set both sensitivities to 3.5 volts.

It is important to clarify that, VPI defines both sensitivities (lower and upper) equal, even though, experimentally, each branch of the modulator could have different V_c .

In this case the “LowerArmPhaseSense” parameter does not have any effect, since the lower arm of the interferometer is disabled.

Name	Value	Unit
Physical		
f VpiDC	3.5	V
f VpiRF	3.5	V
f InsertionLoss	6	dB
f ExtinctionRatio	40	dB
LowerArmPhaseSense	NEGATIVE	
f dVpiDC_dTemperatu	0	V/d...
f dVpiRF_dTemperatu	0	V/d...
f OperatingTemperatu	25	degC
f ReferenceTemperatu	25	degC

Figure 2.14 Modulator physical parameters

Then, for obtaining the modulator transfer function, we performed a bias sweep from 0 to 7 volts with a step width of 0.1 volts.

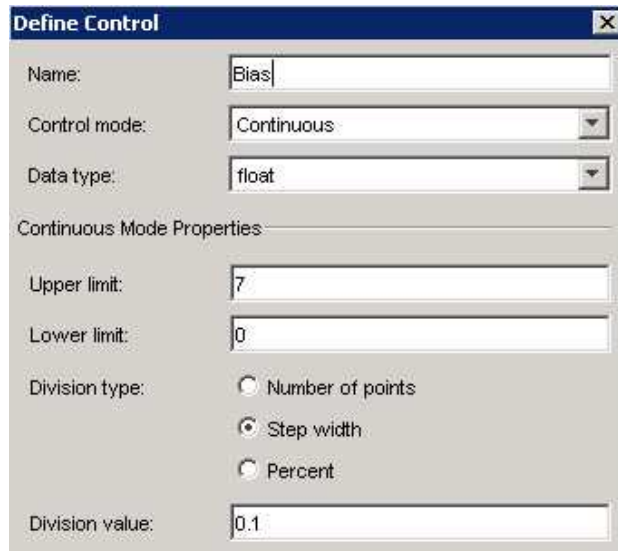


Figure 2.15 Bias sweep configuration

- **Results**

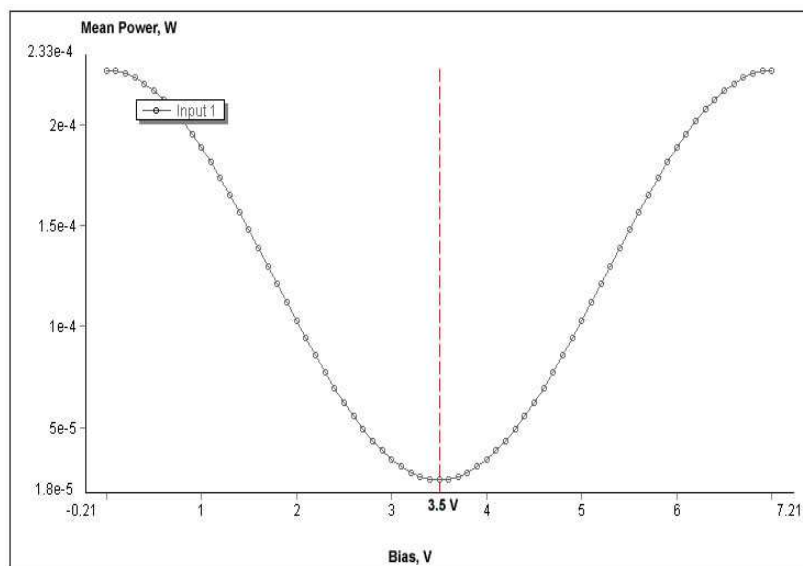


Figure 2.16. Transfer Function of an Asymmetric MZ Modulator

Figure 2.16 shows the MZ modulator transfer shows the MZ modulator transfer shows the MZ modulator transfer function in an asymmetric configuration. It corresponds with the DC component of (47), where the half – wave voltage is equal to the sensitivity of the electrodes (3.5 volts), as it has been demonstrated in section 2.2.1.2.

3. ASYMMETRIC-MODULATION BIAS CONTROLLED METHOD (ABCM)

3.1 Description and Mathematical Analysis

This first technique is devoted to verify that we can accomplish a high degree of accuracy when we calculate chromatic dispersion using a RF modulated signal's amplitude term instead of the phase term.

In the same way as in Peucheret's method, the idea consists on finding the envelope dips (where the sinusoidal argument takes a well-known value); and then, through a direct mathematical development, the total amount of dispersion can be calculated. However, in this case no RF Frequency sweep is required. We will choose a fixed frequency appropriately and we will make a bias voltage sweep instead.

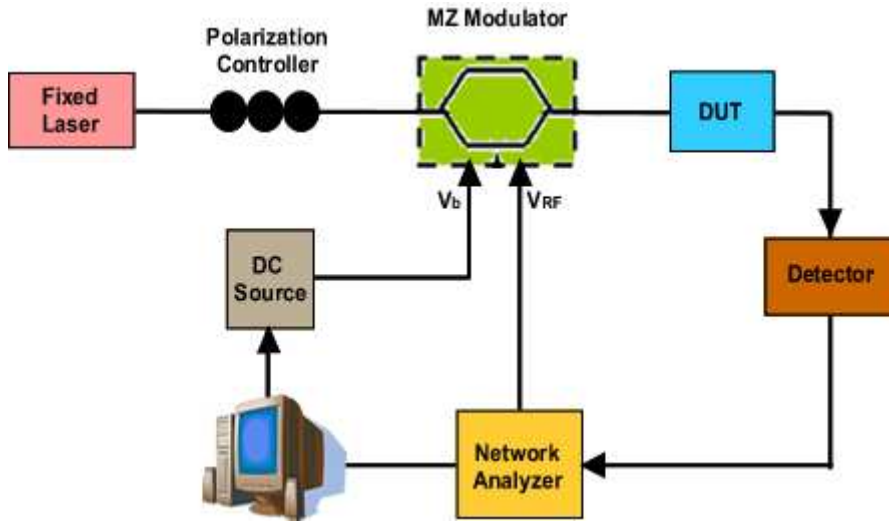


Figure 3.1 ABCM basic setup

The setup used in this method consists on a laser source operating at a fixed wave length (third window) whose output gets into a Dual drive Mach-Zehnder Modulator in asymmetric configuration. The optical signal is not altered at the modulator's upper branch, while at the lower branch, it is phase modulated by a RF tone inserted together with a bias voltage. The sum of both branches' signals results in an amplitude-modulated signal.

The modulator's output passes through the DUT, where it acquires the phase shifts, and then through the detector, obtaining expression (17) as we already verified in section 2.2.2:

$$P_d = \frac{A_0^2 \cos^2\left(\frac{\theta_b}{2}\right)}{4} - \frac{A_0^2 A_m \cos\left(\frac{\theta_b}{2}\right) \sin\left(\frac{\varphi^+ + \varphi^-}{2} - \varphi_0 + \frac{\theta_b}{2}\right) \cos\left(\omega_m t + \frac{\varphi^+ - \varphi^-}{2}\right)}{4}$$

The first term is the DC component and the second one is the RF first harmonic. Analyzing this second term we notice that in the amplitude factor the cosine function depends exclusively on the bias voltage value; so that it yields "zeros" in fixed locations: $V_b = (2n+1)V_{\pi}$; however, the

sine function depends on the semi sum of the phase shifts at both sidebands as well. Dispersion information is contained in this last term, so we need to determine the location of the zeros yielded by the sine function, defined as “moving zeros”, to calculate D value.

In absence of dispersion (no phase shifts in the sine’s argument), the moving zeros will be located at $V_b = 2nV_\pi$, therefore, under dispersion effects, these zeros will be shifted a certain distance from these reference locations positively or negatively, according to the dispersion’s magnitude and sign.

To explain the complete procedure to calculate the chromatic dispersion, we start looking for an expression that relates the sum of phase shifts term with D value.

The phase shifts inserted at both sidebands can be expressed using the Taylor Expansion defined in

$$\varphi^+ = \varphi_0 - \tau_g(\Delta\omega) + \frac{1}{2} \left(\frac{\partial \tau_g}{\partial \omega} \right) (\Delta\omega)^2 \quad (34)$$

$$\varphi^- = \varphi_0 - \tau_g(-\Delta\omega) + \frac{1}{2} \left(\frac{\partial \tau_g}{\partial \omega} \right) (-\Delta\omega)^2 \quad (35)$$

$$\frac{\partial \tau_g}{\partial \omega} = -\frac{2\pi c}{\omega_0^2} D = -\frac{\lambda_0^2}{2\pi c} D \quad (36)$$

Note that in contrast to section X where all quantities were given as distributed quantities along the fiber length, here we consider the total dispersion (after multiplying by total length). Applying expression (7) we have:

Then, replacing (36) in expressions (34) and (35) and forming the sum of phase shifts term, we obtain:

$$\varphi^+ + \varphi^- - 2\varphi_0 = \sum \varphi = \frac{2\pi D \lambda_0^2 f_m^2}{c} \quad (37)$$

where λ_0 is the operating wave length, f_m is the RF tone frequency and c the velocity of light in vacuum.

Now, in order to get an amplitude dip (zero), the sine’s argument must be equal to $n\pi$, so we have:

$$\begin{aligned} \frac{\varphi^+ + \varphi^-}{2} - \varphi_0 + \frac{\theta_b}{2} &= n\pi \\ \varphi^+ + \varphi^- - 2\varphi_0 + \theta_b &= 2n\pi \end{aligned} \quad (38)$$

where $\theta_b = \frac{\pi}{V_\pi} V_b$. Thus, if we replace expression (37) in expression (38), we obtain the exact locations of moving zeros and the final expression to calculate D :

$$\begin{aligned} \frac{2\pi D \lambda_0^2 f_m^2}{c} + \frac{\pi}{V_\pi} V_b &= 2n\pi \\ V_b &= \left(2n - \frac{2\lambda_0^2 f_m^2}{c} D \right) V_\pi \end{aligned} \quad (39)$$

$$\Rightarrow D = \left(2n - \frac{V_b}{V_\pi}\right) \frac{c}{2\lambda_0^2 f_m^2} \quad (40)$$

where V_b is the voltage necessary to get the n_{th} moving zero, f_m is the RF frequency, and c and λ_0 are the velocity of light and the operating wavelength respectively.

In this analysis, according to the setup, we considered that the RF modulating signal and the Bias voltage are inserted into the same electrode, however if we decide to use a different electrode for each one, the final expression obtained will be the same as in (40), but with a plus sign instead of the minus one.

We notice how the level of accuracy in D calculation depends on the Bias voltage step width (V_b sweep resolution) and the RF frequency chosen. In numerical terms, a 0.01 V error in V_b measurement represents approximately a $180/f_m^2$ ps/nm error in D calculation (with f_m in GHz, $c = 3 \times 10^8$ m/s and $\lambda_0 = 1559$ nm). Therefore, once we have fixed a proper Bias voltage resolution (conditioned by equipment available), we can minimize the error yielded in measurements by choosing a high enough RF frequency, but then the Taylor approximation for the dispersion may fail because we would get too much far from the optical carrier (See expression (34) and (35)).

The explanation above tries to establish the lower edges for both bias voltage resolution and RF frequency; however, there are also some restrictions which do not allow increasing these parameters too much.

In the case of the bias voltage resolution, after a determined level, if we keep reducing the step width, there will be almost no improvement in D resolution, but there will be an unnecessary extra processing charge.

In terms of RF frequency, if we look back to expression (40), we observe that for big dispersion values, the frequency must be low enough to avoid the bias voltage corresponding to the n_{th} dip gets too much close to $\pm nV_\pi$ (depending on dispersion sign), because if so, it will be difficult to distinguish the “moving zeros” from the “fixed zeros”.

3.2 VPI simulations

This section is devoted to illustrate and verify the mathematical analysis' results obtained for the ABCM, working in an ideal simulation schematic (noise-free transmission channel, no equipment limitations, etc), and it also gives us the chance to analyze the method's behavior while we change its different parameters, so that we can identify the operation edges for each case. In this purpose, we will expose the complete process to carry out ABCM using this powerful simulation tool.

On a first stage, after making a Bias sweep, VPI will return Amplitude-vs-Bias graphics where we can easily locate the amplitude dips, obtain the respective bias voltages; and finally by applying expression (40), calculate D value.

On a second stage, in order to observe the method's behavior when we vary a determined parameter, VPI provides us multidimensional sweeping options and Text Visualization modules, which allow the processing and storage of large amounts of data samples.

It is also important to highlight that along this section all setups will use a Mach – Zehnder modulator in asymmetric configuration, whose operation method was described in section 2.2.1 and whose transfer function was already obtained using VPI.

3.2.1 Analysis of the dispersion inserted by the DUT

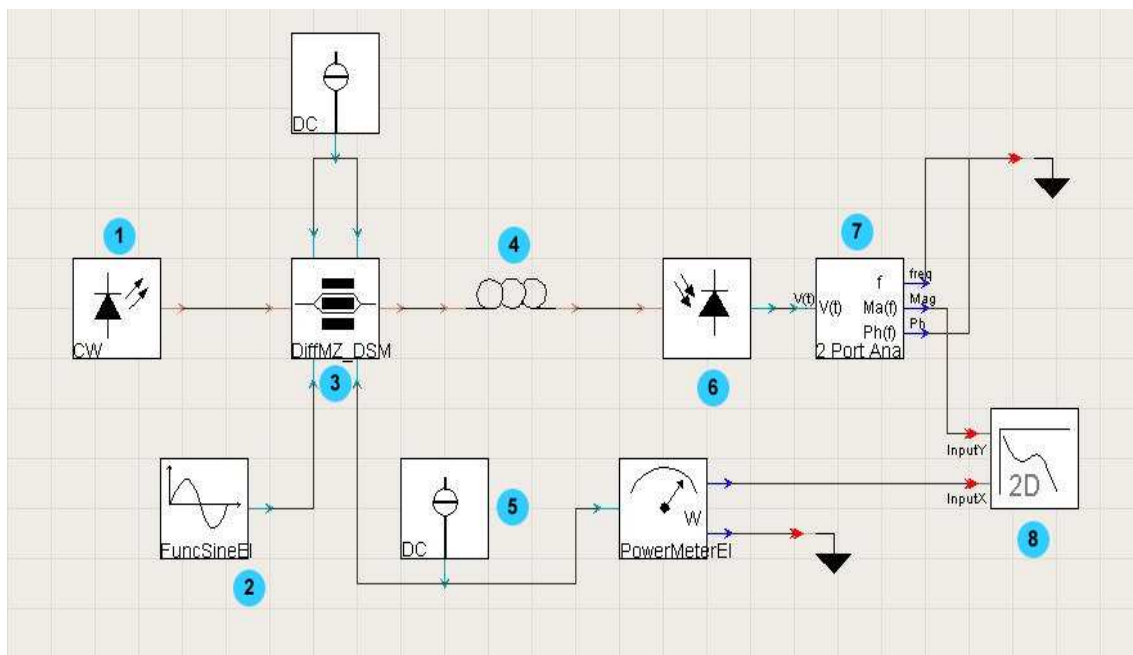


Figure 3.2 VPI setup for ABCM: 1- Optical source 2- Sine function generator 3- MZM 4- Fiber section 5- DC source 6- Photodetector 7- Phase and Magnitude detector 8- 2D Analyzer

In this first part, we will use the setup featured in Figure 3.2. We will display an amplitude-vs-bias graphic for three specific situations: when the setup includes a DUT (fiber section) with positive and negative dispersion, and without the DUT.

By this analysis, we want to identify the “moving zeros”, verify they are separated a distance from each other, and observe the shift caused by the dispersion effect.

We will make a bias sweep from -1 to 8 V with a step width of 0.01 V and a fixed RF frequency. We fill the setup's parameters with the same values as in section 2.2.6.6, except for a few changes:

- RF amplitude is set to 0.03 V and RF frequency will be 2GHz.
- The fiber section, when required, will have 80Km of length and a dispersion-per-meter value equal to 17 , which makes a total dispersion of
- The Phase Detector's frequency must be set to the RF frequency (2GHz).

Results

After running these three simulations (DUT with null, positive and negative dispersion, and 2GHz RF frequency), the graphics obtained are shown in figure Y. On the top, we have the result for a non-dispersive DUT simulation. The graphic is a rectified sine function $|\sin(\theta_B)|$, where the amplitude dips (both fixed and moving zeros) are located at $V_b = 0, \pm V_\pi, \pm 2V_\pi, \pm 3V_\pi, \dots$. This behavior is verified in section 3.1, where we concluded that in absence of dispersion (no phase shifts at the sidebands nor at the carrier), the amplitude term will be only composed by the product of two bias-dependent sinusoidal functions:

$$A \cos\left(\frac{\theta_b}{2}\right) \sin\left(\frac{\theta_b}{2}\right) \equiv \frac{A}{2} \sin(\theta_b)$$

Otherwise, the graphic on the center, which corresponds to the DUT with positive dispersion, lets us distinguish the fixed and moving zeros. The first ones, as in the previous simulation, are located at $V_b = \pm V_\pi, \pm 3V_\pi, \pm 5V_\pi \dots$ (odd positions). However, the moving zeros have suffered a certain shift to the left from their reference positions $V_b = 0, \pm 2V_\pi, \pm 4V_\pi, \dots$ (even positions). This shift is due the phases sum term within the sine function argument, as explained in section 3.1. Therefore, the amplitude term results:

$$A \cos\left(\frac{\theta_b}{2}\right) \sin\left(\frac{\varphi^+ + \varphi^-}{2} - \varphi_0 + \frac{\theta_b}{2}\right)$$

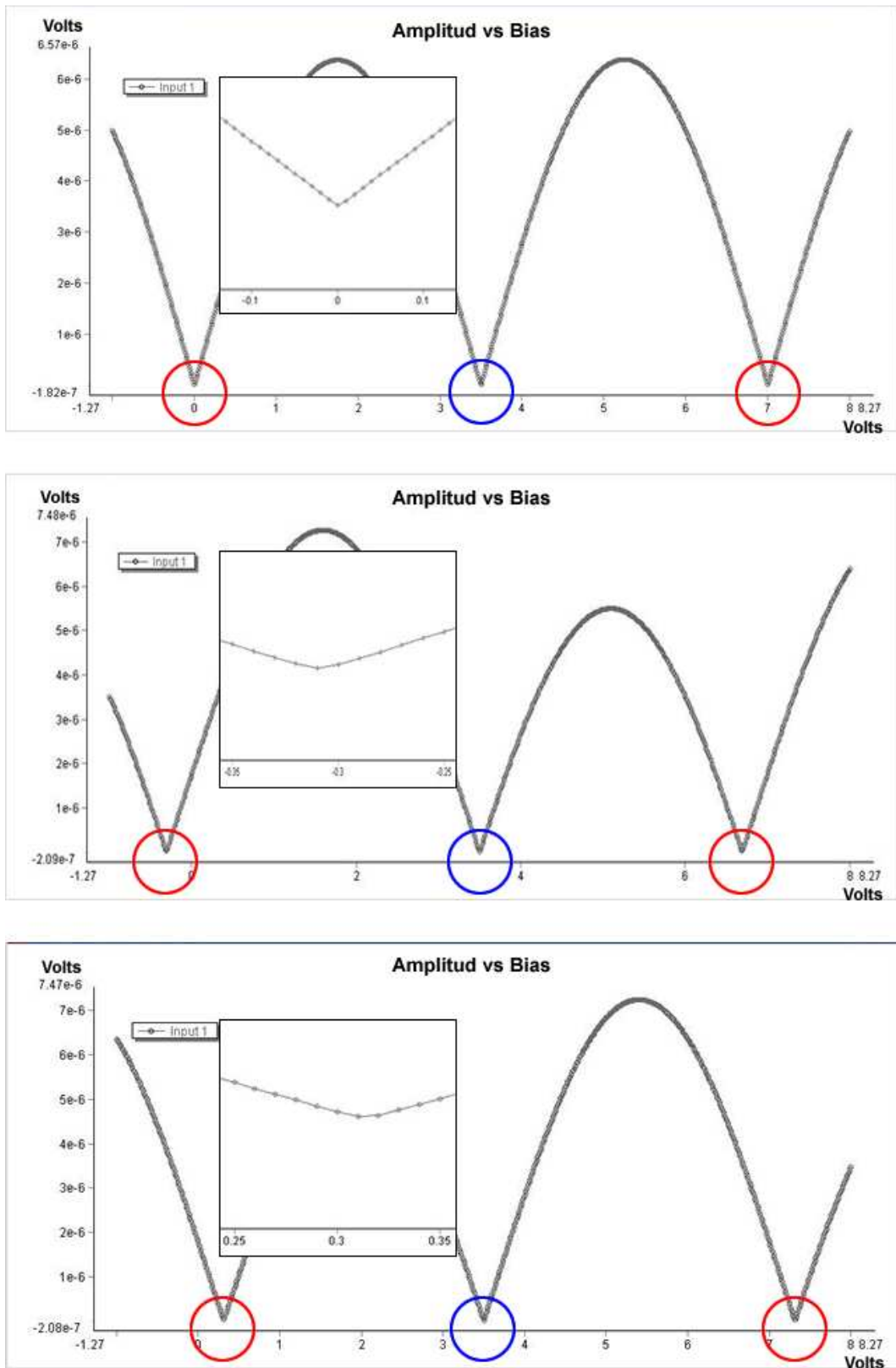


Figure 3.3 Amplitude-vs-Bias graphics for: a. null dispersion (top) b. Positive dispersion (center) c. Negative dispersion (bottom). Fixed zeros in blue, moving zeros in red

Finally, the graphic on the bottom was obtained using a DUT with negative dispersion. Its behavior is similar to the previous case except for the fact that the moving zeros have displaced to the right this time. Therefore, it verifies that expression (40), used for D calculation, contemplates the sign of dispersion.

In general, the moving zeros play an essential part in ABCM, as we only need to identify their locations in the Bias voltage axis and directly replace these values in expression (40) to obtain D .

If we look at the zoomed-in image in Figure 3.3.b, we notice that the shift suffered by the moving zeros is equal to -310 mV. Thus, if we replace this value in expression (40) for $n = 0$, we have:

$$D = \left(\frac{0.31}{3.5}\right) \frac{3 \times 10^8}{2 \times 1559.25^2 \times 4^2}$$

$$D = 1366 \text{ ps/nm}$$

We observe that the dispersion calculated has an error equal to 6 ps/nm (0,44%) with respect to the nominal value, which can be included within the acceptable error range.

We also observe from setup in Figure 3.2 that in all these simulations both the bias voltage and the RF tone are input through the same electrode. Nevertheless, in the mathematical development we verified that it is also possible to apply both signals through different branches, and we will then use expression (40) with the opposite sign.

Figure 3.4 features the Amplitude-vs-Bias graphic obtained for a DUT with positive dispersion using only one electrode. We notice how the moving zeros have suffered a shift of the same magnitude as in the previous case but to the opposite direction. This fact explains the sign change in expression (40).

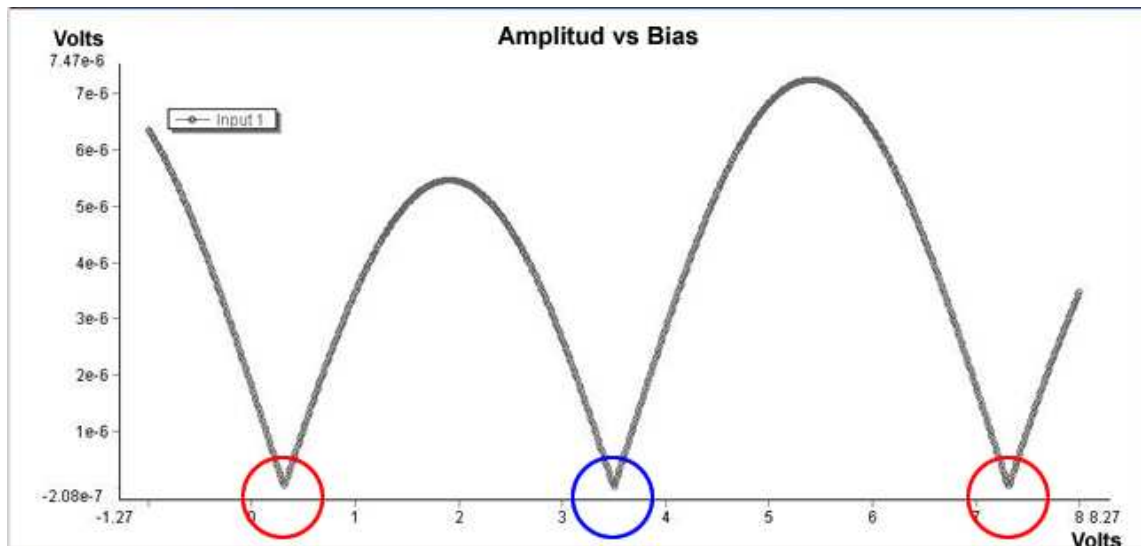


Figure 3.4 Amplitude-vs-Bias graphic for Positive Dispersion inputting Bias and RF tone through different branches. Fixed zeros in blue, moving zeros in red

We ran the same schematic but considering a 6 GHz RF Frequency this time. Figure 3.5 provides the resulting amplitude-vs-bias graphic (we kept the DUT's nominal dispersion equal to 1360 ps/nm).

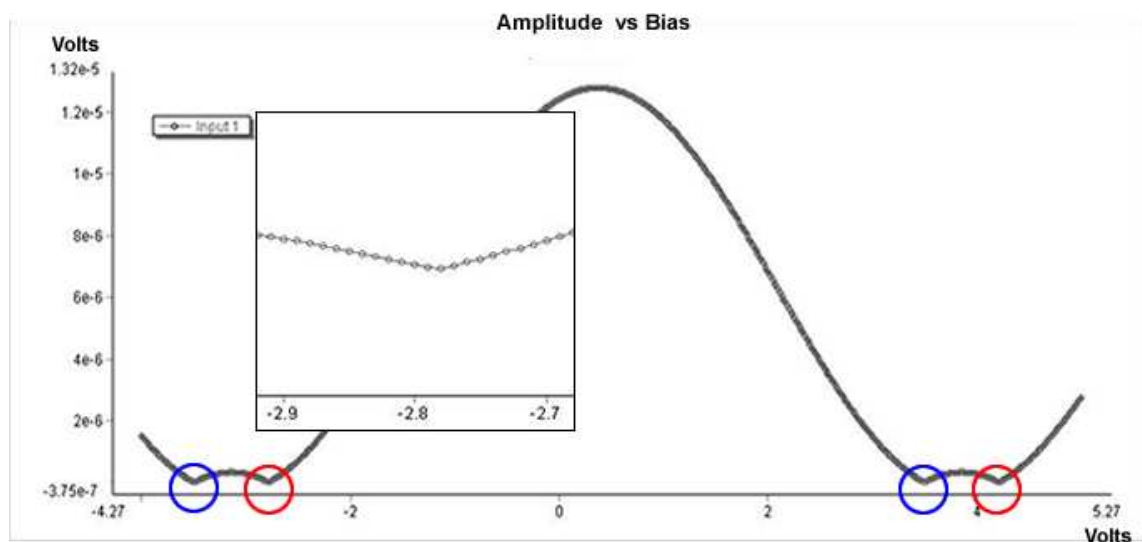


Figure 3.5 Amplitude-vs-Bias graphic for a 1360 ps/nm nominal dispersion with a 6GHz RF frequency. Fixed zeros in blue, moving zeros in red

As it is shown in Figure 3.5, the moving zeros' shift in this case is equal to -2.78 V. Thus, if we replace this value in expression (40) considering the new RF frequency, it results:

$$1361 \text{ ps/nm}$$

Dispersion value obtained in this case approximates better to the nominal dispersion value (1360 ps/nm) as compared to the 2 GHz simulation. This behavior matches with the analysis in section 3.1, where we stated that if we keep the same Bias voltage resolution, value gets closer to the nominal value as we increase RF frequency.

3.2.2 Analysis of the effect caused by the setup's main parameters

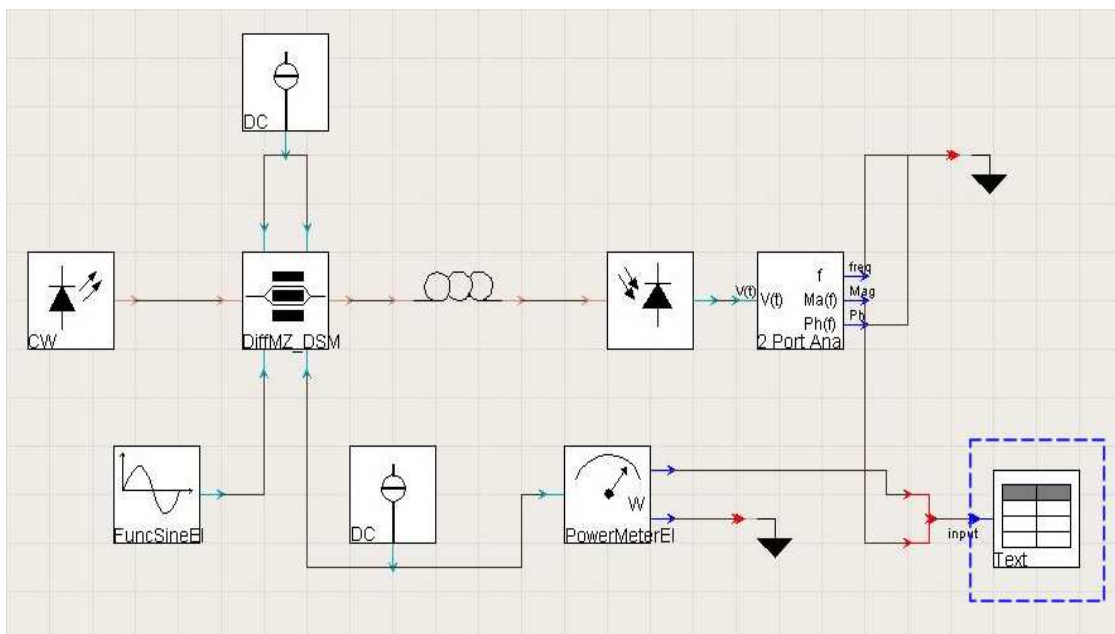


Figure 3.6 VPI setup for ABCM (Second stage). Highlighted with discontinuous line: Text module

In this section, we will run the ABCM while varying some key parameters of the setup in Figure 3.6, to evaluate its performance in different contexts and identify the best operating conditions. For this purpose, we will make use of the bidimensional sweep option provided in VPI's Sweep Control.

The innermost loop will always be the bias voltage sweep from -3.5 to 0 V with a 0.01 V step width, to obtain the “ $n = 0$ ” dip on each run; while the outermost loop will be the studying

parameter sweep, where the start point, stop point and step width will be properly chosen to illustrate the system's behavior in the best way.

A Vi-Text module will save the resulting data using, generating a .txt file output with the bias voltage and amplitude samples. Finally, a MATLAB program will take charge of processing this file to obtain and plot a vector with the chromatic dispersion values for each sample of the analyzed parameter.

3.2.2.1 RF Frequency Sweep

RF frequency is a key parameter in what respects to ABCM accuracy level. We observe in expression (40) that this parameter together with the bias voltage resolution is directly related to the dispersion resolution. Thus, in this analysis, we will prove that the dispersion value calculated will be closer to its nominal value as we increase the RF frequency, considering that bias step width is fixed at 0.01V. We must consider that as we are working with an ideal characterization of dispersion, the Taylor approximation is valid no matter how far we get from the carrier frequency (RF Frequency can be as high as we want).

Therefore, we will need to obtain the zero-amplitude bias for each RF frequency sample, from 200MHz up to 6.2 GHz with a step width equal to 200MHz. This sweep configuration allows us to characterize the method's behavior with good resolution but without increasing too much the processing time.

Results

The results obtained are featured through figures plotted in Matlab. Figure 3.7 shows the relation between the zero-amplitude bias (for $n = 0$) and the RF frequency. We notice how as we expected from the theoretical analysis, expression (39), the curve decreases with frequency following a parabolic behavior (bigger variation for higher frequencies). This fact demonstrates why at the highest frequencies we are able to measure smaller chromatic dispersion values and still achieve a good accuracy levels with moderate bias resolution.

We also observe that for this particular dispersion value, a 6.2GHz RF frequency implies a null-amplitude bias equal to -2.96 V. Thus, since the bias voltage must be kept under 3.5 V to avoid a cross with the fixed zero, the maximum frequency allowed will be just a little further from this value.

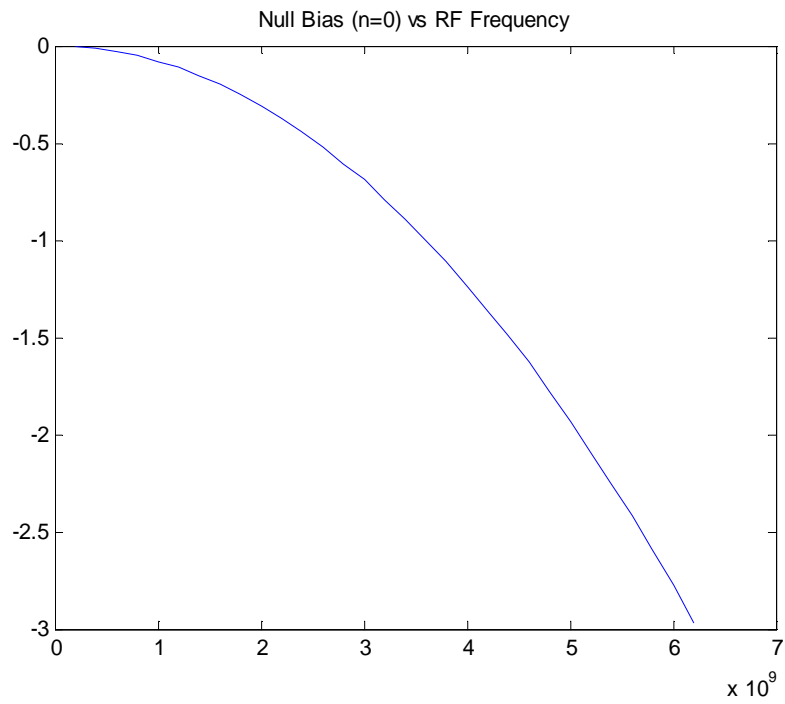


Figure 3.7 Zero-Amplitude Bias-vs-RF Frequency Curve

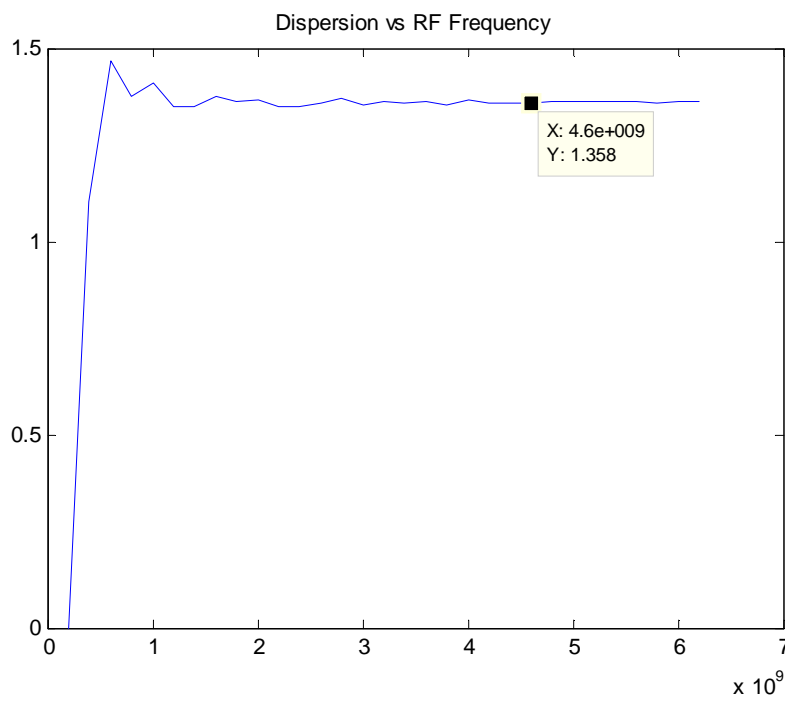


Figure 3.8. Chromatic Dispersion-vs-RF Frequency Curve

Figure 3.8 shows the relation between the RF frequency and the chromatic dispersion for a fixed bias resolution according to expression (40). The graphic starts with a '0' dispersion value for 200MHz, that is, 0 V represents the closest voltage to the zero-amplitude bias, for a step width of 0.01V.

For the next frequency samples, dispersion values obtained differ a lot from the nominal dispersion value (1.36 ps/nm). Thus, if we want this technique to operate at these low frequencies, the bias resolution must be considerably increased.

However, the curve acquires certain stability since approximately 1.4GHz, where the error from the nominal value is kept under 0.02 ps /nm. Although this error is already within the tolerable range, dispersion values keep getting even closer to the nominal value as frequency continues increasing. Thus, we point out another "landmark" at 4.2GHz, where the error observed is kept under 0.003 ps /nm, demarking an almost optimum operating condition.

3.2.2.2 RF Amplitude sweep

The mathematical analysis for RF tone-based chromatic dispersion measurement techniques, states that the optical carrier modulation must be done under small signal condition, that is, the RF tone's amplitude must be small enough to satisfy the approximation in expression (16). Nevertheless, the amplitude level must be kept high enough to face channel noise and devices' insertion loss. In this section we aim at define an upper edge for the tone's amplitude, and determine the effect of over passing it.

In this case the outermost loop will be a RF amplitude sweep from 0.08 V to 2.08 V. The step width will be 0.08V, which means we will have a total of 25 amplitude samples (similar processing load than in previous simulation). Although this number of samples could not be big enough to carry out a good characterization, it is perfectly valid to identify the amplitude tolerable range and measure the error yielded by each sample.

Results

Figure 3.9 shows the null amplitude bias-vs-RF amplitude graphic obtained in this simulation. The curve has a decreasing behavior, experiencing several hops as we increase the amplitude level. We see how the first null-amplitude bias is located at -0.31 V, which matches with the value obtained in previous simulations as well as in the mathematical analysis (considering $D = 1.36$ ps/nm, RF frequency = 2GHz). This bias value represents the longest step in RF amplitude domain, going from 0.08 V to 0.72 V. Therefore, we have just found a valid operation range for this parameter.

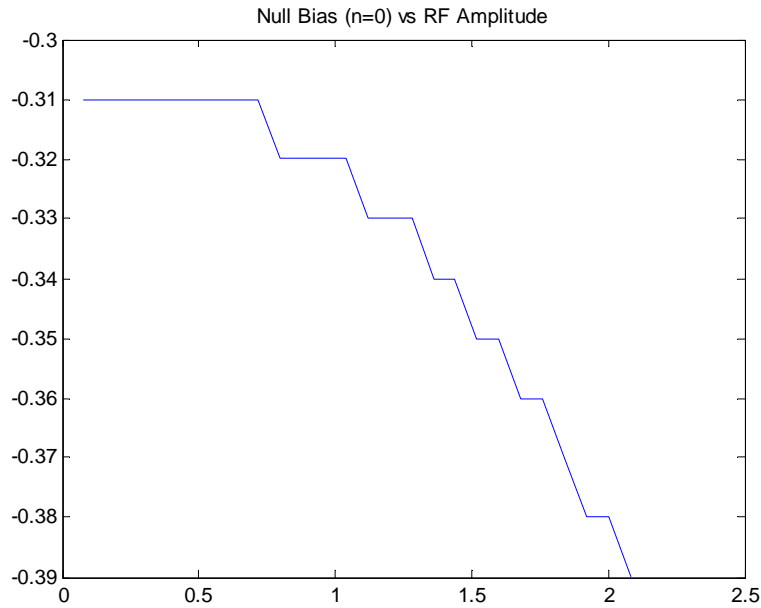


Figure 3.9. Zero-Amplitude Bias-vs-RF Amplitude Curve

The main effect of the hops in Figure 3.9 can be analyzed in Figure 3.10. If we look at the curve's shape we realize of the linear relation between the null amplitude bias and chromatic dispersion coefficient. The dispersion value which corresponds to -0.31 V (first step) is equal to 1.366 ps/nm; that is, a 0.006 ps /nm error (0.44%). Thus, as we expected, this step is within the tolerable range.

The second step, which at 0.8 with a -0.32 V null bias, yields a dispersion of 1.410 ps/nm, that is, a 0.5 ps/NM error (3,67%). This value is a little far away from the nominal dispersion, and for most chromatic dispersion compensating systems it is considered out of the acceptable range. The other steps are completely out of range with values that reach an error near 25% and must be dismissed.

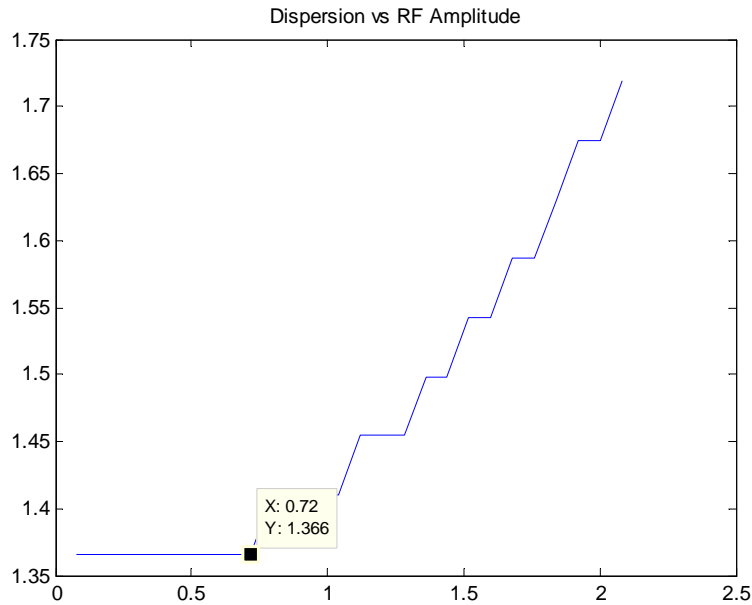


Figure 3.10. Chromatic Dispersion-vs-RF Amplitude Curve

3.2.2.3 Nominal Dispersion Sweep

The final parameter to be studied is the nominal dispersion set on the DUT (a fiber section in this setup). We want to verify that ABCM keeps a good performance, no matter of the amount of dispersion to measure.

Analyzing expression (40), since the RF frequency has a fixed value, the maximum and minimum dispersion values we can measure depend on the maximum (modulator's V_{π}) and minimum (bias step width) values the null amplitude bias can take. However, we observe that if we choose a frequency within the range obtained in section 3.2.2.1 (1.5GHz- 6GHz), even if we set an extremely low or high dispersion value, the bias voltage required will be totally reachable. Therefore, this analysis will not focus on finding edges for the amount of dispersion, but on studying the nominal dispersion's relation with bias resolution.

In this case the outermost loop of the bidimensional sweep should be the DUT's total dispersion. Nevertheless, unlike previous simulations, here we cannot handle directly the chromatic dispersion as an independent parameter. The dispersion parameter is defined by the product of the fiber's length and the dispersion slope value. We have to choose one of these two parameters to be swept and the other one must be kept fixed. Thus, in order to simulate a real optical environment we decided to sweep the fiber's length from 0 to 160 000 meters with a step width of 5000 meters.

Results

The curve in figure 3.11 features the expected linear relation between dispersion value and null-amplitude bias along the whole range. This behavior is also exposed in Figure 3.12 relating dispersion calculated with its nominal value. However, we realize that the curve has a slope scarcely over 1, and we can identify two “drop points” located at 0.68 and 1.87 approximately.

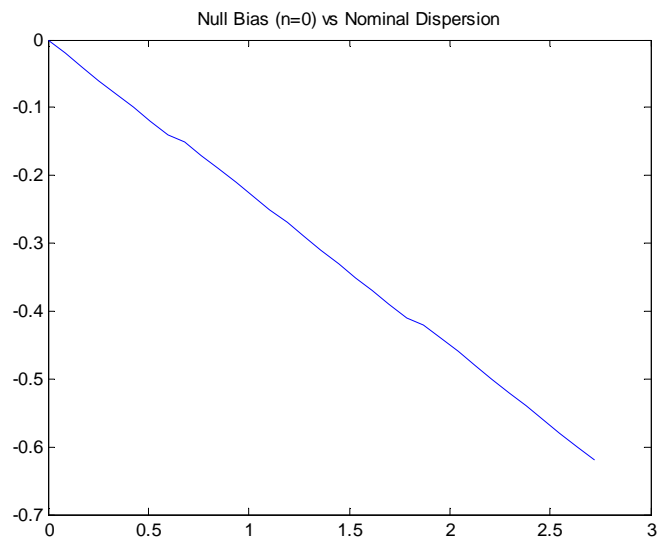


Figure 3.11 Zero-Amplitude Bias-vs-Nominal Dispersion Curve

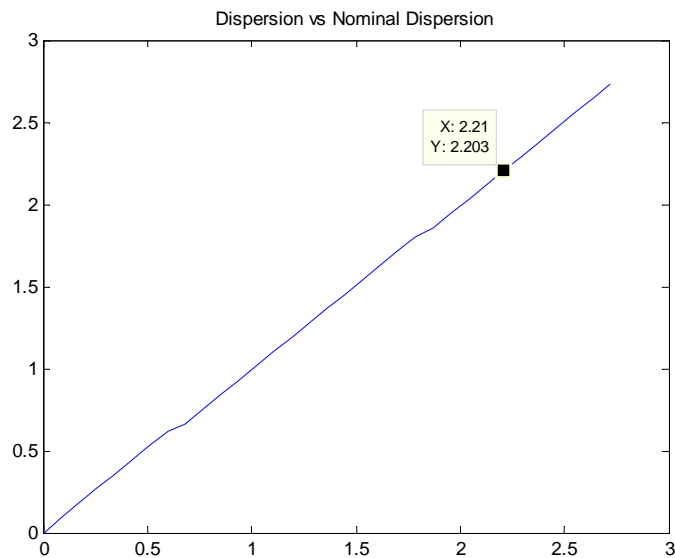


Figure 3.12 Chromatic Dispersion-vs-Nominal Dispersion Curve

To give an explanation to the special features highlighted above, we must focus on the bias voltage resolution and evaluate its effect on the dispersion calculation replacing it in expression (40).

If we consider that the bias samples are separated 0.01V, we know that the maximum error contemplated in the bias measurement will be of 0.005 V, which means a 0.022 ps/nm error. This value is exactly the highest difference observed in the graphic between the dispersion calculated and its nominal value, that is, the dispersion value calculated is rounded up until it overpasses this limit (at the drop points) where it is rounded down and so on.

Therefore, this analysis verifies the fact that there is no other issue with the nominal dispersion additional to the error related with the bias resolution. Moreover, this error itself is not a big inconvenience for calculations, as it is kept within a tolerable range (+- 0.022 ps/nm).

3.3 Experiments

3.3.1 Laboratory Equipment

Next we will describe the devices used in ABCM's setup

3.3.1.1 Optical and Electrical Sources

3.3.1.1.1 Laser New Focus 6427

This device (Figure 3.13) will be the light source to carry out chromatic dispersion measurement in ABCM. It is a tunable laser and it also features control of the output power up to 7 dBm. It can be connected to a PC through a GPIB port, so that its parameters can be controlled remotely, which will not be necessary in this experiment as we work on a fixed optical frequency.



Figure 3.13 Laser New Focus 6427

The most relevant technical features of New Focus 6427 are shown in Table 3.1.

Laser NEW FOCUS 6427	
Optical BW	1520 - 1570 nm
Optical Power	-3 - 7 dBm
Connetor Type	FC/APC

Table 3.1. NEW FOCUS 6427 Features.

3.3.1.1.2 Programmable DC Source PROMAX FA-851

This instrument (Figure 3.14) will provide the DC voltage to be inserted in the modulator as the bias voltage. It will be connected to the PC through its RS-232 port, so that a Matlab program will automatically set the bias voltage to be inserted into the modulator along the whole bias sweep. This procedure will be required for both the Transfer function and ABCM.

In addition, since it has 3 power supply outputs available, it will also feed up the O/E detector.



Figure 3.14 FA-851

3.3.1.2 Optical devices

3.3.1.2.1 Modulator FUJITSU FTM7921ER/052 H74M-5208-062

Fujitsu FTM7921ER/052 H74M-5208-062 (Figure 3.15) is a dual drive modulator which has an input for each of its two interferometric branches. In this experiment we will work on the modulator's asymmetric configuration, that is, we will apply the bias voltage and the RF signal through the same input while the other one stays in open circuit.

This modulator disposes of two arms with SMA adapters which are bind to the electrodes through a GPO connector. We will only use one of them, so the bias voltage and the RF signal will be inserted together through a bias-tee. Since the electro-optical effect by which the light gets modulated in the MZ modulator is polarization dependent, the input fiber to the Fujitsu modulator is polarization maintaining (PM), meaning it only allows the propagation of one specific light polarization, so that we will require a polarization controller in order to minimize the insertion loss.

Since standard fiber presents a cylindrical symmetry, the light beam can be polarized on any direction perpendicular to its axis. Thus, some devices include a polarization preserver fiber with cylindrical section at the input, so that light's polarization follows a determined fixed direction. In fact, this preserver fiber will reduce or suppress the light component with polarization in the perpendicular direction. This fact implies a power loss if the input polarization doesn't match with preserver fiber polarization.



Figure 3.15 FUJITSU FTM7921ER/052 H74M-5208-062

The most relevant technical features of this modulator can be observed in table 3.2.

FUJITSU FTM7921ER/052 H74M-5208-062 Modulator	
Optical BW	1530 - 1608 nm
Electrical BW	8.5 GHz
Electrode Impedance	50 Ω
Insertion Loss (IL)	6 - 7 dB (según banda)
$V_{\pi} (V_{\max} - V_{\min})$	4 V
Optical connectors type	FC/UPC

Table 3.2. FUJITSU FTM7921ER/052 H74M-5208-062 features.

3.3.1.2.2 Polarization Controller

In Fujitsu Modulator description we explained why a polarization controller is required to make the light at the input acquire a polarization very similar to the one of the PM fiber.

In this setup our polarization control will be based on applying mechanic deformations to the standard fiber, as it is shown on Figure 3.16. As seen, the optical fiber coils up around each of three mobile parts with 180° rotation capability. As obtained in ..., we will have to twirl the fiber twice at the mobile parts on the extremes and four times at the one on the center.



Figure 3.16. Polarization Controller

3.3.1.3 Passive Devices

3.3.1.3.1 Bias-tee

This device (Figure 3.17) is required to insert both RF signal and bias voltage through the same modulator's arm. It is just a kind of multiplexor which has 3 ports organized in a T distribution, so that the RF signal (which can go from 45 MHz to 26.5 GHz) and the bias voltage are entered through two different SMA connectors and get out together through an only one output connected to the modulator.

In conclusion, the bias tee lets us multiplex two electrical signals in the same cable, one in Radiofrequency and the other in DC.



Figure 3.17. Bias tee

3.3.1.3.2 Optical detector Agère

This device (Figure 3.18) takes charge of transforming optical power received into an electrical current. In this process the carrier wave of the signal at the output of MZ modulator will be cancelled out and we will just keep the modulating wave. The detector's output is connected to the Network Analyzer to measure the amplitude required for ABCM.

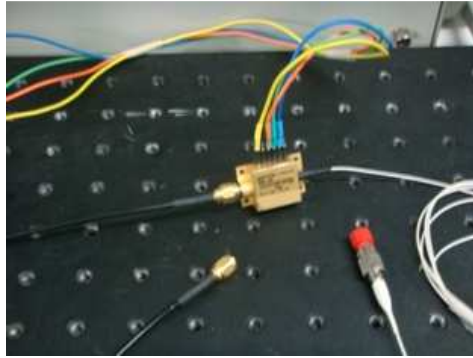


Figure 3.18. AGERE Systems 2860E

The most relevant features of AGERE Systems 2860E are shown in table 3.3.

Optical Detector OC-192/STM-64	
Optical BW	1280 - 1580 nm
Optical BW	30 KHz-9 GHz
Vcc (Power supply)	8 V

Table 3.3. AGERE Systems 2860E features

3.3.1.4 Devices under test (DUTs)

3.3.1.4.1 Fiber Brag Grating PIRELLI CDC-04074

Fiber Brag Grating Pirelli (Figure 3.19) is designed to compensate for the amount of dispersion that 80 km of fiber would yield. These 80 Km are verified considering the device presents a 1252.35 ps/nm total dispersion and under third window we estimate a 16ps/nm·km dispersion slope.

$$l_{FIBER} = \frac{1252.35 \text{ ps/nm}}{16 \text{ ps/(nm}\cdot\text{km)}} = 78,27 \approx 80 \text{ Km}$$

Since this is a dispersion compensating device, the sign of dispersion will be opposite to that in the fiber.

This is a narrow band device as we can observe in the specifications (table 3.9). Nevertheless, since the laser New Focus 6427 has a tunable frequency set containing the FBG's operating band, we will just have to adjust the laser output wavelength to the FBG band.



Figure 3.19. PIRELLI CDC-04074

The most relevant features of the device are shown in table 3.4.

Pirelli CDC-04074	
Optical BW	1557.27 - 1561.19 nm
Nominal Dispersion	1252.35 ps/nm
Insertion Loss	6.18 dB
Connector Type	FC/UPC

Table 3.4. CDC-04074 features

3.3.1.4.2 Chromatic Dispersion Compensating Fiber

This is a very special type of fiber with much more dispersion than standard fiber and with the opposite sign.

Unlike Pirelli FBG, the own fiber acts as the source of dispersion, thus, it has no restriction about optical bandwidth. It has FC/APC connector at both extremes; this is why we will need adapter fiber sections in between to connect it to the modulator in one extreme and to the optical detector in the other, since they both have UPC connectors.

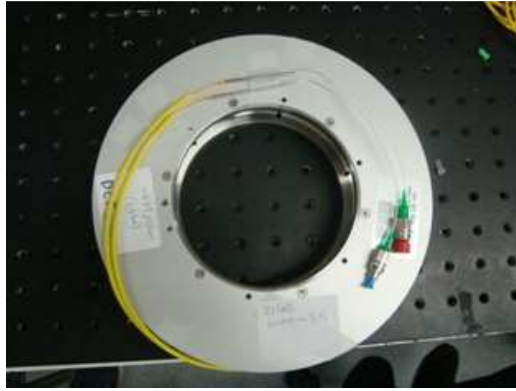


Figure 3.20 Chromatic Dispersion Compensating Fiber

The most relevant features of this device are shown in table 3.5.

Dispersion Compensating Fiber	
Nominal Dispersion	671 ps/nm
Insertion Loss (1575 nm)	5.15 dB
Connector Type	FC/APC

Table 3.5. Dispersion Compensating Fiber features

3.3.1.5 Measurement Devices

3.3.1.5.1 Network Analyzer HP 8753D

For the setup in this experiment we need a Network Analyzer. We will use a HP 8753D model (Figure 3.21). This device will let us carry out dispersion measurements required for ABCM.

Besides taking charge of measurements, HP 8753D will be useful as a RF signal supplier through its port 2, and will be able to adjust its power and frequency. Therefore, binding in mind that the RF signal is obtained from port 1 and the output signal of the setup is inserted through port 2, we will work with parameter S21 in amplitude mode.



Figure 3.21 HP 8753D

The most relevant features of the Network Analyzer as both measurer and signal generator are shown in tables 3.6 and 3.7 respectively.

Network Analyzer HP 8753D (measurer)	
BW	30 KHz - 6 GHz
Maximum input power	10 dBm
Connectors type	N

Table 3.6. HP 8753D measurer features

Network Analyzer HP 8753D (Signal Generator)	
BW	30 KHz - 6 GHz
Maximum output power	10 dBm
Mínimum output power	- 15dBm
Connectors type	N

Table 3.7. HP 8753D signal generator features

3.3.1.5.2 Optical Multimeter HP 8153A

This device (Figure 3.22) is used specifically to make power measurements. This procedure is very important for instance to obtain Transfer Functions and to detect bad connections or dirty or damaged fibers in our setups.

It has a GPIB port, so it can be connected to a PC and be controlled automatically through a Matlab program.

This device, if configured in RMT (remote) mode, can be used together with another instrument to carry out Transfer Functions in an automatic way, all controlled by a very simple Matlab code.



Figure 3.22 HP 8153A

This device has an analog output through a BNC connector. This output is used by the multimeter to provide an output signal between 0 and 2 volts in relation to the received optical signal.

The most relevant technical features of HP 8153A for our own application are shown in table 3.8.

Multimeter HP 8153A	
Optical BW	450 - 1700 nm
Supported Error	$\pm 2.2\%$
Power margin	-110 - 27 dBm
Connector type	SC/UPC

Table 3.8. HP 8153A features.

3.3.2 Experimental Transfer Function

3.3.2.1 Setup

To obtain the transfer function of the Mach-Zehnder Modulator used in this experiment we need to deploy the setup shown in Figure 3.23.

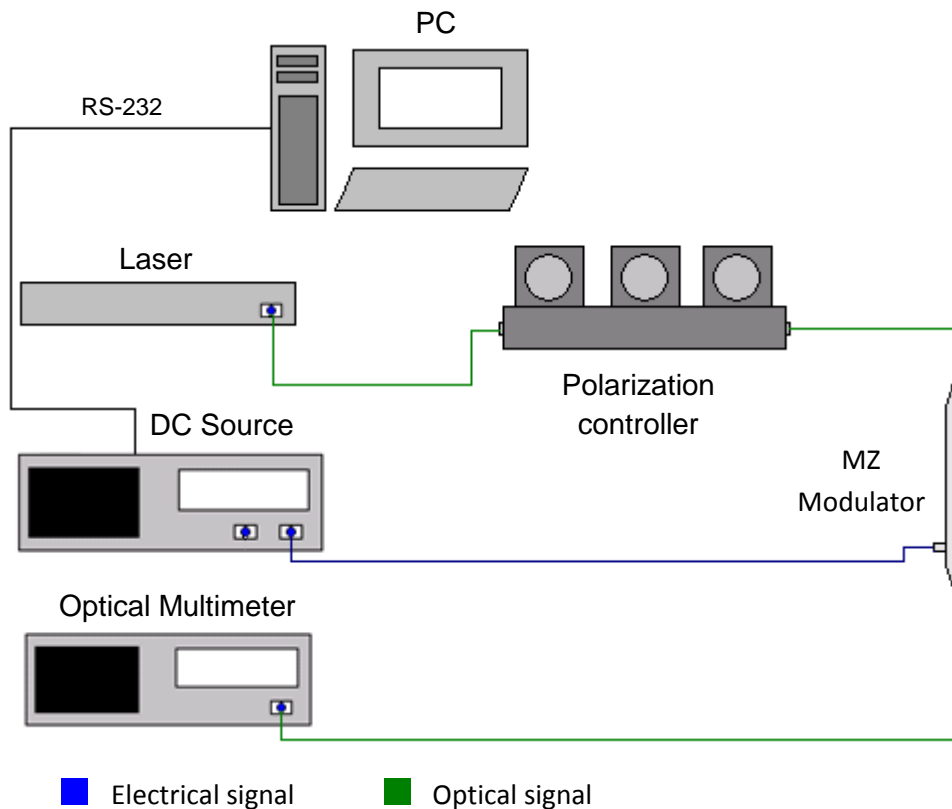


Figure 3.23 Experimental Transfer Function setup

As we can see in Figure 3.23, first we must connect the modulator's optical input to the laser source, its output to the optical multimeter, and finally its electrical input to the DC source.

We must take into account that the modulator's output connector is a FC/UPC, while the measurer's input is a SC/UPC. Thus, we will need a fiber section in between with a FC/UPC connector in one extreme and a SC/UPC in the other.

To carry out the transfer function, we will execute a matlab program, through which will ask the user for the start bias voltage, the end bias voltage and the step width.

This program will automatically activate the DC source (since it is connected to the PC through its RS-232 port) and it will vary its voltage periodically. At the same time, the optical multimeter will be capturing the measures.

If we want this procedure to be reliable, the code must be programmed in a way such that the multimeter carries out several (in our case we set it to 3) measurements for each bias voltage sample and then obtains the mean of them.

The power measures obtained will be sent to the PC through GPIB port to make all the necessary calculations.

Finally, the matlab program will feature the results obtained on a power-vs-bias graphic, and it will save the data in a .txt file.

Next section is an example of a transfer function following this procedure.

3.3.2.2 Transfer Function for FUJITSU Modulator

It is important to bind in mind that this is a dual drive modulator, that is, it has two electrical input connectors. Since in this case we will use the modulator in its asymmetric configuration and the signal phase will not be varied at one branch, we will keep one connector in short circuit, and on the other we will insert the DC voltage to carry out the bias sweep.

Here we show the final Transfer Function obtained (including the polarization controller) (see Figure 3.24).

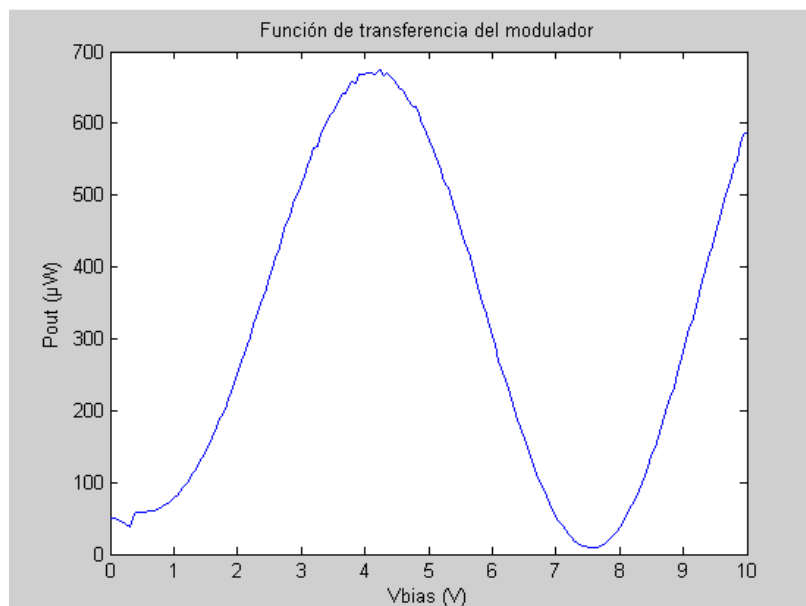


Figure 3.24 FUJITSU FTM7921ER/052 H74M-5208-062

FUJITSU Experimental Features	
V_{π} ($V_{max} - V_{min}$)	$7,6 - 4,23 = 3,37$ V
QP ($(V_{max} - V_{min})/2$)	1,685 V
ER	19 dB

Table 3.9 FUJITSU Experimental features.

3.3.3 ABCM Experiment

3.3.3.1 General description

To carry out the laboratory experiment for ABCM - SC we will design a setup based on the one in Figure 3.2, adapting it to a real environment with the equipment available. The setup is shown in Figure 3.25.

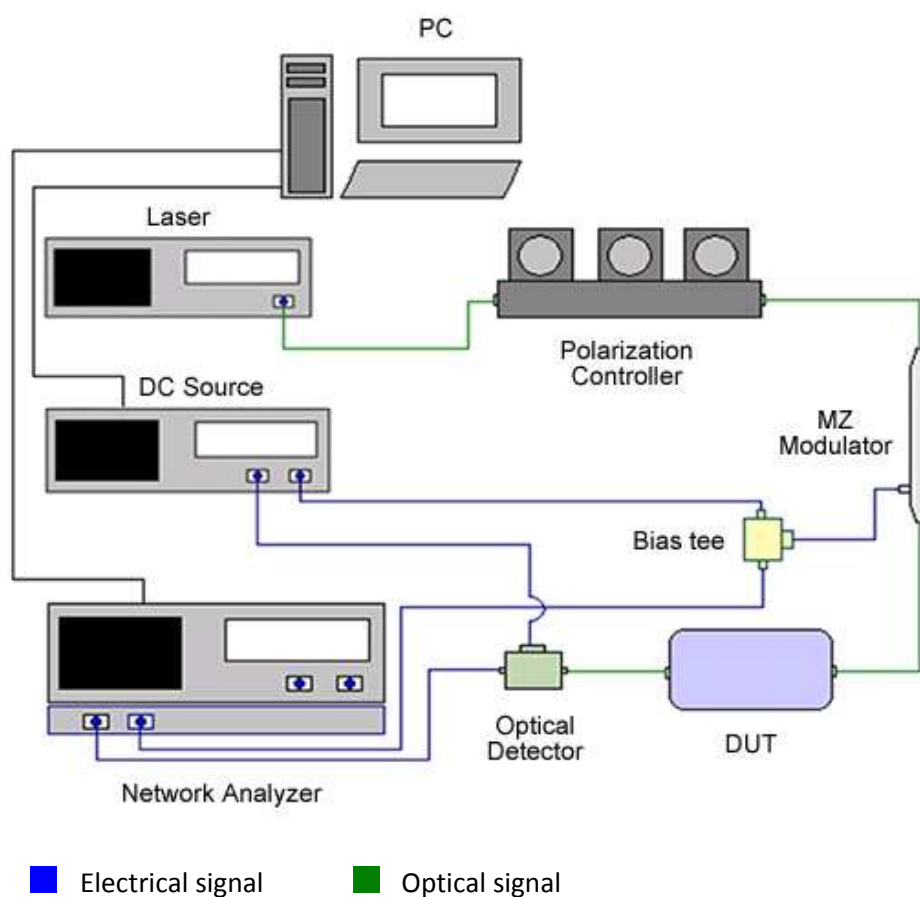


Figure 3.25 ABCM Experimental Setup

We observe from Figure 3.25 that the automatic sweeps and measurements required are controlled by a PC via GPIB and RS 232 connections with the Network Analyzer and DC Source respectively. The software responsible of directing the process is a Matlab program which asks the user for the bias start and end voltages, and the step width.

Once the sweep is correctly set, the DC Source starts supplying the modulator with the corresponding voltage. After a few seconds the Analyzer is ordered to capture the amplitude measures (dB). There will be three measures for each voltage sample, so that the Matlab program will obtain the mean of the three values. This process will be repeated until the DC source arrives to the end voltage indicated.

As we already mentioned, the DUTs used in these experiments will be a Fiber Bragg Grating (FBG) and a Dispersion Compensating Fiber (DCF).

Before we start with the measurements, we must obtain the modulator's Transfer Function. As we know from ABCM mathematical analysis (expression 39), in absence of dispersion the moving zeros are located at V_{pi} odd factors (0, $2V_{pi}$, $4V_{pi}$, ...). Thus, the bias sweep must go at least from 0 to $3V_{pi}$ in order to visualize two fixed zeros and one moving zero; this last one will help us to calculate dispersion.

Since we want to perceive the moving zeros displacement, first we must carry out a measurement without the DUT, that is, calibrate the system to obtain the positional reference for the moving zeros (Figure 3.26).

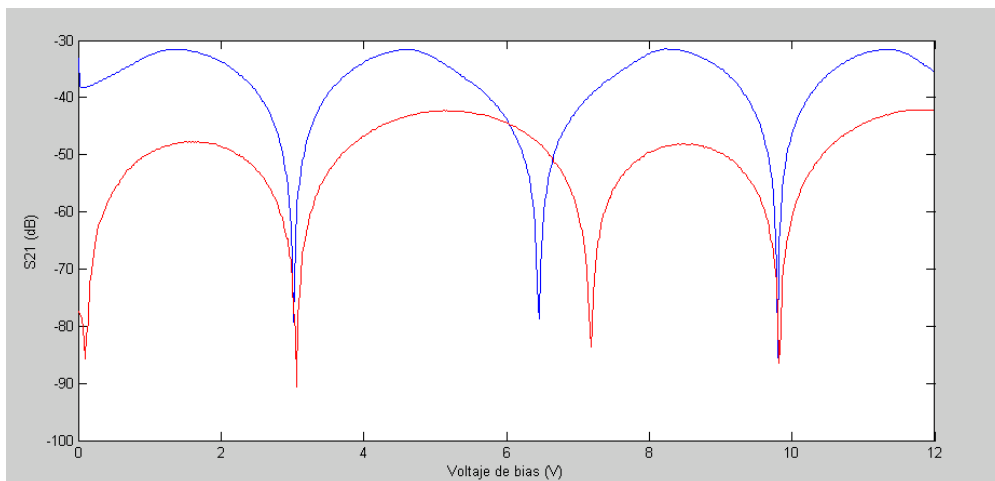


Figure 3.26 Moving Zeros Displacement. Blue: without the DUT. Red: with the DUT.

Once we obtain the displacement, in order to calculate the chromatic dispersion we will have to equal the sine argument to π multiples (where the zeros take place). Since our reference is the case where no dispersion is present, we will carry out the following calculations to obtain the dispersion value:

- Sine argument without the DUT: $\frac{\theta_{b1}}{2} = n\pi$
- Sine argument with the DUT: $\frac{D\pi\lambda_0^2 f_m^2}{c} + \frac{\theta_{b2}}{2} = n\pi$

The difference in bias phase is:

$$\Delta\theta_b = -\frac{D2\pi\lambda_0^2 f_m^2}{c}$$

From where dispersion is:

$$D = -\frac{c \cdot (V_{b2} - V_{b1})}{2V_\pi \lambda_0^2 f_m^2}$$

where $V_2 - V_1$ is the moving zeros' displacement.

An alternative way to calculate dispersion would be just focusing on the case with DUT and obtain the displacement of a moving zero with respect to a fixed zero. Since this distance is equal to V_π in absence of dispersion, we can make the following calculation:

$$V_{moving} - V_{fixed} = V_\pi + \Delta V_b \rightarrow \Delta V_b = V_{moving} - V_{fixed} - V_\pi$$

Once the moving zero displacement value is obtained we just need to replace it on expression (40) as in the previous case:

$$D = -\frac{c \cdot \Delta V_b}{2V_\pi \lambda_0^2 f_m^2}$$

3.3.3.2 Setup characterization

As it was explained in VPI simulation section, there is a strong trade off RF signal power (amplitude) and frequency election.

RF frequency choice: We already highlighted the zeros displacement dependence with the modulating frequency (RF), as if this frequency is too low the displacements yielded would be insignificant. Moreover, we must take into account that the measurement equipment has a certain resolution and error margin, which can generate small errors in measurements. In this specific case, these errors are expressed in small displacements of the zeros, thus, if RF frequency is too low, the small displacements yielded could be confused with those measurement imperfections mentioned.

On the other hand, we know that if the RF frequency is too high the moving zeros displacement could be so big that they could overlap or overpass the fixed zeros locations. Another restriction for the upper edge of the frequency is the fact that Taylor approximation used in the mathematical analysis loses validity as the bands get further from the carrier.

Therefore, if we use as reference the RF frequency interval obtained for the simulation analysis and we test it on our laboratory setup, we determined that the best possible value to carry out the measurements is 3 GHz.

RF power choice: As it was also explained in the mathematical and simulation analysis, the RF power (amplitude) must be low enough to respect the small signal condition. That amplitude level in power terms is around -5 dBm, which is the value we will use in the experiments.

Now, for the choice of the **frequency and power of the optical source** (laser) we must just focus on restrictions imposed by the devices to be measured (DUTs). In the case of the laser frequency must be set to 1559 nm, as that is the central frequency of the FBG's narrow bandwidth.

For the optical source, as we can see in table 3.10, the power value used depends on the DUT we want to work with.

Optical Signal Power values	
FBG	3 dBm
Compensating Fiber	5 dBm

Table 3.10 Optical Power values

These different power values are due to the different connectors on the DUTs. In the case of FBG, the input is directly connected to the modulator's output as both devices have FC/UPC connectors, and the same thing happens at the output, which can be directly connected to the detector.

Otherwise, if we use the DCF as our DUT, we must put two fiber sections in between, one at the input and the other at the output. Both fibers must have one FC/APC extreme and the other FC/UPC, so that we can connect the modulator's output (FC/UPC) with the DCF's input (FC/APC), and in the same way, DCF's output (FC/APC) with detector's input (FC/UPC). These fiber sections yield an increment in power loss due to its connectors. Therefore, we have 2 additional connectors with respect to the FBG case, so, if we estimate 0.6 dB for each connector, it results on a 1.2 dB total loss increment, despite of the 0.5 extra insertion loss of the DCF with respect to the FBG.. This is why for DCF use 2 dB extra power in the optical source.

Another important parameter to be determined to carry out measurements with ABCM is the maximum allowed Bias step width. This value is conditioned by the minimum dispersion value

we expect to measure, in this case it is 671ps/nm corresponding to the Fiber section; and also it depends on RF frequency set (3GHz). Thus, the maximum step width allowed for the bias sweep is obtained as follows:

$$D = -\frac{c \cdot (V_{b2} - V_{b1})}{2V_{\pi} \lambda_0^2 f_m^2}; \quad -\frac{D \cdot 2V_{\pi} \lambda_0^2 f_m^2}{c} = (V_{b2} - V_{b1})$$

$$(V_{b2} - V_{b1}) = -\frac{671 \cdot 2 \cdot 3,37 \cdot (1559 \times 10^{-9})^2 (3 \times 10^9)^2}{3 \times 10^8};$$

$$(V_{b2} - V_{b1}) = 329,75mV$$

Once we found the maximum bias step width we can use, we proceed to choose a proper value for this parameter considering a certain security margin; therefore we choose a step width of 200mV. This value is five times bigger than the step width set for the simulations, however, it still provides good accuracy in measurements.

One final consideration about the equipment is related to the Dual drive Mach-Zehnder Modulator available. This Modulator has one positive input and also a negative one, so that if we insert both the RF signal and the bias voltage through the positive input, we will obtain a positive phase shift, otherwise, if we use the negative input we will have a negative phase shift.

In this particular method, this above feature implies that in Figure 42 the moving zeros will suffer a displacement to the x axis positive or negative direction if we use the positive or negative input respectively.

3.3.3.3 Results

3.3.3.3.1 Results obtained with the FBG

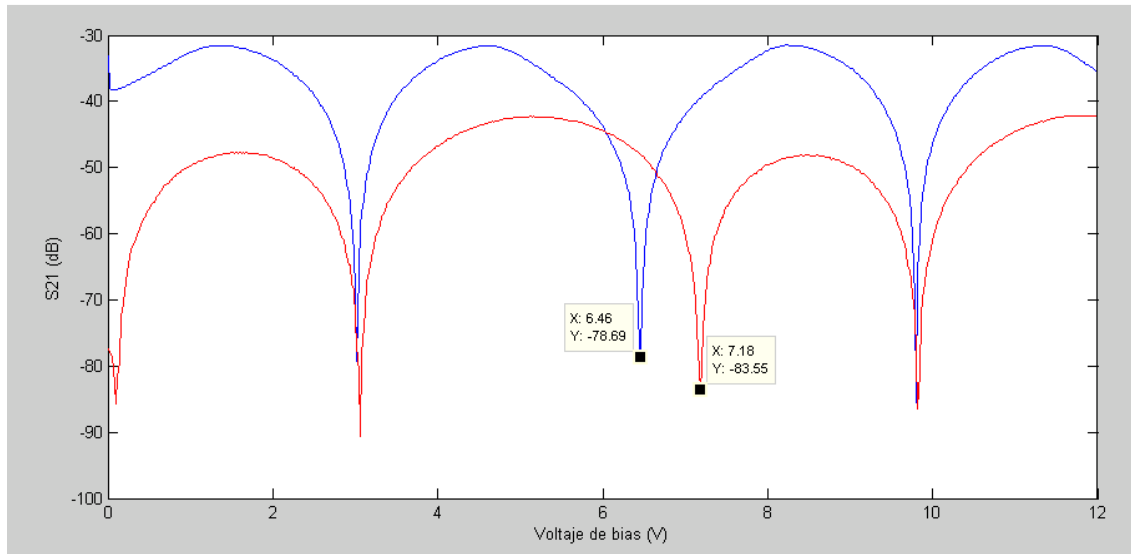


Figure 3.27 ABCM measures obtained for FBG

As we can see in Figure 3.27, there is a significant displacement of the moving zeros but also a small displacement of the fixed zeros about 0.01 from its natural location. This can be attributed to some bias drift of the modulator, so we will consider this value as a calibration reference to calculate the moving zero exact displacement.

$$(V_{b2} - V_{b1}) = (7,18 - 6,46) - 0,1 = 0,62V$$

Once we have the real displacement of the moving zeros we just need to apply expression (40) to calculate chromatic dispersion. Thus, considering V_{π} value obtained in FUJITSU modulator Transfer function of section 3.3.2.2, we have:

$$D = -\frac{c \cdot (V_{b2} - V_{b1})}{2V_{\pi} \lambda_0^2 f_m^2} = \frac{3 \times 10^8 \cdot 0,62}{2 \cdot 3,37 (1559 \times 10^{-9})^2 (3 \times 10^9)^2} = -1,26159 ns/nm = -1261,59 ps/nm$$

Measured Dispersion vs Nominal Dispersion	
Measured value	- 1261,59 ps/nm
Nominal value	- 1252,35 ps/nm

Table 3.11 Measured Dispersion vs Nominal Dispersion for FBG

3.3.3.3.2 Results obtained with the DCF

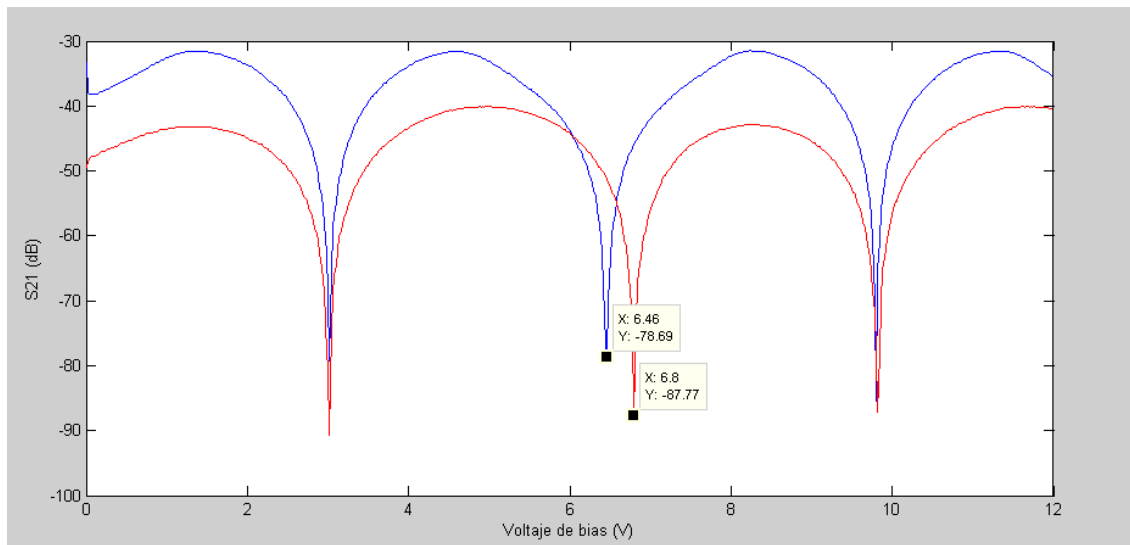


Figure 3.28 ABCM measures obtained for DCF

In this case, as we notice in Figure 3.28, there is no displacement for the fixed zeros, that is, no calibration is required this time. Therefore, the calculation corresponding to chromatic dispersion final expression is as follows:

$$D = -\frac{c \cdot (V_{b2} - V_{b1})}{2V_{\pi} \lambda_0^2 f_m^2} = \frac{3 \times 10^8 (6,8 - 6,46)}{2 \cdot 3,37 (1559 \times 10^{-9})^2 (3 \times 10^9)^2} = -0,69184 ns / nm = -691,84 ps / nm$$

Measured Dispersion vs Nominal Dispersion	
Measured value	- 691,84 ps/nm
Nominal value	- 671ps/nm

Table 3.12 Measured Dispersion vs Nominal Dispersion for DCF

As we can observe in tables 3.11 and 3.12, the dispersion values obtained are very close to their nominal values; that is, both measurements were carried out with the expected accuracy.

4. ASYMMETRIC MODULATION BIAS-CONTROLLED METHOD - SUPPRESSED CARRIER (PROOF OF CONCEPT)

4.1 Description and Mathematical Analysis

Even though the ABCM exposes the general concept of this PFC, its usage is devoted to laboratory tests, due to the unavoidable carrier alteration (altering data detection) yielded when we carry out the bias voltage sweep. Thus, if we want to implement a high-accuracy dispersion monitoring system and apply it in an optical communication network without altering the data recovery, the setup must be redesigned.

Therefore, in this chapter we present a new approach for on-line chromatic dispersion monitoring but still based on RF tone addition. The tone's amplitude must be such that in the resulting modulated signal the carrier gets cancelled (carrier suppression), so that it does not interfere with the intensity modulated optical carrier (data stream) when both signals are combined.

Once again the bias voltage sweep applied together with the RF tone takes charge of changing the optical phase shift between the RF bands and the carrier, so that at the monitoring point the voltage difference between the zero-amplitude bias corresponding to the RF frequency and to its second harmonic can be used to calculate dispersion coefficient.

Operating principle

The basic scheme of ABCM - SC is shown in Figure 4.1. At the emitter side the output from a laser source is split into two branches. At the upper branch the optical carrier is intensity modulated by the data, while at the other branch the optical signal passes through a phase modulator controlled by the RF tone and the DC voltage signal $V_B(t)$ going at a constant slow time rate from $-V_\pi$ to V_π (at least), where V_π is the modulator's half wave voltage.

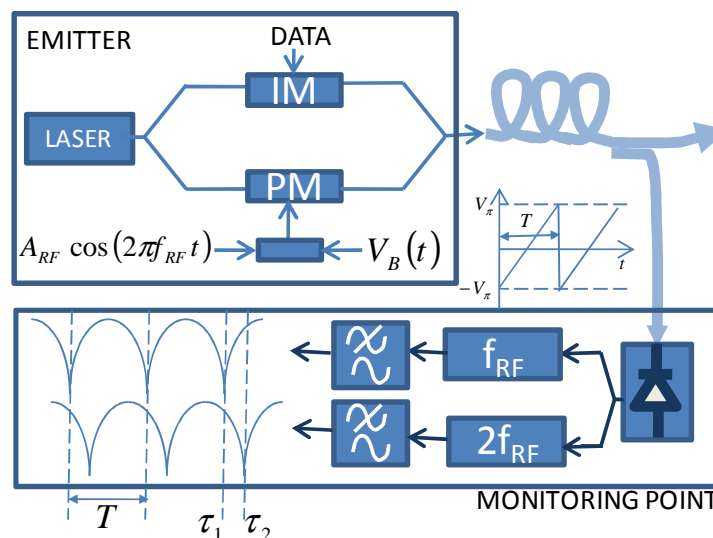


Figure 4.1 General schematic for Dispersion Monitoring System

We mentioned that in this PFC we will strictly focus on verifying the method's mathematical basis and evaluating its performance in terms of accuracy and stability. Therefore, to simplify the study, no intensity-modulated data will be considered at the upper branch (optical signal passes unaltered).

The phase modulated optical signal at the lower branch is expressed as follows:

$$E_{out} = E_{in} e^{j\theta_b} e^{j\theta_{RF}} \quad (41)$$

where $\theta_b = \frac{\pi V_b}{V_\pi}$ and $\theta_{RF} = \frac{\pi V_{RF}}{V_\pi}$.

Since we want to cancel out the carrier component at the lower branch, in this case we will not work under a small signal condition, but we will use the Bessel functions expansion to find out the proper RF tone amplitude.

Using again low-pass equivalent expressions we have:

$$E_{out} = \frac{A_0}{2} \text{Re} [e^{j\theta_b} e^{j\theta_{RF}}] \quad (42)$$

$$E_{out} = \frac{A_0}{2} \text{Re} [e^{j\theta_b} e^{jm \cos(\omega_m t)}] \quad (43)$$

where m is the modulation index. So if we make use of the Jacobi-Anger identity:

$$e^{jz \cos \phi} = \sum_{n=-\infty}^{\infty} j^n J_n(z) e^{jn\phi} \quad (44)$$

and we express the RF-dependent exponential term considering it up to 2^o order, we obtain:

$$E_{out} = \frac{A_0}{2} \text{Re} [e^{j\theta_b} (J_0(m) + jJ_1(m)e^{j\omega_m t} + jJ_1(m)e^{-j\omega_m t} - jJ_2(m)e^{j2\omega_m t} - jJ_2(m)e^{-j2\omega_m t})] \quad (45)$$

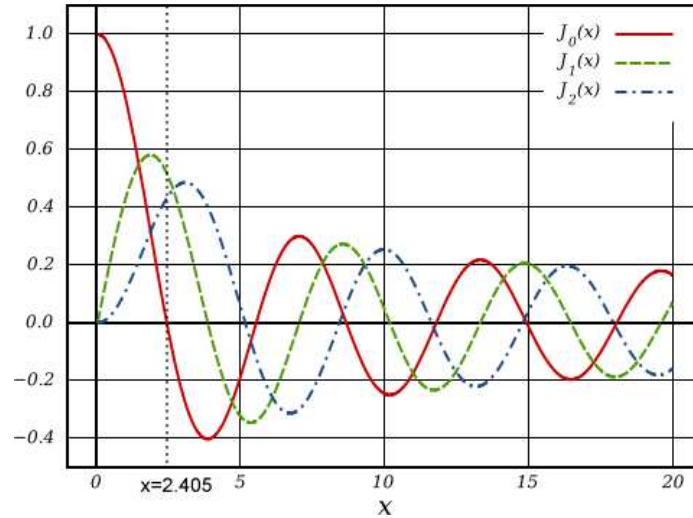


Figure 4.2 Bessel Functions: order 0 (red), order 1 (green) and order 2 (blue)

Now, looking at Figure 4.2, we realize that $J_0(m)$ acquires a null value for $m = 2.405$. Then, the three Bessel terms' values will be:

$$J_0(2.405) \cong 0$$

$$J_1(2.405) \cong 0.52$$

$$J_2(2.405) \cong 0.43$$

Replacing these values in expression (45), it results:

$$E_{out} = \frac{A_0}{2} \text{Re}[e^{j\theta_b}(j0.52(e^{j\omega_m t} + e^{-j\omega_m t}) - 0.43(e^{j2\omega_m t} + e^{-j2\omega_m t})))] \quad (46)$$

Expression (46) represents the output of the phase modulator, where as we can see, the carrier's component has been suppressed. Thus, the data at the upper branch will be kept unaltered when combining the two signals.

We must emphasize the fact that as we are not considering a small signal condition for the RF tone, we need to ensure a proper splitting ratio between the branches to keep the effective optical modulation index within moderate values. Here is where the role of the couplers within the setup acquires importance.

If we define a coupling factor " α ", the signal at the DUT's input will be:

$$E_{DUT_in} = \frac{A_0}{2} \text{Re}[1 - \alpha + \alpha e^{j\theta_b}(j0.52(e^{j\omega_m t} + e^{-j\omega_m t}) - 0.43(e^{j2\omega_m t} + e^{-j2\omega_m t})))] \quad (47)$$

Then, passing it through the DUT, we have:

$$\begin{aligned}
 E_{DUTout} &= \\
 &= \frac{A_0}{2} \text{Re} \left[(1 - \alpha) e^{j\phi_0} + \alpha e^{j\theta_b} (j0.52(e^{j\omega_m t} e^{j\phi_1^+} + e^{-j\omega_m t} e^{j\phi_1^-}) - 0.43(e^{j2\omega_m t} e^{j\phi_2^+} + e^{-j2\omega_m t} e^{j\phi_2^-})) \right] \\
 &= \frac{A_0}{2} \text{Re} \left[(1 - \alpha) e^{j\phi_0} \right. \\
 &\quad \left. + \alpha e^{j\theta_b} \left(j0.52 e^{j\frac{\phi_1^+ + \phi_1^-}{2}} (e^{j\omega_m t} e^{j\frac{\phi_1^+ - \phi_1^-}{2}} + e^{-j\omega_m t} e^{-j\frac{\phi_1^+ - \phi_1^-}{2}}) \right. \right. \\
 &\quad \left. \left. - 0.43 e^{j\frac{\phi_2^+ + \phi_2^-}{2}} (e^{j2\omega_m t} e^{j\frac{\phi_2^+ - \phi_2^-}{2}} + e^{-j2\omega_m t} e^{-j\frac{\phi_2^+ - \phi_2^-}{2}}) \right) \right] \\
 &= \frac{A_0}{2} (1 - \alpha) \cos(\omega_0 t + \phi_0) - A_0 \alpha 0.52 \sin(\omega_0 t + \frac{\phi_1^+ + \phi_1^-}{2} + \theta_b) \cos\left(\omega_m t + \frac{\phi_1^+ - \phi_1^-}{2}\right) - \\
 &\quad A_0 \alpha 0.43 \cos(\omega_0 t + \frac{\phi_2^+ + \phi_2^-}{2} + \theta_b) \cos\left(2\omega_m t + \frac{\phi_2^+ - \phi_2^-}{2}\right) \quad (49)
 \end{aligned}$$

Expression (49) illustrates how the carrier and the first and second harmonics' sidebands have acquired a certain phase shift coming from the dispersive system (DUT), so that, like in the previous method, an accurate detection and measurement of the phase shift are essential for chromatic dispersion calculation.

Therefore, at the monitoring point, after applying a square-law detection, neglecting terms affected by α^2 , the detected power will be:

$$\begin{aligned}
 P_d &= \frac{|E_{DUTout}|^2}{2} \\
 P_d &= \frac{(1-\alpha)^2 A_0^2}{16} - \frac{0.52\alpha A_0^2}{4} \sin\left(\frac{\phi_1^+ + \phi_1^-}{2} - \phi_0 + \theta_b\right) \cos\left(\omega_m t + \frac{\phi_1^+ - \phi_1^-}{2}\right) - \frac{0.53\alpha A_0^2}{4} \cos\left(\frac{\phi_2^+ + \phi_2^-}{2} - \right. \\
 &\quad \left. \phi_0 + \theta_b\right) \cos\left(2\omega_m t + \frac{\phi_2^+ - \phi_2^-}{2}\right) \quad (50)
 \end{aligned}$$

From the expression obtained above, we must highlight that the really important terms are the sine and the cosine functions, which represent the detected envelopes for the first and the second harmonic respectively. Then, expressing these envelopes in terms of Bias voltage and chromatic dispersion coefficient, we obtain:

$$\left| i_D(f_{RF}) \right| = \left| \sin\left(\frac{\pi}{V_\pi} V_B(t) + \frac{\pi}{c} D \lambda_o^2 f_{RF}^2\right) \right| \quad (51)$$

$$\left| i_D(2f_{RF}) \right| = \left| \cos\left(\frac{\pi}{V_\pi} V_B(t) + \frac{\pi}{c} D \lambda_o^2 (2f_{RF})^2\right) \right| \quad (52)$$

where c is the velocity of light in vacuum and λ_0 is the carrier's wavelength. Both envelopes present a relative electrical phase shift which depends on the D value.

Now, we have to carry out the mathematical development for the case when we get an amplitude zero at both harmonics, as it is explained below:

1st harmonic:

$$\frac{\pi}{V_\pi} V_{b1} + \frac{\pi D \lambda_0^2 f_m^2}{c} = n\pi \quad (53)$$

2nd harmonic:

$$\frac{\pi}{V_\pi} V_{b2} + \frac{\pi D \lambda_0^2 (2f_m)^2}{c} = (2n + 1) \frac{\pi}{2} \quad (54)$$

From expressions (53) and (54) we finally obtain a direct expression to calculate D :

$$D = \left(\frac{1}{2} - \frac{V_{b2} - V_{b1}}{V_\pi} \right) \frac{c}{3\lambda_0^2 f_m^2} \quad (55)$$

In absence of dispersion both envelopes are $\pi/2$ out of phase and then $\Delta V/V_\pi = 0.5$, so, in the same way we infer that $\Delta V/V_\pi < 0.5$ for $D > 0$ and $\Delta V/V_\pi > 0.5$ for $D < 0$. Therefore, both magnitude and sign of the dispersion coefficient can be obtained with this technique, subject to the periodic nature of the two detected envelopes which limits, on a first look, the maximum dispersion magnitude that can be unambiguously determined (in section 4.2.2.1 we will discuss how this is actually not a limitation). Dispersion monitoring window and dispersion resolution are in fact key parameters of any chromatic dispersion monitoring system based on pilot tones which set a trade-off in the RF frequency choice.

4.2 VPI simulations

As it was done for the ABCM, now we are going to demonstrate the validity of ABCM – SC through a theoretical and numerical analysis, using the VPI simulation tool. The procedure will be the same except for the fact that we first need to determine the appropriate RF Tone amplitude to accomplish the “ $m = 2.405$ ” condition (necessary to cancel the carrier).

It must be emphasized that for the RF modulation we consider phase instead of intensity modulation, and therefore we must find a proper way of simulating it with VPI. We found that the better way to do it is by using a generic MZ modulator block in which the sign of the phase shift acquired by each of the two interferometric branches is the same (set “LowerArmPhaseSense” to positive) and then we enter the same RF tone in both electrodes. See Figure 4.3.

We will set the modulator's V_π at 3.5 V, so that, we can now obtain the A_{RF} value required from the expression below:

$$m = \frac{\pi A_{RF}}{V_{\pi}}$$

Thus, we have:

$$A_{RF} = \frac{\pi 2.405}{3.5}$$

Therefore,

$$A_{RF} = 2.68 \text{ V}$$

As we are working in a simulation environment (ideal conditions) this value can be directly set as the RF tone amplitude.

Figure 4.3 features a basic Phase modulation schema, representing the lower branch on ABCM - SC setup. Through this simulation we will make sure that the carrier cancellation is done correctly. To carry out the simulation, in addition to the 2.68V RF amplitude, the optical source, MZM and RF Frequency must be configured with the same parameters we will use in the main simulation. The bias voltage into the phase modulator in the final setup (Figure 4.3) will be the parameter that sets the phase difference between sidebands and carrier to yield detected RF amplitude nulls, but for now, in order to get the RF amplitude value required for carrier cancellation into the PM branch of Figure 4.3 it does not have any relevant effect but adding a constant phase shift that does not affect the optical spectrum, and therefore we just set it to zero.

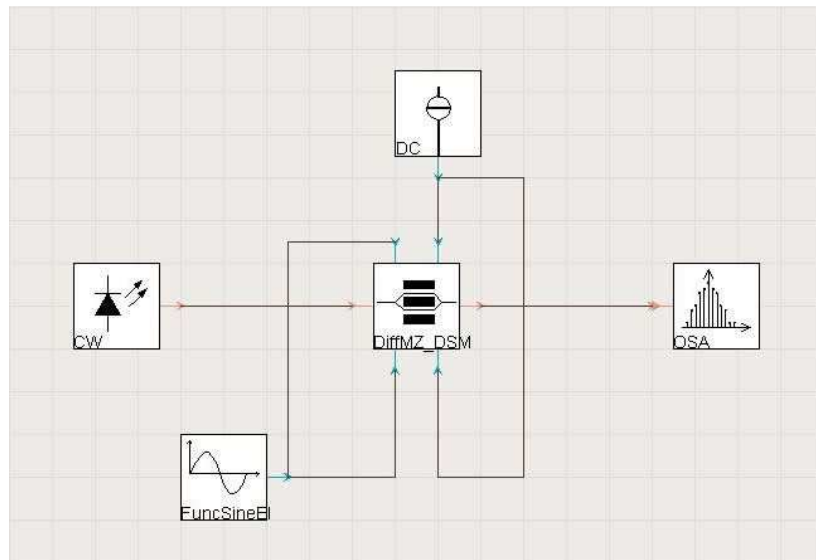


Figure 4.3 VPI schematic for phase modulation with carrier suppression

The graphic displayed by the Spectrum Analyzer in figure 32 is indeed the one we expected. It presents several pairs of sidebands, whose amplitudes decrease as they get further from

harmonic 0 (carrier frequency), and the most important aspect is that the optical carrier has been reduced to an almost imperceptible power level.

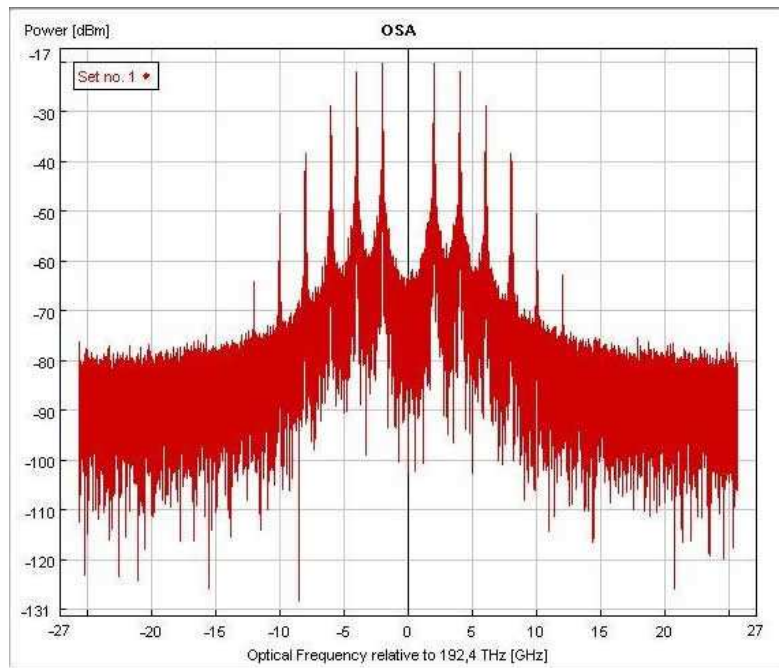


Figure 4.4 Spectrum of the phase modulated optical signal

Figure 4.5 shows a zoomed-in image of the optical spectrum which only exposes the most important features of ABCM - SC: the two main pairs of sidebands (for the first and the second harmonics) with similar power levels and the suppressed carrier (- 63 dBm).

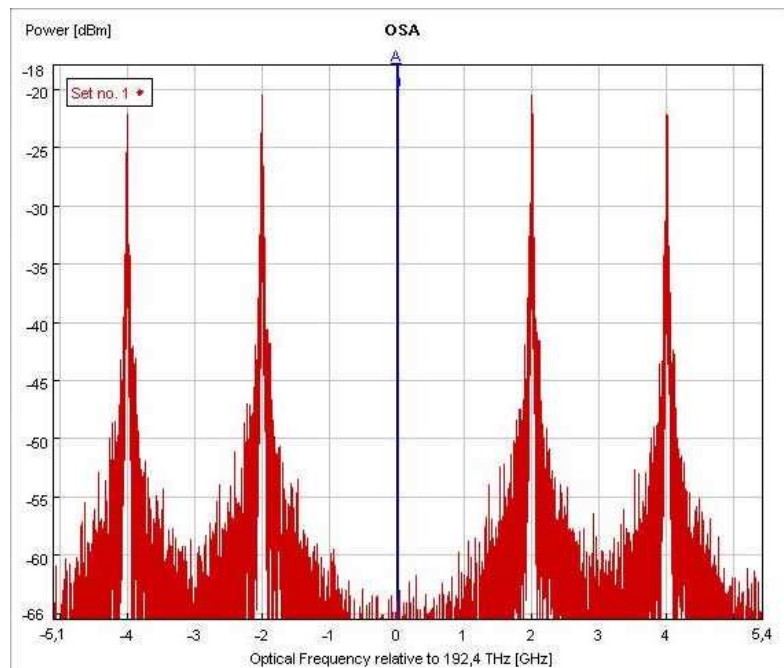


Figure 4.5 Zoom on Figure 4.4 highlighting main sidebands and suppressed carrier

Now, once we have all the parameters settings, we deploy the setup shown in Figure 4.6, which includes the emitter part and the monitoring point described in the operating principle section.

Most modules in this setup were already used in the ABCM simulation; however we notice the presence of some new devices: the couplers located before and after the modulator, and whose main task is to generate a considerable magnitude difference between the upper and the lower branches for the low modulation index condition to hold.

We also notice we have two phase and magnitude detectors, this is because we need to recover the amplitudes of the two harmonics. These amplitudes will be displayed through their respective XY visualizer (2D Analyzer). The 'x axis' for both harmonics will be the bias voltage signal applied on the modulator.

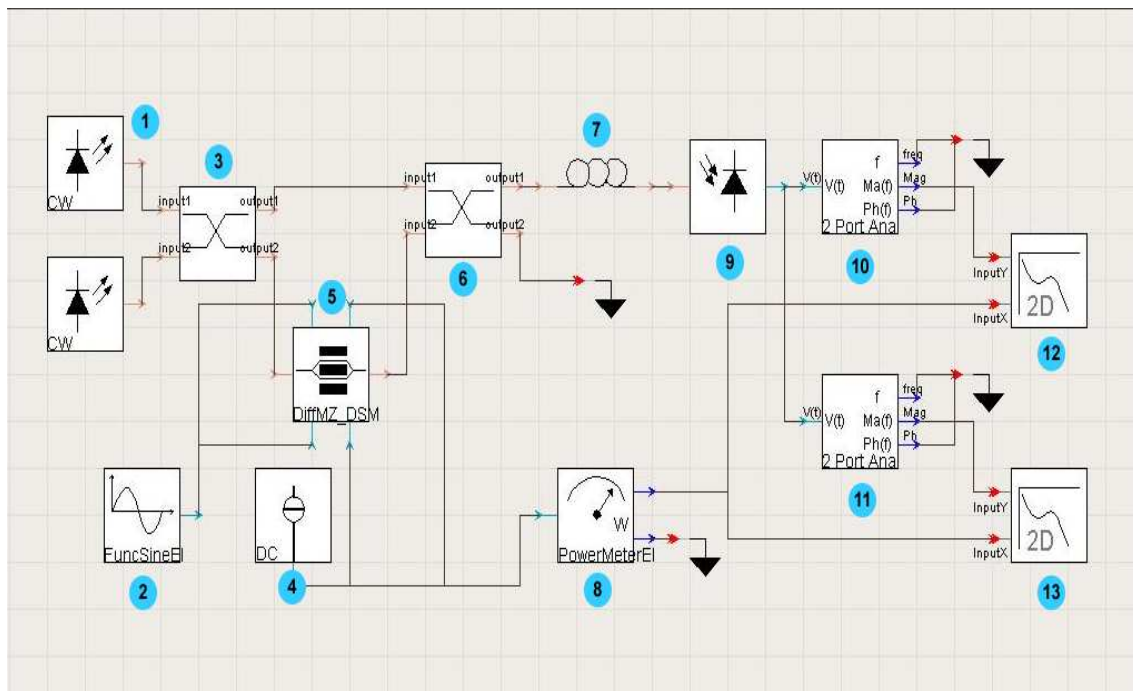


Figure 4.6 VPI schematic for ABCM - SC: 1- Optical source 2- Sine generator 3- Input coupler 4- DC source 5- MZM 6- Output coupler 7- Fiber section 8- Power meter 9- Photo detector 10- 1st harmonic amplitude and phase detector 11- 2nd harmonic amplitude and phase detector 12- 1st harmonic XY visualizer 13- 2nd harmonic XY visualizer

Another important issue about this setup is related with the Mach-Zehnder configuration. As we can observe in the setup in figure 31, we want to emulate a phase modulator behavior using a dual-drive MZM. We input the same RF tone and the same bias voltage into both electrodes and set the POSITIVE polarity in the modulator.

This section will be also divided into two main stages. The first one focuses on the analysis of dispersion inserted by the DUT. The complete procedure to calculate chromatic dispersion with this simulation environment will be the following:

- We obtain one amplitude-vs-bias graphic for each harmonic in order to identify the amplitude dips.
- We choose any pair of dips (the “ $n = 0$ ” ones for this experiment) and obtain their respective bias voltages.
- Finally, we calculate the chromatic dispersion coefficient manually, replacing these values in expression (55).

On the second stage, we will study ABCM - SC behavior while sweeping some key parameters such as the RF frequency, the nominal dispersion, the RF Amplitude and coupling factor (α).

4.2.1 Analysis of the dispersion inserted by the DUT

In this section, we will run the setup shown in figure 34. After the electrical signal is recovered by the photo detector, it is split into two signals to obtain the amplitude value for the first and second harmonics. Thus, in the XY visualizers, we will display an amplitude-vs-bias graphic for each harmonic.

The bias voltage sweep will go from -1 to 8 V, because this range will give us the chance to observe at least two amplitude dips for each harmonic; and the bias step width will be 0.01 V.

Now, just to summarize the configuration parameters which differ from the ones of previous cases, we have:

- The RF tone’s amplitude is set to 2.68 V according with carrier-suppression analysis
- There is a 0.5/0.5 coupler located before the modulator and a 0.15/0.85 coupler after the modulator. For this last device, the 0.15 input corresponds with the modulator’s output and the 0.85 input to the non-modulated optical signal.
- The amplitude/phase detector on the top will be set to 2 GHz (RF frequency) and the one on the bottom to 4 GHz (2xRF frequency).

Results

Figure 4.7 features the amplitude-vs-bias graphics obtained for both harmonics from this simulation.

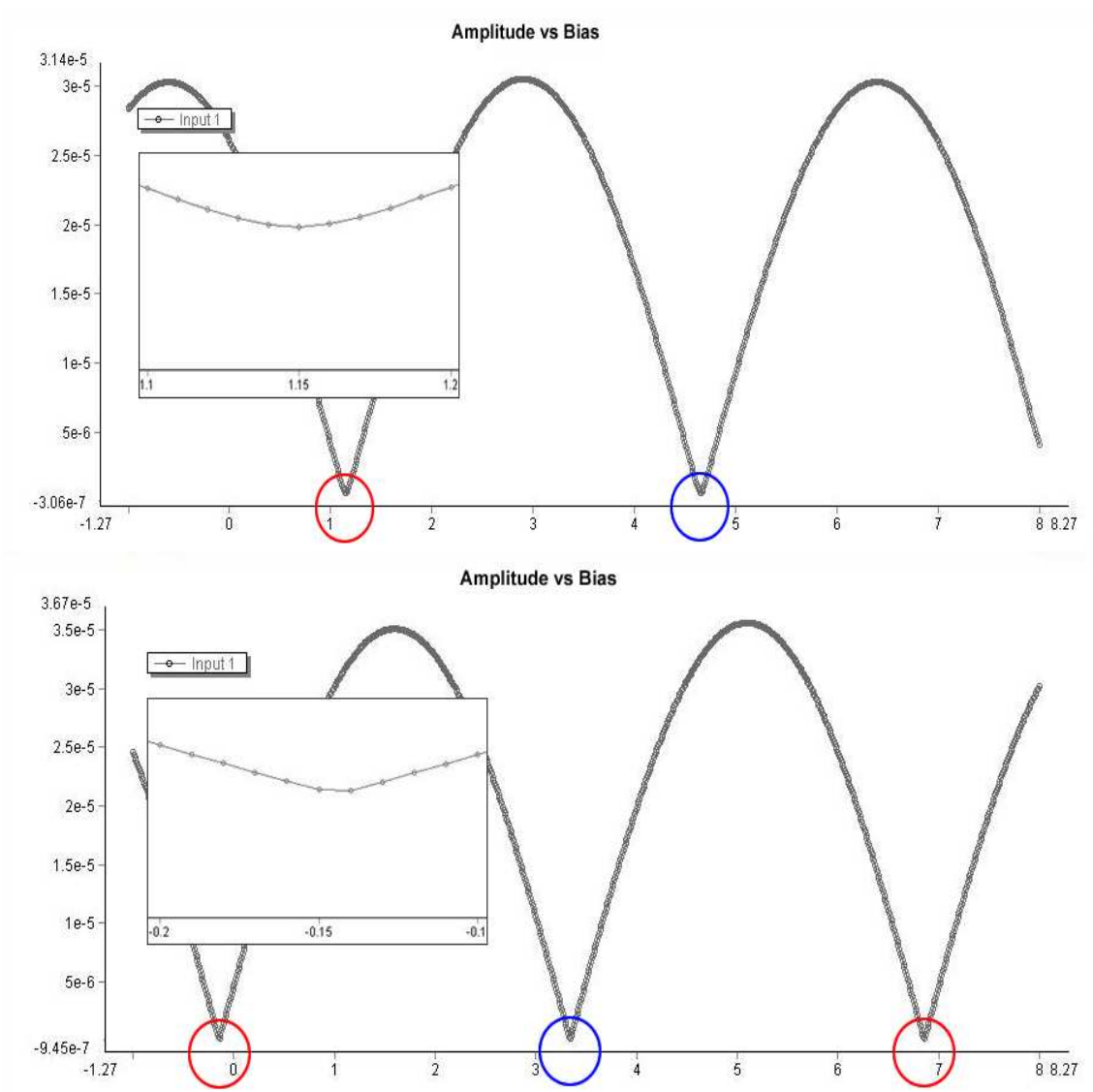


Figure 4.7 Amplitude-vs-Bias graphics for: 1st harmonic (top) 2nd harmonic (bottom)

From Figure 4.7 we obtain the null bias voltages corresponding to the first and second harmonic (V_{b1} and V_{b2}) which are -0.14 and 1.15 respectively. We just need to replace these values in expression (55) to directly calculate the D value, as follows:

$$D = \left(\frac{1}{2} - \frac{V_{b2} - V_{b1}}{V_{\pi}} \right) \frac{c}{3\lambda_0^2 f_m^2}$$

We know that $c = 3 \times 10^8$ m/s, $\lambda_0 = 1559.25$ nm, $f_m = 2$ GHz and $V_{\pi} = 3.5$ V, so we finally have:

$$D = \left(\frac{1}{2} - \frac{1.15 - (-0.14)}{3.5} \right) \frac{3 \times 10^8}{3 \times 1559.25^2 \times 2^2}$$

$$D = 1351 \text{ ps/nm}$$

According with the results obtained above, the total chromatic dispersion calculated with ABCM - SC has a 9ps/nm error (0.66%) with respect to its nominal value, which is reasonable.

It is also important to remark that we could have chosen any pair of dips ($n = 1, 2, 3 \dots$) as all of them keep a 3.5 V (V_{π}) difference between each other, so that the difference between the two harmonics' amplitude dips (key factor in this method) is kept constant.

4.2.2 Analysis of the effect caused by the setup's parameters

In this section we will analyze the impact of varying some key parameters within ABCM - SC schema. These parameters will be the RF frequency, the RF amplitude, Nominal dispersion and the Coupling factor of the coupler located immediately after MZM in the setup.

For this simulation the setup featured in Figure 4.6 will suffer some modifications as it is shown in Figure 4.8. We will replace the XY analyzers by the V_i Text Modules, because we need to save the data sample in .txt files to be later processed by a Matlab program. Two .txt files will be generated for each parameter instead of a single file, one file for the first harmonic and the other for the second harmonic.

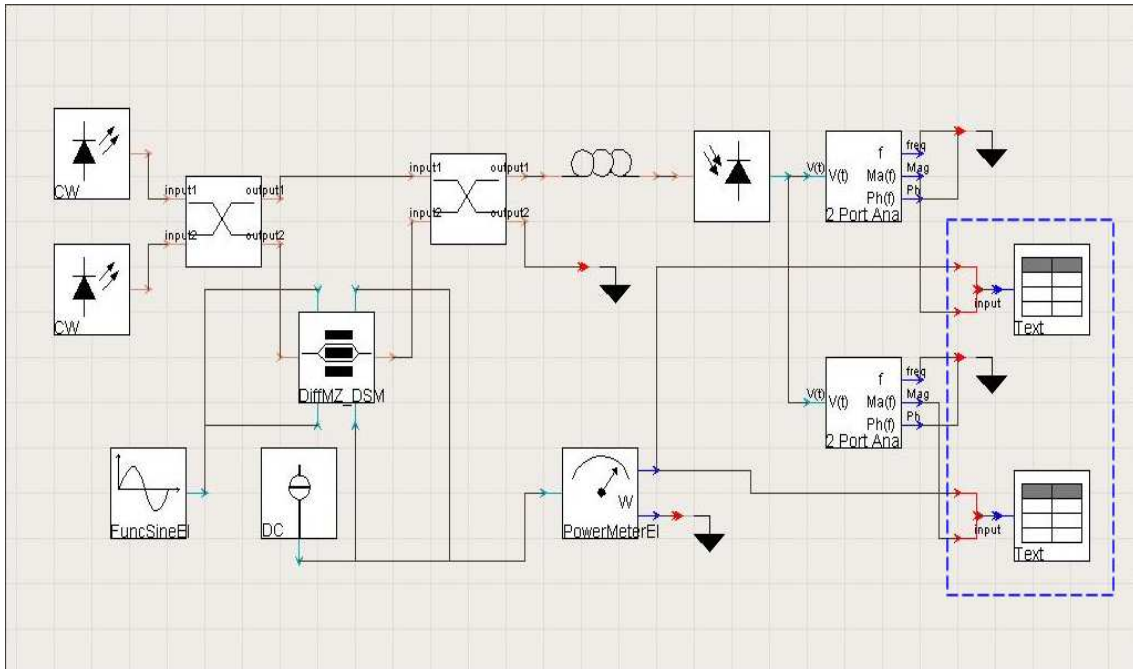


Figure 4.8 VPI setup for ABCM - SC (Second stage). Highlighted with discontinuous line: Text module

With respect to the sweeping process, the innermost loop parameter will be the bias voltage inserted into the MZM, but as this value is the same for both harmonics, the upper and lower limits must be properly chosen so that it contains the zero amplitude bias of both harmonics.

Therefore, looking at expressions (53) and (54), the “=0” dips for the first and the second harmonics will be located between -3.5 V and 0 V , and between $-\sqrt{2}$ and $\sqrt{2}$ respectively. If we join these two ranges together we conclude that the bias voltage sweep must go from -3.5 V to 1.75 V .

The outermost loop will be composed by the sweep control of the parameters we want to study.

4.2.2.1 RF Frequency Sweep

The RF frequency is one of the most important parameters within ABCM – SC setup because of its direct presence in the final expression to calculate chromatic dispersion, (55), and its interdependence with bias resolution.

Our goal in this analysis will be to identify the RF frequency level edges to guarantee a high degree of accuracy and efficiency when applying the technique.

We already verified the good performance of ABCM – SC for a RF frequency equal to 2 GHz . This fact gives us a good reference point to configure the sweep. We also know from ABCM analysis that the lower edge is determined by the bias voltage step width (0.01 V for all simulations in this PFC).

With respect to the upper edge, the only limitation is related with the dips location since we need to associate each dip with its respective order ($n = \dots -2, -1, 0, 1, 2, 3 \dots$). Thus, in order to avoid any mistake while assigning the “ n ” value to a dip, we must restrict the possible dips locations to determined ranges.

Looking at expression (53) and (54) we infer that for a positive dispersion value the zero-amplitude bias corresponding with the first and the second harmonics must be located within $[(n - 1) V_{\pi}, nV_{\pi}]$ and $[\frac{(2n-1)V_{\pi}}{2}, \frac{(2n+1)V_{\pi}}{2}]$ respectively. In this particular case ($n = 0$), the valid ranges would be $[-V_{\pi}, 0]$ for the first harmonic and $[-V_{\pi}/2, V_{\pi}/2]$ for the second harmonic.

The RF frequency sweep chosen will go from 200 MHz to 2 GHz with a 200 MHz step width.

Results

After running the simulation, we obtained the two .txt files and we processed them by a modified version of the Matlab program used in ABCM. This Matlab code is new due to the fact that it processes both .txt files in a single run and looks for the dips within the corresponding range for the first and the second harmonics, and obviously it uses expression (55) instead of expression (40) to calculate chromatic dispersion.

We finally obtained the graphics featured in Figure 4.9 and 4.10. Figure 4.9 describes the relation between Null Bias delta ($V_{b2} - V_{b1}$) and RF frequency. We can notice the curve’s parabolic shape since the bias is proportional to the RF frequency square power according to expression (55).

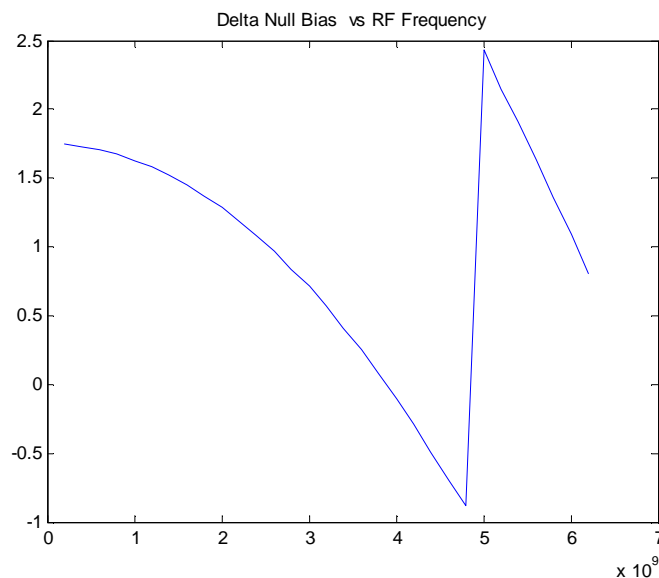


Figure 4.9 Zero-Amplitude Bias Delta-vs-RF frequency Curve

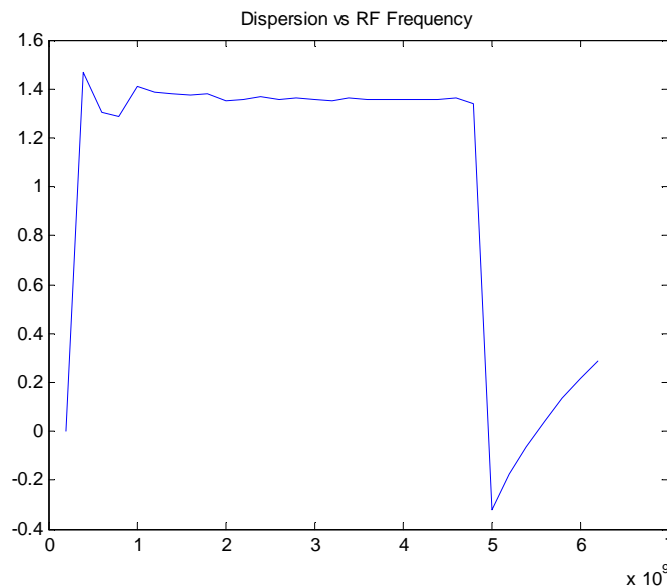


Figure 4.10 Chromatic Dispersion-vs-RF frequency Curve

We observe, just as in ABCM simulation, how the Null-amplitude bias delta decreases as frequency increases; however, it doesn't keep the same behaviour till the end, yielding a level hop around 4.8 GHz. This feature reflects that we have arrived to the upper edge for the RF frequency, which indicates that at this frequency value the zero amplitude bias from one of the two harmonics has over passed the allowed range, so the rest of the graphic should be dismissed.

However, unlike ABCM, if we look at expression (55), it does not depend on “ n ”; thus, it is not necessary to know the dips' order as long as we make sure both dips correspond to the same order. Nevertheless, for this particular analysis we decided to restrict the possible dips location to finite ranges to simplify the dips obtaining algorithm.

This level hop at 4.8 GHz is also featured in figure 38, which shows dispersion-vs-RF Frequency relation. Here we can see how the dispersion level approximates to the nominal value (1.36 ps/nm) and gets even closer to it for 1 GHz. If we want to make a comparison with ABCM, we can state that in this case the graphic reaches a good stability sooner, however, the maximum frequency allowed is around 4.8GHz.

4.2.2.2 RF Amplitude Sweep

In ABCM - SC, the RF Amplitude acquires an even more important role than in ABCM. It is the main parameter to handle during the carrier suppression process, which is a particular consequence of the phase modulation of the optical carrier.

We know from the introduction section that the main purpose of cancelling the optical carrier in the RF tone phase modulated signal is to avoid altering the recovery of data when both signals are combined. This is in fact the reason why this technique can be applied to a real-time optical network monitoring system, unlike ABCM.

However, the accuracy of the dispersion measurement is not related with the data alteration along transmission, but with keeping the signals' amplitude level within the acceptable range to support the approximations of the mathematical analysis. Thus, we need to yield a considerable difference level between the carrier and the two first harmonics' sidebands, and between these ones and the rest of the harmonics.

The considerations exposed above establish an important restriction to the RF amplitude value in terms of data preservation and accuracy in measurements.

First, we will focus on the carrier cancellation issue. We will carry out a certain number of simulations with the schematic featured in Figure 4.3, while we sweep manually the RF amplitude around values close to the ideal one obtained in the math analysis (2.68 V). The exact values will be: 2.60, 2.65, 2.70, 2.75, 2.80 and 2.85 V.

After running these simulations, the Optical Spectrum Analyzer Module yielded a different spectral representation for each run as it is shown in Figure 4.11. We observe that the first harmonic has an amplitude level around -20 dBm along all simulations; however, the carrier suffers a considerable level variation on each RF amplitude step.

The carrier level increases as we get further from 2.68, so that we have almost 20 dB of difference from the extreme values to the center. This behavior demonstrates how susceptible the carrier level is to RF amplitude variations. Therefore, we must keep this parameter as close as possible to the reference value if we want to achieve a good carrier cancellation.

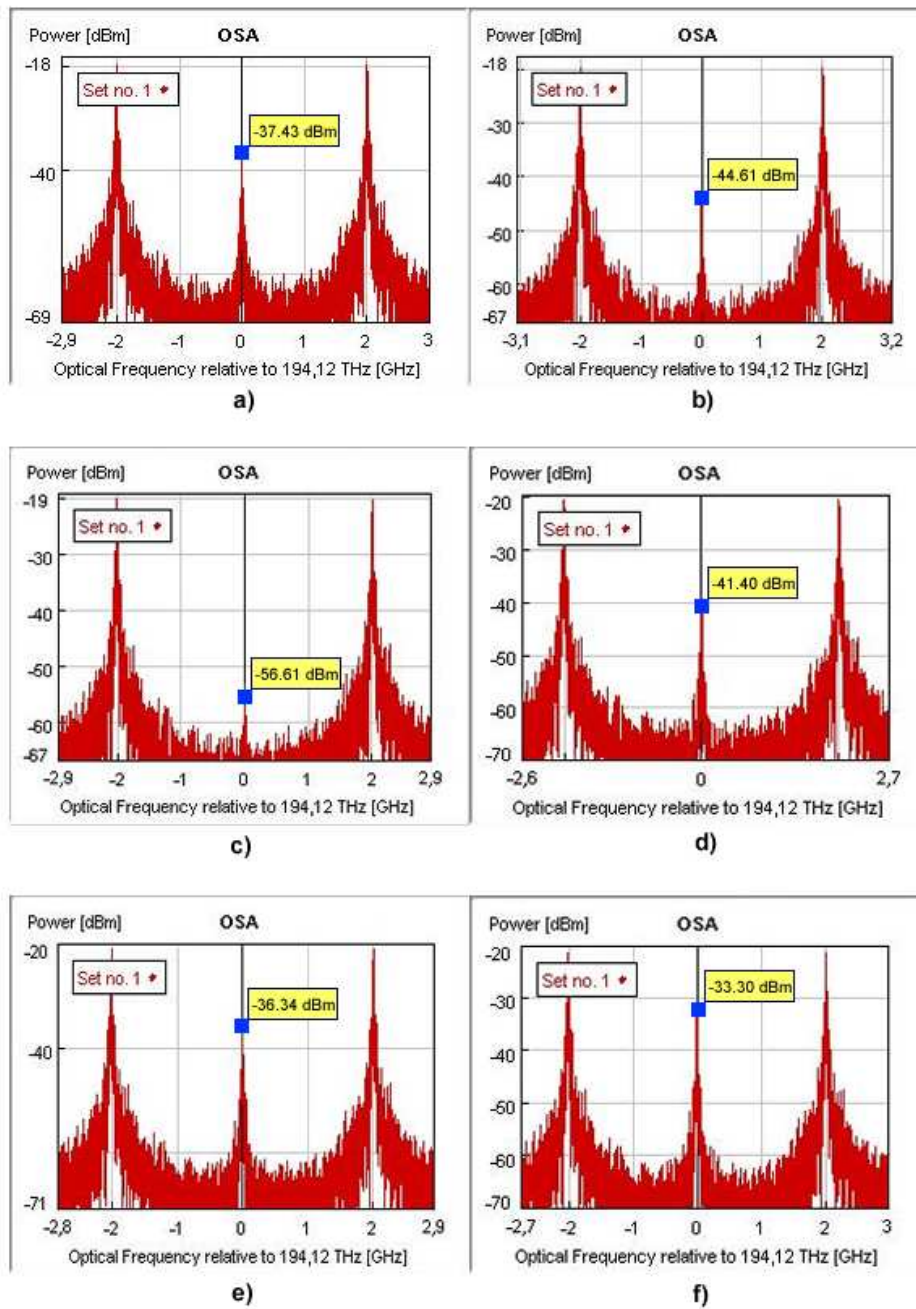


Figure 4.11 Spectrums of the phase modulated optical signal obtained with RF amplitude equal to: a) 2.60 V b) 2.65 V c) 2.70 V d) 2.75 V e) 2.80 V f) 2.85 V

On the other hand, we need to evaluate the technique's behavior in terms of accuracy, just as we have been doing in the previous analysis. We will make a large RF amplitude sweep so that we can easily identify the lower and upper edges of the acceptable range. The RF amplitude (outermost loop) will go from 0.12 V to 4.12 V as these values are far enough from the reference level to perceive measurement errors. The step width will be of 0.16 V, which makes a total of 26 samples.

Results

The results corresponding to this simulation are featured in the Harmonics Null-Amplitude Bias Difference-vs-RF amplitude curve and in the Dispersion-vs-RF amplitude curve in Figure 4.12 and 4.13 respectively.

We observe in figure 41 how the curve starts with 2 ps/nm dispersion at 0.12 V and then it approximates very quickly to the nominal dispersion (1.36 ps/nm), reaching the closest value (1.351 ps/nm) at 0.8 V and keeping this until 2.9 V. The range we have just delimited is where the RF amplitude must be allocated in order to preserve ABCM -SC accuracy.

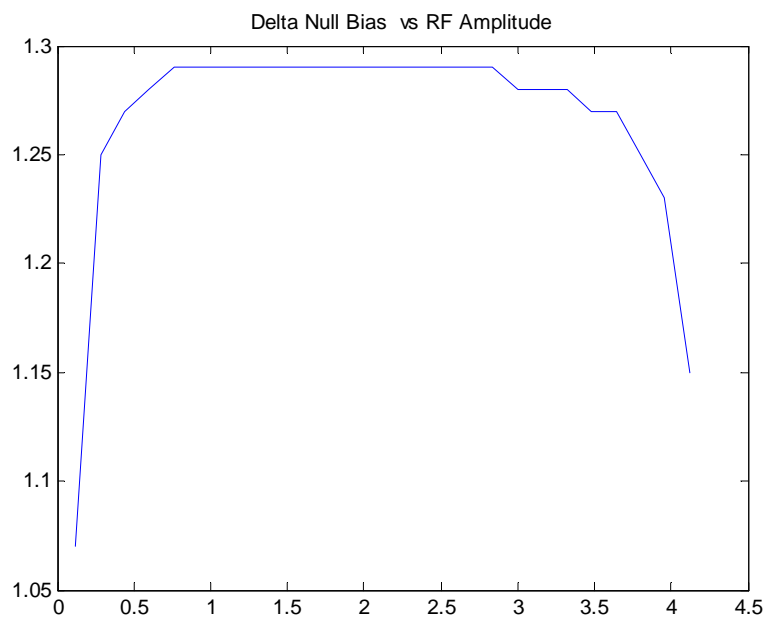


Figure 4.12 Zero-amplitude Bias Delta-vs-RF amplitude curve

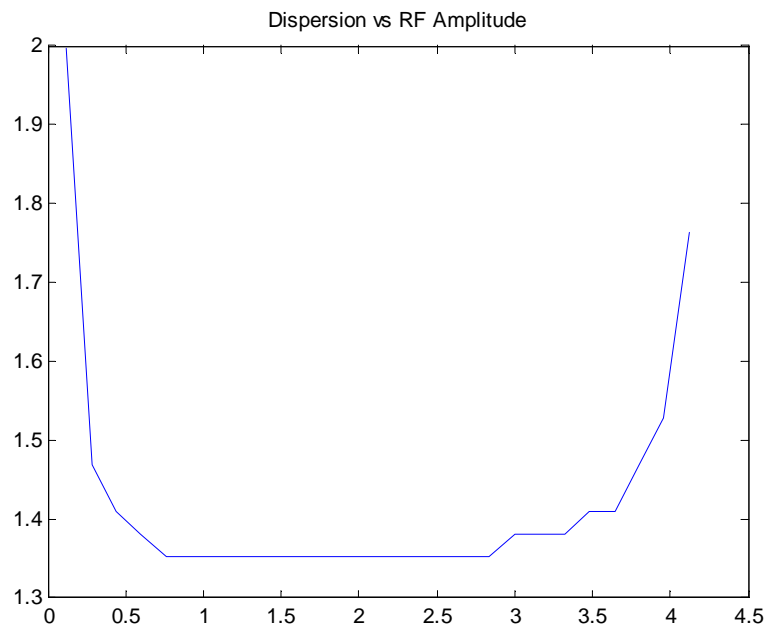


Figure 4.13 Chromatic Dispersion-vs-RF amplitude curve

Going deeper into the analysis, we realize that the upper and lower edges of the range obtained are not equidistant from 2.68 V; this means, the carrier suppression is not the main property involved while evaluating results. Thus, it is more important to keep the RF amplitude small enough with respect to the signal traveling in upper branch.

In conclusion, we can state that the most important issue within ABCM - SC is related with the accuracy in the dispersion measurement. We have to determine a range of RF amplitude possible values; however, since this method is supposed to be applied on a real time optical network, we must set this value as close as possible to the reference value obtained in carrier suppression analysis. It is also important to conduct BER measures for the modulation format to avoid affecting transmitted data.

4.2.2.3 Nominal Dispersion Sweep

The analysis of Nominal Dispersion parameter has nothing new with respect to the one carried out for ABCM. We observe from expression (55) that the relation between the dispersion and the RF frequency is very similar to the one we had for ABCM in expression (40). Thus, we assume that if we work within the range obtained in the RF frequency sweep section, we will not have any problems while measuring very high or very low dispersion values.

Therefore, this analysis will once again focus on describing how the variation of nominal dispersion (set in the fiber section) affects the method's accuracy, and we will also study its relation with the bias resolution.

As we are using the same fiber module as DUT, the outermost loop for the bidimensional sweep will be the fiber's length, which will go from 0 to 160 km with a step width of 5 km.

Results

Figure 4.14 represents Null amplitude Bias Delta voltage-vs-Nominal Dispersion Curve, which has a linear behavior from the beginning to the end. This linearity is also observed in figure 4.15, containing the relation between the measured dispersion and the nominal dispersion.

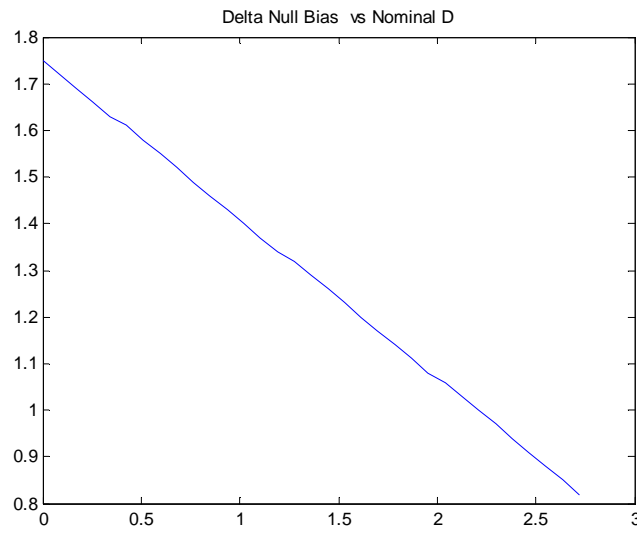


Figure 4.14 Zero-amplitude Bias Delta-vs-Nominal Dispersion Curve

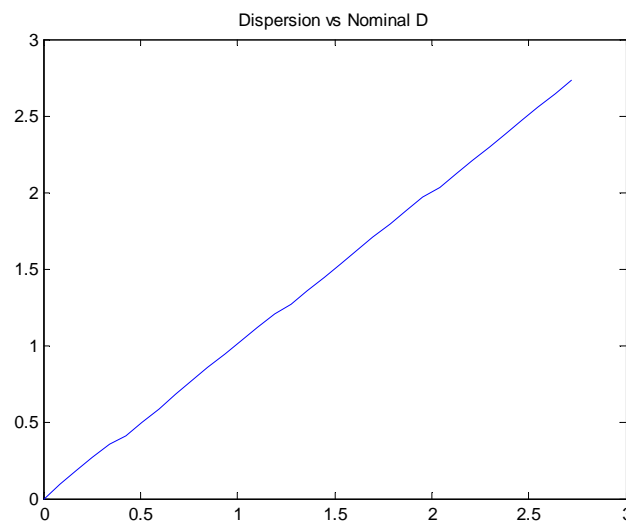


Figure 4.15 Chromatic Dispersion-vs-Nominal Dispersion Curve

The most salient point in Figure 4.15 is that once again the nominal dispersion value has an almost imperceptible effect on the dispersion calculated, so that the ABCM - SC is able to keep a good performance no matter the level of dispersion the optical system has, subject to the limit of maximum measureable dispersion which depends on the RF frequency.

4.2.2.4 Coupling factor Sweep

The presence of couplers within the setup is one of the new features introduced by ABCM - SC.

We will carry out a bidimensional sweep with the coupling factor (α) as the outermost loop parameter, going from 0.51 to 0.99 (the number indicates the factor applied to the upper branch).

Results

We obtained the Null amplitude Bias Delta-vs-Alpha and Dispersion-vs-Alpha curves featured in Figure 4.16 and Figure 4.17 respectively.

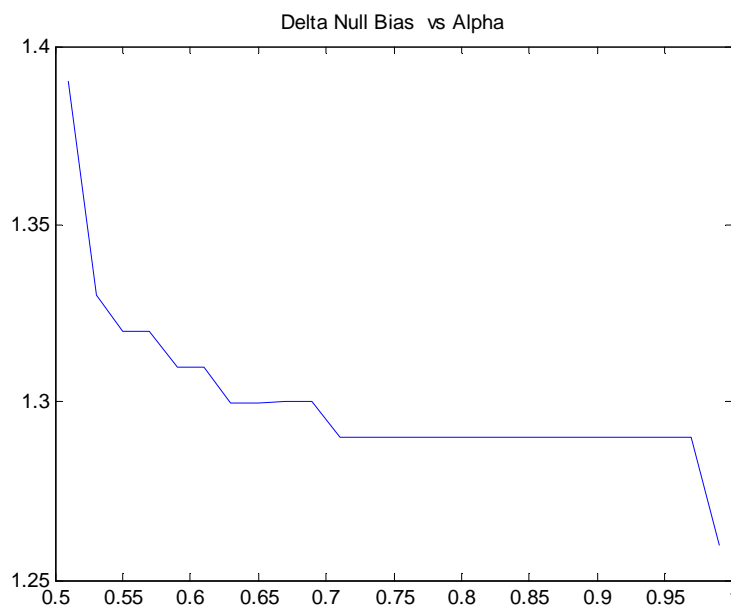


Figure 4.16 Zero-amplitude Bias Delta-vs-Alpha Curve

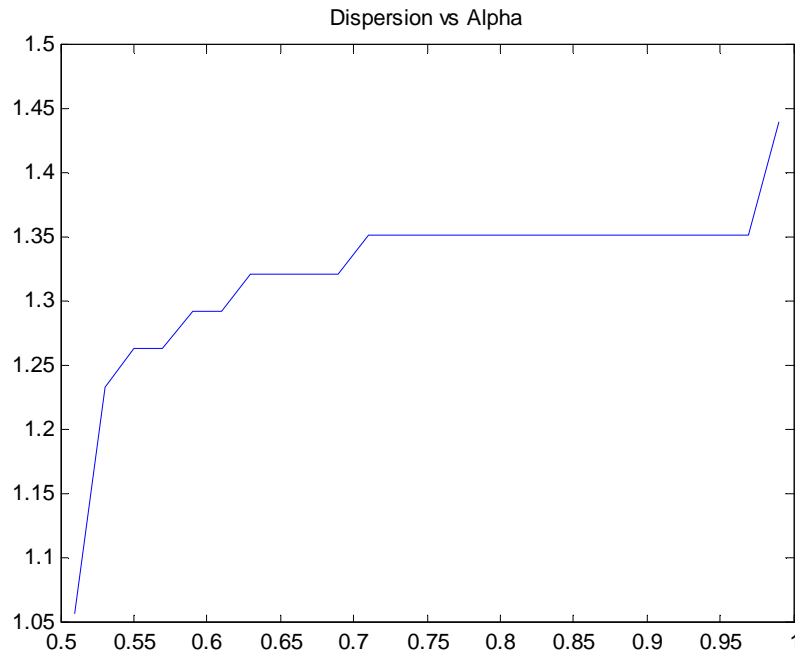


Figure 4.17 Chromatic Dispersion-vs-Alpha Curve

We notice the graphics obtained have a quite similar behavior to the ones obtained in the RF amplitude analysis. This fact shows how both parameters are, in different levels, involved on yielding the magnitude difference between the optical carrier and the first and second harmonics. Now, observing Dispersion-vs-Alpha curve on itself, we realize it starts with a dispersion value around 1 ps/nm at 0.51 alpha sample, and then dispersion increases following a “steps” shape, and getting the closest to nominal dispersion, with a 1.351 ps/nm value at around 0.75 α . Therefore, this last alpha value represents the minimum point or lower edge to maximum accuracy in chromatic dispersion calculation.

We can see how the dispersion calculated keeps unaltered almost until the end of α 's range; however from 0.97 α the curve starts growing again. Anyway, it is totally inefficient to use couplers with those alpha values in real environments.

4.3 Experiments

4.3.1 Laboratory Equipment

Next we will describe the devices need to carry out ABCM – SC which were not used in ABCM.

4.3.1.1 Optical Coupler

This is a passive device used in optical systems for multiplexing (branching or joining) the optical signal from one or more light sources to one or more light receiving devices. The power distribution into the outputs depends on the wavelength and the polarization. The couplers

available in the laboratory were fabricated by thermally fusing the fibers so that their cores get into intimate contact. The coupling factor () is reached by using different fiber lengths to connect inputs and outputs.

In this experiment we will use two couplers within the setup: a 50/50 coupler immediately after the laser source to split the optical signal into the two branches (the upper branches simulating the data flow and the lower one to be phase modulated by the RF tone); and a 80/20 coupler between the emitter side and the monitoring point in order to achieve the amplitude level difference between signals of both branches.

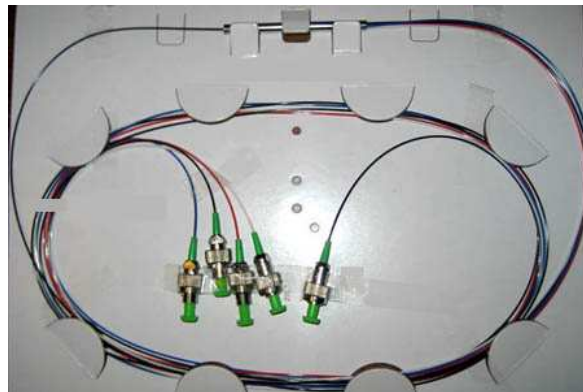


Figure 4.18 Optical Coupler

4.3.1.2 Laser HP 83424A

This instrument (Figure 4.19) can be used as a light source in measurements which do not require wavelength tuning and where its frequencies margin is contained within the laser's supportable bandwidth. This is why it can be used for instance to obtain the Transfer Functions of the modulator. This laser does not have a power regulator at the output, so that the power provided has a constant value (see table 4.1).

In this experiment, the HP 83424A will be used as a secondary light source in the carrier suppression setup in order to heterodyne the RF tone phase modulated signal, so that the carrier and the sidebands are displaced to a frequency range supportable by the electrical spectrum analyzer.



Figure 4.19 HP 83424A

The most relevant technical features of HP 83424A are shown in table 4.1.

HP 83424A Laser	
Optical BW	1553 nm
Optical Power	3 dBm
Type of connector	FC/UPC

Table 4.1 HP 83424A Laser features

4.3.1.3 Agilent Spectrum Analyzer

In this experiment all measurements will be obtained by using an Agilent super heterodyne Spectrum Analyzer. This device will display the spectrum components of the modulated signal (sidebands and carrier), so that we can manually cancel out any of these components by just adjusting the bias voltage (in the dispersion measurement experiment) or RF signal (in the carrier suppression experiment).

Since this device is an electrical Spectrum Analyzer, we will have to optically heterodyne the phase modulated optical signal with the carrier from an additional laser such that the spectral difference between both lasers is contained within the SA frequency range. Thus, we will be recover the downconverted signal with a detector and display it on the SA to carry out measurements.

It also provides an electrical output with enough power to be used as a RF source in the phase modulation process.



Figure 4.20 HP Agilent Spectrum Analyzer

4.3.2 General description of the experiment

This section will be divided into two well-defined experiments. First we will focus on the emitter side of the setup. We will regulate the RF power level and the position of the polarization controller's arms to achieve a robust cancellation of the optical carrier.

In the second part, we will implement the monitoring point of the setup, adding the DUT to be characterized and a DC signal (bias voltage) together with the RF tone with the specific amplitude required to carry out the carrier suppression in the phase modulation. The goal will be to determine manually the bias voltage values which cancel the first and the second harmonics respectively. Finally, these voltages will be replaced in ABCM -SC final expression, (55), to calculate the total amount of dispersion inserted by the DUT.

4.3.3 Setup characterization

Now we will explain the choice of the main parameters (RF power and frequency, Optical power and frequency, etc).

RF frequency choice: Looking at expression (55) we notice that relation between RF frequency and dispersion resolution is the same as in the ABCM. This means that as the frequency increases, the dispersion resolution increases too (bias step width is kept constant).

There is an upper limit for the RF frequency since we want to avoid overlaps between the zeros ranges. Otherwise, the lower limit is determined, as mentioned in section 4.2.2.1, by the bias step width (minimum value the bias voltage can take).

Considering all the above and the range obtained in the simulation of section 4.2.2.1 (from 0.8 GHz to 6 GHz), we conclude that the ideal range for the RF frequency is very similar to the one of ABCM. However, since we want to verify that in a real environment when the RF frequency is reduced we get closer to Taylor expansion and compensate the loss of resolution, this time we will work in the resolution limit, so we will place the frequency at the beginning of the tolerable range: 1 GHz.

RF power choice: This parameter is essential in the first part of the experiment; where we want to achieve the optical carrier cancellation. This value under ideal conditions could be calculated starting from the V_{π} of the modulator as explained in section 4.2. However, in this case we cannot rely on this theoretical value because there are many potential causes of power loss within the experimental setup; therefore, the correct procedure is to adjust manually the RF power while we see the carrier power level on the SA display and verify it gets cancelled.

With respect to the optical source, we know that the **optical frequency and optical power** are related to the DUT and the setup's total loss estimation respectively. Thus, as DUTs to be used are the same than for ABCM, we will use the same fixed wavelength for the main laser source (1559 nm). And, as a matter of fact, the secondary laser' wavelength must be such that the frequency difference between them is supportable by the optical detector and the Spectrum Analyzer. After some tests we determined that the best wavelength is 1568 nm (heterodyned carrier is located around 11 GHz on the SA).

In the case of the optical power, we observe that the setup is almost the same as for ABCM, except for the inclusion of the couplers. Thus, we decided to add 2 dB to the values fixed for ABCM experiments, so we have: 5 dBm using FBG and 7 dBm using DCF.

Finally, we determine the maximum allowed Bias step width in this case. Here we start from expression (53) (first harmonic) and expression (54) (second harmonic), considering the DUT to be characterized is the FBG ($D = 1252$ ps/nm), so we have:

For the 1st harmonic ($n = 0$)

$$\begin{aligned} \frac{\pi}{V_{\pi}} \Delta V_{b1} + \frac{\pi D \lambda_0^2 f_m^2}{c} &= n\pi \\ \Delta V_{b1} &= -\frac{D \lambda_0^2 f_m^2}{c} V_{\pi} \\ \Delta V_{b1} &= -\frac{1252 \cdot (1559 \times 10^{-9})^2 (3 \times 10^9)^2}{3 \times 10^8} 3.44 \\ \Delta V_{b1} &= 313.82 \text{ mV} \end{aligned}$$

For the 2nd harmonic ($n=0$)

$$\begin{aligned} \frac{\pi}{V_{\pi}} \Delta V_{b2} + \frac{\pi D \lambda_0^2 (2f_m)^2}{c} &= (2n + 1) \frac{\pi}{2} \\ \Delta V_{b2} &= \left(\frac{1}{2} - \frac{D \lambda_0^2 (2f_m)^2}{c} \right) V_{\pi} \\ \Delta V_{b2} &= \left(\frac{1}{2} - \frac{1252 \cdot (1559 \times 10^{-9})^2 (6 \times 10^9)^2}{3 \times 10^8} \right) 3.44 \\ \Delta V_{b2} &= 1256.13 \text{ mV} \end{aligned}$$

Therefore, the maximum Bias step width is limited by first harmonic expression (the smallest value) and it is 313.82 mV.

We notice that the value obtained is very close to the one for the ABCM experiment, it means, we can also use a 200 mV step width between bias samples.

4.3.4 Carrier Suppression Experiment

In this first part the goal was to obtain a carrier-suppressed optical phase modulation with state of the art equipment.

Therefore, in order to verify that we can indeed cancel the carrier within the RF tone addition process, we used an AVANEX phase modulator with $V_{\pi} = 6.12$ driven by a 22 dBm, 1GHz RF tone to modulate the optical carrier.

This optical phase modulated signal was heterodyned with the second laser in order to obtain a replica of the optical spectrum in an electrical spectrum analyzer range as it is shown in Figure 4.22.

We observe we got a carrier suppression of 25 dB, and the first and second harmonic optical modulation bands feature similar levels so that significant amplitude detection at the monitoring point is expected at both frequencies when mixed with a powerful carrier (containing data) in the detector.

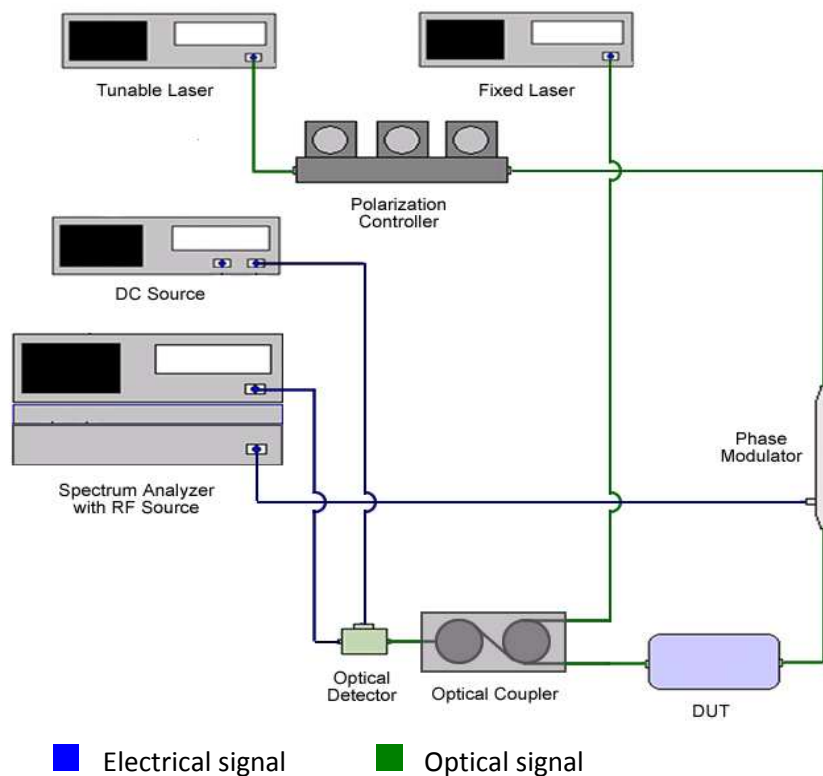


Figure 4.21. Setup for the Carrier cancellation Procedure

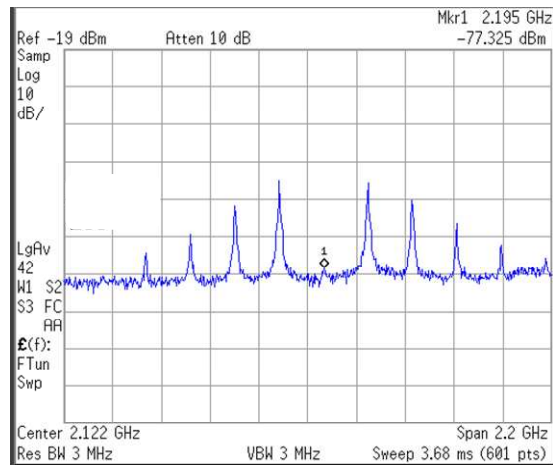


Figure 4.22 Spectrum analyzer capture corresponding to the heterodyning of the phase modulated signal with 20 dBm RF amplitude.

4.3.5 Dispersion Measurement Experiment

In this second stage is where the dispersion measurement takes real place. We set up an emitter following the scheme in Figure 4.23 using FUJITSU MZM with $V_{\pi} = 3.44$ V. The upper branch, which in a real application should be intensity modulated by the data to be sent, in this validity test is left unmodulated so that only the carrier passes through.

The lower branch is driven by a 18 dBm, 1 GHz tone and a continuous DC voltage through the bias tee. The DC voltage applied to the bias tee acts as the low frequency signal controlling the phase offset between bands and carrier in Fig. 4.24 and, once again for validity test purposes it was varied manually.

The output of the modulator is applied to the corresponding DUT (FBG), and after detection, captured in a spectrum analyzer. The RF amplitude tone used should give a spectrum outcome as in Figure for the phase modulated signal.

Since we do not have independent access to the phase modulated branch, we confirm the carrier suppression achievement by checking that the 1 GHz and 2 GHz detected levels at the modulator output with zero DC voltage have very close values (see Bessel Functions theory in section 4.1).

Thus, we need to vary the DC voltage until at the DUT output we get a cancellation of detected power at 1 GHz. We will continue to increase the DC voltage until the 2 GHz tone disappears. Therefore, applying expression (55) we obtain the total amount of dispersion.

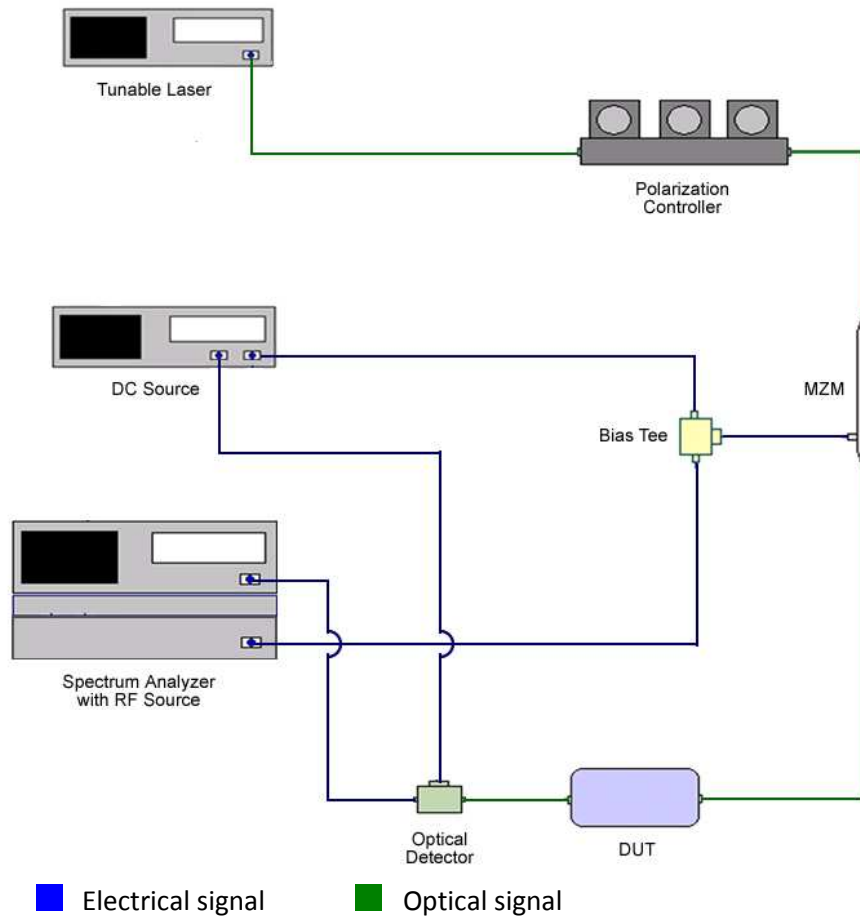


Figure 4.23 Setup for ABCM –SC Experiment

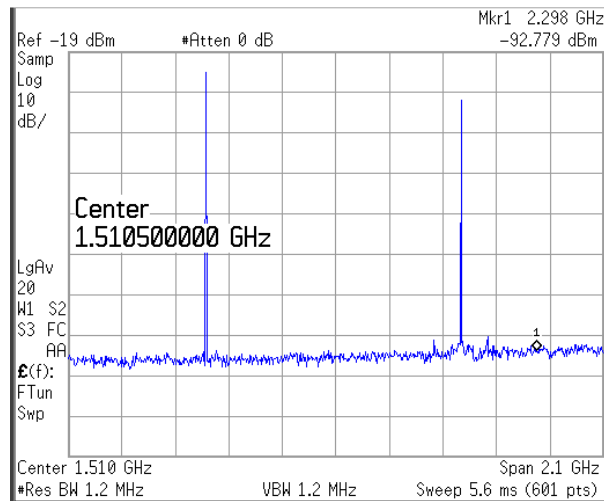


Figure 4.24 Spectrum analyzer capture of the output of the dual-drive modulator with zero phase modulator DC voltage

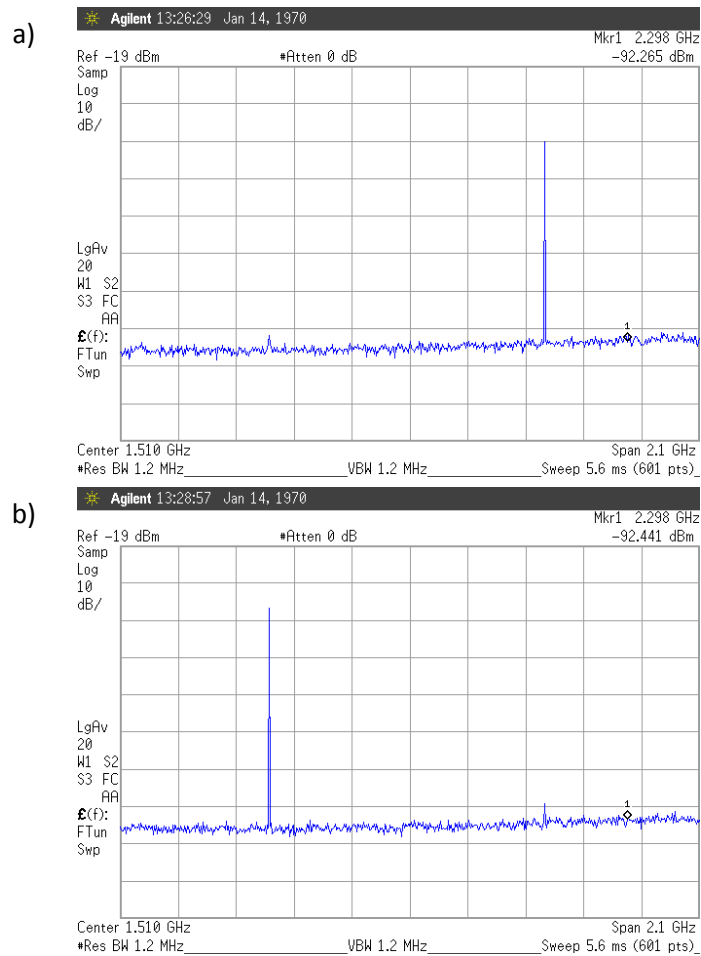


Figure 4.25 a) Spectrum analyzer capture of the output of the dual-drive modulator with zero phase modulator DC voltage b) Spectrum analyzer capture of the output of the DCF with a 2.2 V. phase modulator DC voltage c) same as b) but for a 4.05 V. DC voltage.

Results

Therefore, applying expression (55) we finally obtain:

$$D = \left(\frac{1}{2} - \frac{4.03 - 2.2}{3.44} \right) \frac{3 \times 10^8}{3 \times (1559 \times 10^{-9})^2 (1 \times 10^9)^2}$$

$$D = -1.3157$$

Measured Dispersion vs Nominal Dispersion	
Measured value	-1315,70 ps/nm
Nominal value	-1252,35 ps/nm

Table 4.2 Measured Dispersion vs Nominal Dispersion for FBG

We can see from the dispersion value obtained that even when we have approximated fairly well to the nominal value (which is the best reference we have about FBG real dispersion value), it is not as good as in the ABCM experiment. This fact may be because we are not working under a small signal condition, that is, there is not enough difference level between the sidebands and the carrier with data.

Thus, to solve this issue we should use a phase modulator with the output connected to a 80/20 coupler to yield a significant amplitude difference between the phase modulated signal and the upper optical carrier. Therefore, the optimum setup for this experiment should be the one shown in Figure 4.26.

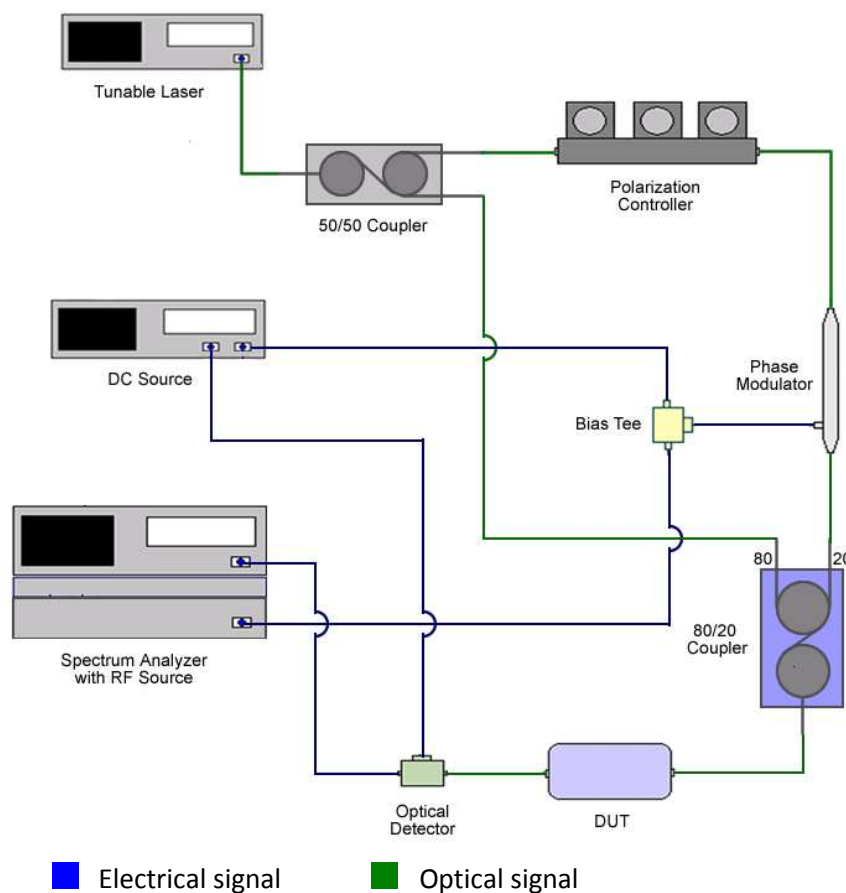


Figure 4.26 Optimum ABCM-SC Setup (not implemented)

5. CONCLUSIONS AND FUTURE LINES

We can state that all the objectives specified in chapter 1 have been accomplished along the chapters of this PFC, and, as happens with all new and innovative proposals, some new studying topics and possible applications emerged from this study. The main purpose of the project was to introduce two new methods for measuring chromatic dispersion: ABCM and ABCM – SC, therefore, the conclusions will be organized according to the chapters which contemplate each method.

Chapter 3. Asymmetric Modulation Bias Controlled Method (ABCM)

ABCM was introduced as a solid alternative for conventional RF tone based dispersion measurement techniques. We specifically analyzed the method's close relation with Peucheret's (calculates dispersion from the amplitude term), highlighting the improved features of ABCM, specially the fact of replacing the RF sweep by a bias voltage sweep, allowing free choice of the RF frequency which is a fundamental parameter in the dispersion measurement.

Bias voltage was identified as a key handling parameter in dispersion measurement, taking advantage of the fundamental role acquired in RF tone modulation by using a Mach-Zehnder in asymmetric configuration.

We were able to obtain a direct expression to calculate chromatic dispersion, (40). We verified that through this expression both the magnitude and sign of dispersion can be determined.

Within the zero-amplitude Bias obtaining process, we realized how the combined performance of "moving zeros" (contain dispersion information) together with "fixed zeros" (serve as reference) yield a self-referenced measurement system.

In terms of accuracy in the measurements, the VPI simulator helped us to determine the best operation conditions for the most relevant parameters involved. The following table summarizes the study of all these parameters:

Parameter	Features
RF Frequency	<ul style="list-style-type: none"> Establishes an interdependence with Bias resolution. As it increases, the system is able to measure smaller dispersion values (better resolution) but smaller maximum dispersion value The acceptable range starts from 1.5 GHz (ideal conditions) From a practical viewpoint, if too high a poorer approximation of the local D is obtained
RF Amplitude	<ul style="list-style-type: none"> Must be kept under a small signal condition The acceptable range ends at 0.8 V (ideal conditions). From a practical viewpoint, If too low we do not get a enough dip's definition
Nominal Dispersion	<ul style="list-style-type: none"> There is no restriction for the total amount of dispersion to be measured. Accuracy just depends on Bias Resolution

In the experimental section we verified that the accuracy reached by ABCM under real laboratory conditions is acceptable; however, we notice that the calibration of the system is extremely important, since small variations of the V_{π} or the zero-amplitude bias represent important variations in the D value obtained.

Chapter 4. Asymmetric Modulation Bias Controlled Method with Suppressed Carrier (ABCM - SC)

We redefined successfully the setup of ABCM to adapt it to a real time dispersion monitoring environment, and in this purpose we had to challenge some of RF tone based measuring methods conventional properties:

- The RF tone amplitude was out of the small signal condition range, as we needed to reach a value near the 20 dBm to cancel out the optical carrier according to Bessel Functions theory.
- The tone addition modulation was a phase modulation instead of an intensity modulation.
- The system required the determination of the bias required to cancel the detected first and second harmonics to calculate chromatic dispersion. The difference in the bias required to cancel each one of the harmonics gives the ABCM –SC the self-reference feature.

The small signal requirement to yield significant a level difference between the carrier with modulated data and the phase modulated signal was achieved by including optical couplers within the setup.

One of the advantages of ABCM – SC is the fact of isolating the carrier suppression and the dispersion measurement procedures in the emitter side and the monitoring point respectively, simplifying the support and failures detection tasks.

The main features of the parameters studied in the simulation section for ABCM - SC are exposed in the following table:

Parameter	Features
RF Frequency	<ul style="list-style-type: none"> • Establishes interdependence with Bias resolution. • As it increases, the system is able to measure smaller dispersion values(better resolution) but smaller maximum dispersion value • The acceptable range starts from 0.8 GHz (ideal conditions) • From a practical viewpoint, if too high a poorer approximation of D is obtained
RF Amplitude	<ul style="list-style-type: none"> • Must be set according to the Modulator's V_{π} value • Establishes a trade-off between alteration of data (carrier suppression) and accuracy.
Nominal Dispersion	<ul style="list-style-type: none"> • There is no restriction for the total amount of dispersion to be measured. • Accuracy just depends on Bias Resolution
Coupling factor	<ul style="list-style-type: none"> • Lower edge located around 0.8 (for the data signal) • Upper values (bigger than 0.9) are dismissed due to inefficiency issues.

Finally, the experimental section has verified the feasibility of the ABCM-SC.

Future Lines

The ABCM has been proposed as a low-cost chromatic dispersion measurement system. Here we have experimentally proven its validity in a setup which has included a costly vectorial network analyzer. As a future line it is proposed to setup a simplified low-cost system using mixers and low-cost detectors and to explore the possibility of building an integrated low-cost ABCM measurement system.

To study ABCM – SC considering the transmission of real intensity modulated data and to analyze some key parameters related like BER, SNR, etc.

To automate both methods exposed by a software application with a graphical interface, to make it more suitable to final users.

6. ANNEX

- **Matlab Program used in section 3.3.2.1 to obtain the Transfer Function of a Modulator**

```
function varargout = fun_trasf(varargin)
2 % FUN_TRASF M-file for fun_trasf.fig
3 % FUN_TRASF, by itself, creates a new FUN_TRASF or raises the existing
4 % singleton*.
5 %
6 % H = FUN_TRASF returns the handle to a new FUN_TRASF or the handle to
7 % the existing singleton*.
8 %
9 % FUN_TRASF('CALLBACK',hObject,eventData,handles,...) calls the local
10 % function named CALLBACK in FUN_TRASF.M with the given input arguments.
11 %
12 % FUN_TRASF('Property','Value',...) creates a new FUN_TRASF or raises the
13 % existing singleton*. Starting from the left, property value pairs are
14 % applied to the GUI before fun_trasf_OpeningFcn gets called. An
15 % unrecognized property name or invalid value makes property application
16 % stop. All inputs are passed to fun_trasf_OpeningFcn via varargin.
17 %
18 % *See GUI Options on GUIDE's Tools menu. Choose "GUI allows only one
19 % instance to run (singleton)".
20 %
21 % See also: GUIDE, GUIDATA, GUIHANDLES
22
23 % Edit the above text to modify the response to help fun_trasf
24
25 % Last Modified by GUIDE v2.5 12-Jan-2010 17:06:47
26
27 % Begin initialization code - DO NOT EDIT
28 gui_Singleton = 1;
29 gui_State = struct('gui_Name', mfilename, ...
30 'gui_Singleton', gui_Singleton, ...
31 'gui_OpeningFcn', @fun_trasf_OpeningFcn, ...
32 'gui_OutputFcn', @fun_trasf_OutputFcn, ...
33 'gui_LayoutFcn', [], ...
34 'gui_Callback', []);
35 if nargin && ischar(varargin{1})
36 gui_State.gui_Callback = str2func(varargin{1});
37 end
38
39 if nargin
40 [varargout{1:nargout}] = gui_mainfcn(gui_State, varargin{:});
41 else
42 gui_mainfcn(gui_State, varargin{:});
43 end
44 % End initialization code - DO NOT EDIT
45
46
47 % --- Executes just before fun_trasf is made visible.
48 function fun_trasf_OpeningFcn(hObject, eventdata, handles, varargin)
49 % This function has no output args, see OutputFcn.
50 % hObject handle to figure
51 % eventdata reserved - to be defined in a future version of MATLAB
52 % handles structure with handles and user data (see GUIDATA)
53 % varargin command line arguments to fun_trasf (see VARARGIN)
54
55 % Choose default command line output for fun_trasf
56 handles.output = hObject;
```

```
12/02/10 18:35 C:\Users\cristhian86\Downloads\Fiber-Test\fun_trasf.m 2 of 8
57
58 % Update handles structure
59 guidata(hObject, handles);
60
61 imagen = imread( 'optic_fiber.jpg' );
62 axes( handles.axes3 );
63 image( imagen );
64 axis off;
65
66 % UIWAIT makes fun_trasf wait for user response (see UIRESUME)
67 % uiwait(handles.figure1);
68
69
70 % --- Outputs from this function are returned to the command line.
71 function varargout = fun_trasf_OutputFcn(hObject, eventdata, handles)
72 % varargout cell array for returning output args (see VARARGOUT);
73 % hObject handle to figure
74 % eventdata reserved - to be defined in a future version of MATLAB
75 % handles structure with handles and user data (see GUIDATA)
76
77 % Get default command line output from handles structure
78 varargout{1} = handles.output;
79
80
81 % --- Executes on button press in unidaddBm.
82 function unidaddBm_Callback(hObject, eventdata, handles)
83 % hObject handle to unidaddBm (see GCBO)
84 % eventdata reserved - to be defined in a future version of MATLAB
85 % handles structure with handles and user data (see GUIDATA)
86
87 % Hint: get(hObject,'Value') returns toggle state of unidaddBm
88
89
90 % --- Executes on button press in unidaduW.
91 function unidaduW_Callback(hObject, eventdata, handles)
92 % hObject handle to unidaduW (see GCBO)
93 % eventdata reserved - to be defined in a future version of MATLAB
94 % handles structure with handles and user data (see GUIDATA)
95
96 % Hint: get(hObject,'Value') returns toggle state of unidaduW
97
98
99 % --- Executes on button press in Ayuda.
100 function Ayuda_Callback(hObject, eventdata, handles)
101 % hObject handle to Ayuda (see GCBO)
102 % eventdata reserved - to be defined in a future version of MATLAB
103 % handles structure with handles and user data (see GUIDATA)
104
105 %Cargamos la imagen desde LA CARPETA WORK DEL MATLAB!!
106 %uiopen('C:\Documents and Settings\Administrador\Escritorio\TFC
ARNAU_PATRI\GUI_Arnau_Patri\ayuda_fun_transf.fig')
107 h=figure(ayuda_fun_transf);
108
109
110 %imagen = imread( 'ayuda_fun_transf.jpg' );
111 %axes( handles.axes2 );
12/02/10 18:35 C:\Users\cristhian86\Downloads\Fiber-Test\fun_trasf.m 3 of 8
112 %image( imagen );
113 %axis off;
114
115 %open ayuda_fun_transf.fig
```

```
116
117 function VbiasIn_Callback(hObject, eventdata, handles)
118 % hObject handle to VbiasIn (see GCBO)
119 % eventdata reserved - to be defined in a future version of MATLAB
120 % handles structure with handles and user data (see GUIDATA)
121
122 % Hints: get(hObject,'String') returns contents of VbiasIn as text
123 % str2double(get(hObject,'String')) returns contents of VbiasIn as a double
124 % global VSTART;
125 % global vstart;
126 %VSTART = str2double(get(handles.VbiasIn,'String'));
127 %vstart = str2double(VSTART);
128 %handles.VbiasIn = vstart;
129 %guidata(hObject,handles);
130
131
132 % --- Executes during object creation, after setting all properties.
133 function VbiasIn_CreateFcn(hObject, eventdata, handles)
134 % hObject handle to VbiasIn (see GCBO)
135 % eventdata reserved - to be defined in a future version of MATLAB
136 % handles empty - handles not created until after all CreateFcns called
137
138 % Hint: edit controls usually have a white background on Windows.
139 % See ISPC and COMPUTER.
140 if ispc && isequal(get(hObject,'BackgroundColor'), get
(0,'defaultUicontrolBackgroundColor'))
141 set(hObject,'BackgroundColor','white');
142 end
143
144
145
146 function VbiasFi_Callback(hObject, eventdata, handles)
147 % hObject handle to VbiasFi (see GCBO)
148 % eventdata reserved - to be defined in a future version of MATLAB
149 % handles structure with handles and user data (see GUIDATA)
150
151 % Hints: get(hObject,'String') returns contents of VbiasFi as text
152 % str2double(get(hObject,'String')) returns contents of VbiasFi as a double
153 % global VSTOP;
154 % global vstop;
155 % VSTOP = get(hObject,'String');
156 % vstop = str2double(VSTOP);
157 % handles.VbiasFi = vstop;
158 % guidata(hObject,handles);
159
160
161 % --- Executes during object creation, after setting all properties.
162 function VbiasFi_CreateFcn(hObject, eventdata, handles)
163 % hObject handle to VbiasFi (see GCBO)
164 % eventdata reserved - to be defined in a future version of MATLAB
165 % handles empty - handles not created until after all CreateFcns called
166
167 % Hint: edit controls usually have a white background on Windows.
168 % See ISPC and COMPUTER.
169 if ispc && isequal(get(hObject,'BackgroundColor'), get
(0,'defaultUicontrolBackgroundColor'))
170 set(hObject,'BackgroundColor','white');
171 end
172
173
174
```

```
175 function Resolucion_Callback(hObject, eventdata, handles)
176 % hObject handle to Resolucion (see GCBO)
177 % eventdata reserved - to be defined in a future version of MATLAB
178 % handles structure with handles and user data (see GUIDATA)
179
180 % Hints: get(hObject,'String') returns contents of Resolucion as text
181 % str2double(get(hObject,'String')) returns contents of Resolucion as a
double
182 % global VPASO;
183 % global vpaso;
184 % VPASO = get(hObject,'String');
185 % vpaso = str2double(VPASO);
186 % handles.Resolucion = vpaso;
187 % guidata(hObject,handles);
188
189
190 % --- Executes during object creation, after setting all properties.
191 function Resolucion_CreateFcn(hObject, eventdata, handles)
192 % hObject handle to Resolucion (see GCBO)
193 % eventdata reserved - to be defined in a future version of MATLAB
194 % handles empty - handles not created until after all CreateFcns called
195
196 % Hint: edit controls usually have a white background on Windows.
197 % See ISPC and COMPUTER.
198 if ispc && isequal(get(hObject,'BackgroundColor'), get
(0,'defaultUicontrolBackgroundColor'))
199 set(hObject,'BackgroundColor','white');
200 end
201
202
203 function [Potencia]=HP8153A_pow1()
204
205 %global HP8153A_pow1;
206
207 % Esta funcion entrega la potencia del multmetro HP8153A en Watts
208
209 % Se crea un objeto gpib
210 multimeter=gpib('ni' , 0, 22);
211
212 % Se abre el objeto
213 fopen(multimeter);
214
215 % Se pide la identificacion del instrumento
216 fprintf(multimeter, '*idn?');
217 instrument=fscanf(multimeter);
218
219 % Se configura el instrumento para que realice las mediciones en Watts
12/02/10 18:35 C:\Users\cristhian86\Downloads\Fiber-Test\fun_trasf.m 5 of 8
220 %fprintf(multimeter,'SENS2:POW:UNIT W')
221
222 %Se toman tres mediciones de potencia y se promedian
223 fprintf(multimeter, 'READ:pow?')
224 Potencia1=fscanf(multimeter,'%g');
225 %Pasamos la medida de dBm a mW:
226 PmW1=10^(Potencia1/10);
227
228 fprintf(multimeter, 'READ:pow?')
229 Potencia2=fscanf(multimeter,'%g');
230 %Pasamos la medida de dBm a mW:
231 PmW2=10^(Potencia2/10);
232
233 fprintf(multimeter, 'READ:pow?')
```

```
234 Potencia3=fscanf(multimeter,'%g');
235 %Pasamos la medida de dBm a mW:
236 PmW3=10^(Potencia3/10);
237
238 %*****
239 %*****
240
241 %AMB EL RADIOBUTTON HEM DA CONSEGUIR COMENTAR O DESCOMENTAR AQUESTES LÍNIAS,
242 %NECESITEM AJUDA DE LA CONCHI/OLGA YA!
243
244 Potencia=(PmW1+PmW2+PmW3)/3; %Aquí tenemos la potencia en uW.
245
246 %Pasamos la Potencia de mW a dBm:
247 %Potencia=10*log10(Potencia);
248
249
250 fclose(multimeter)
251 delete(multimeter)
252 clear multimeter
253
254 % --- Executes on button press in Ejecutar.
255 function Ejecutar_Callback(hObject, eventdata, handles)
256 % hObject handle to Ejecutar (see GCBO)
257 % eventdata reserved - to be defined in a future version of MATLAB
258 % handles structure with handles and user data (see GUIDATA)
259
260 %function[]=ftrans_mod_lineal()
261 % Esta función grafica la función de transferencia de un modulador óptico.
262 % Se sirve del HP8153A como medidor de potencia y del AG34970A como fuente
263 % de tensión de bias.
264
265 clc
266 clear all
267
268 data=guidata(gcbo);
269 vstart = str2double(get(data.VbiasIn, 'String'));
270 vstop=str2double(get(data.VbiasFi, 'String'));
271 vpaso=str2double(get(data.Resolucion, 'String'));
272
273
274 %Creamos un fichero para guardar los datos
275 [fitxer,path]=uiputfile('*.dat','Guardar');
12/02/10 18:35 C:\Users\cristhian86\Downloads\Fiber-Test\fun_trasf.m 6 of 8
276 fitxer=sprintf('%s%s',path,fitxer);
277 fi=fopen(fitxer,'wt');
278
279 %Se piden los datos del rango de tensiones y el paso para el voltaje de bias
280 %VSTART = get(hObject,'String');
281
282 %vstart=str2num(VSTART);
283 %vstart=VSTART;
284 fprintf(fi, 'Vbias inicial (V):\t');
285 fprintf(fi, '%g\n',vstart);
286
287
288 %vstop=str2num(VSTOP);
289 %vstop=VSTOP;
290 fprintf(fi, 'Vbias final (V):\t');
291 fprintf(fi, '%g\n',vstop);
292
293
294 %vpaso=str2num(VPASO);
```



```

295 %vpaso=VPASO;
296 vpaso=vpaso*1e-3;
297 fprintf(fi, 'resolucion (V):\t');
298 fprintf(fi, '%g\n\n',vpaso);
299
300 %Creamos un contador para el vector de datos adquiridos
301 j=1;
302 fprintf(fi, 'Vbias (V)\tPout ( $\mu$ W)\n');
303
304 %Bucle de adquisición de datos
305 for i=vstart:vpaso:vstop
306
307 %*****
308 %DC(i);
309 s1=serial('COM1' );
310
311 fopen(s1);
312
313 % fprintf(s1, '*IDN?');
314 % nombre = fscanf(s1)
315 v=i;
316
317 fprintf(s1, 'CHAN1:VOLT %g;CURR 1.0',v);
318 pause(2)
319 fprintf(s1, '*VOLT?');
320 voltage = fscanf(s1)
321
322 fclose(s1);
323 delete(s1);
324 clear s1;
325
326 %*****AJUDA OLGA!!!!
327 %Aquí pasem de mW a uW, amb els dBm també multipliquem igual????
328
329 pause(5)
330 potencia = HP8153A_pow1; % Medicion de potencia en Watts (W)
331 %potencia = potencia*1e6; % Medicion de potencia en Micro Watts ( $\mu$ W)
12/02/10 18:35 C:\Users\cristhian86\Downloads\Fiber-Test\fun_trasf.m 7 of 8
332 potencia = potencia*1e3; % Medicion de potencia en Micro Watts ( $\mu$ W)
333 pot(j) = potencia;
334 j=j+1;
335 fprintf(fi, '%g\t',i);
336 fprintf(fi, '%g\n',potencia);
337 end
338
339 st=fclose(fi);
340
341 %En el vector "pot" tenemos las medidas
342 %Se grafica las funcion de transferencia del Modulador
343 vbias=[vstart:vpaso:vstop];
344 %close all
345 figure
346 plot(vbias,pot)
347 title('Función de transferencia del modulador');
348 zoom on
349 ylabel('Pout ( $\mu$ W)');
350 xlabel('Vbias (V)');
351
352
353 % --- Executes on button press in Limpiar_Variables.
354 function Limpiar_Variables_Callback(hObject, eventdata, handles)
355 % hObject handle to Limpiar_Variables (see GCBO)

```

```
356 % eventdata reserved - to be defined in a future version of MATLAB
357 % handles structure with handles and user data (see GUIDATA)
358
359
360 % --- Executes on button press in Salir.
361 function Salir_Callback(hObject, eventdata, handles)
362 % hObject handle to Salir (see GCBO)
363 % eventdata reserved - to be defined in a future version of MATLAB
364 % handles structure with handles and user data (see GUIDATA)
365 close(gcf)
366
367
368 % --- Executes during object creation, after setting all properties.
369 function axes2_CreateFcn(hObject, eventdata, handles)
370 % hObject handle to axes2 (see GCBO)
371 % eventdata reserved - to be defined in a future version of MATLAB
372 % handles empty - handles not created until after all CreateFcns called
373
374 % Hint: place code in OpeningFcn to populate axes2
375
376
377 % --- Executes during object creation, after setting all properties.
378 function uipanel1_CreateFcn(hObject, eventdata, handles)
379 % hObject handle to uipanel1 (see GCBO)
380 % eventdata reserved - to be defined in a future version of MATLAB
381 % handles empty - handles not created until after all CreateFcns called
382
383
384 % --- Executes on button press in pushbutton5.
385 function pushbutton5_Callback(hObject, eventdata, handles)
386 % hObject handle to pushbutton5 (see GCBO)
387 % eventdata reserved - to be defined in a future version of MATLAB
12/02/10 18:35 C:\Users\cristhian86\Downloads\Fiber-Test\fun_trasf.m 8 of 8
388 % handles structure with handles and user data (see GUIDATA)
389 o=figure(montaje_fun_transf);
```

- **Matlab Program to obtain the Null Amplitude Bias vs RF frequency and Dispersion vs RF frequency graphics in section 3.2.2.1**

```

1  clc
2  clear all
3
4
5  %----- The files are loaded
-----
6  load lcRFsweep.txt
7
8  %----- Simulation data
-----
9  Freq_Laser=192.4e12;
10 Bias_Resolution=0.01;
11 Volt_I=-3.5;
12 Volt_F=0;
13 Vpi=3.5;
14
15
16 %----- Frequency Resolution
-----
17 Freq=(200e6:200e6:6.2e9);
18 Delta_Freq=200e6;
19
20
21 %----- Amplitude minimums
-----
22 AMP=lcRFsweep(:,2);
23 a=4;
24 aux=(Volt_F-Volt_I)/Bias_Resolution;
25 b=aux+1; % Number of steps of the bias sweep
26
27 bias=lcRFsweep(1:b,1);
28
29 null_bias=zeros([(Freq(length(Freq))-Freq(1))/(Delta_Freq),1]);
30
31 for i=1:([(Freq(length(Freq))-Freq(1))/(Delta_Freq))+1]
32 [minimum,index]= min(AMP(a:b));
33 null_bias(i)=bias(index+3);
34 a=b+4;
35 b=a+aux-3;
36 end
37
38 null_bias
39
40
41
42 %----- Dispersion in ps/nm
-----
43
44 n=0;
45 c=3e8;
46 Wlength = c/Freq_Laser;
47
48 dispersion=zeros([(Freq(length(Freq))-Freq(1))/(Delta_Freq),1]);
49
50 for i=1:([(Freq(length(Freq))-Freq(1))/(Delta_Freq))+1]
51 dispersion(i)=(2*n-null_bias(i)/Vpi)*(c/(2*Wlength*Wlength*Freq(i)*Freq(i)));
14/02/10 11:20 C:\MATLAB7\work\lc_RF_sweep.m 2 of 2
52
53 end

```

```
54
55 dispersion
56
57 figure
58
59 plot(Freq,null_bias)
60 title('Null Bias (n=0) vs RF Frequency');
61 figure
62
63 plot(Freq,dispersion)
64 title('Dispersion vs RF Frequency');
```

- **Matlab Program to obtain the Null Amplitude Bias vs RF amplitude and Dispersion vs RF amplitude graphics in section 3.2.2.2**

```

1 clc
2 clear all
3 close all
4
5 %----- The files are loaded
-----
6 load lcAmpSweep.txt
7
8 %----- Simulation data
-----
9 Freq_Laser=192.4e12;
10 Bias_Resolution=0.01;
11 Volt_I=-3.5;
12 Volt_F=0;
13 Vpi=3.5;
14
15
16 %----- Frequency Resolution
-----
17 Amp=(0.08:0.08:2.08);
18 Delta_Amp=0.08;
19
20
21 %----- Amplitude minimums
-----
22 AMP=lcAmpSweep(:,2);
23 a=10;
24 aux=(Volt_F-Volt_I)/Bias_Resolution;
25 b=aux+1; % Number of steps of the bias sweep
26
27 bias=lcAmpSweep(1:b,1);
28
29 null_bias=zeros([(Amp(length(Amp))-Amp(1))/(Delta_Amp),1]);
30
31 for i=1:(((Amp(length(Amp))-Amp(1))/(Delta_Amp))+1)
32 [minimum,index]= min(AMP(a:b));
33 null_bias(i)=bias(index+9);
34 a=b+10;
35 b=a+aux-9;
36 end
37
38 null_bias
39
40
41
42 %----- Dispersion in ps/nm
-----
43
44 n=0;
45 c=3e8;
46 Wlength = c/Freq_Laser;
47 RFfreq = 2e9;
48
49 dispersion=zeros([(Amp(length(Amp))-Amp(1))/(Delta_Amp),1]);
50
51 for i=1:(((Amp(length(Amp))-Amp(1))/(Delta_Amp))+1)
14/02/10 11:04 C:\MATLAB7\work\lc_AMsweep.m 2 of 2
52 dispersion(i)=(2*n-null_bias(i)/Vpi)*(c/(2*Wlength*Wlength*RFfreq*RFfreq));
53

```

```
54 end
55
56 dispersion
57
58 figure(1)
59
60 plot(Amp,null_bias)
61 title('Null Bias (n=0) vs RF Amplitude');
62 figure(2)
63
64 plot(Amp,dispersion)
65 title('Dispersion vs RF Amplitude');
```

- **Matlab Program to obtain the Null Amplitude Bias vs Nominal Dispersion and Dispersion vs Nominal Dispersion graphics in section 3.2.2.3**

```

clc
2 clear all
3 close all
4
5 %----- The files are loaded
-----
6 load lcDswEEP.txt
7
8 %----- Simulation data
-----
9 Freq_Laser=192.4e12;
10 Bias_Resolution=0.01;
11 Volt_I=-3.5;
12 Volt_F=0;
13 Vpi=3.5;
14
15
16 %----- Frequency Resolution
-----
17 L=(0:5000:160000);
18 Delta_L=5000;
19 Dnom=L*17e-6;
20 Delta_D=Delta_L*17e-6;
21 %----- Amplitude minimums
-----
22 AMP=lcDswEEP(:,2);
23 a=3;
24 aux=(Volt_F-Volt_I)/Bias_Resolution;
25 b=aux+1; % Number of steps of the bias sweep
26
27 bias=lcDswEEP(1:b,1);
28
29 null_bias=zeros([(Dnom(length(Dnom))-Dnom(1))/(Delta_D),1]);
30
31 for i=1:([(Dnom(length(Dnom))-Dnom(1))/(Delta_D))+1)
32 [minimum,index]= min(AMP(a:b));
33 null_bias(i)=bias(index+2);
34 a=b+3;
35 b=a+aux-2;
36 end
37
38 null_bias
39
40
41
42 %----- Dispersion in ps/nm
-----
43
44 n=0;
45 c=3e8;
46 Wlength = c/Freq_Laser;
47 RFfreq = 2e9;
48
49 dispersion=zeros([(Dnom(length(Dnom))-Dnom(1))/(Delta_D),1]);
50
51 for i=1:([(Dnom(length(Dnom))-Dnom(1))/(Delta_D))+1)
14/02/10 11:21 C:\MATLAB7\work\lc_DswEEP.m 2 of 2
52 dispersion(i)=(2*n-null_bias(i)/Vpi)*(c/(2*Wlength*Wlength*RFfreq*RFfreq));
53

```

```
54 end
55
56 dispersion
57
58 figure(1)
59
60 plot(Dnom,null_bias)
61 title('Null Bias (n=0) vs Nominal Dispersion' );
62 figure(2)
63
64 plot(Dnom,dispersion)
65 title('Dispersion vs Nominal Dispersion');
```


- **Matlab Program to obtain the Null Amplitude Bias Difference vs RF frequency and Dispersion vs RF frequency graphics in section 4.2.2.1**

```

clc
2 clear all
3 close all
4
5 %----- The files are loaded
-----
6 load monRFsweepv1.txt
7 load monRFsweepv2.txt
8
9 %----- Simulation data
-----
10 Freq_Laser=192.4e12;
11 Bias_Resolution=0.01;
12 Volth1_I=-3.5;
13 Volth1_F=0;
14 Volth2_I=-1.75;
15 Volth2_F=1.75;
16 Vpi=3.5;
17
18
19 %----- Frequency Resolution
-----
20 Freq=(200e6:200e6:6.2e9);
21 Delta_Freq=200e6;
22
23
24 %----- Amplitude minimums
-----
25 AMP1=monRFsweepv1(:,2);
26 a1=4;
27 aux1=(Volth1_F-Volth1_I)/Bias_Resolution;
28 total1 = (Volth2_F-Volth1_I)/Bias_Resolution;
29 b1=aux1+1; % Number of steps of the bias sweep
30
31 bias1=monRFsweepv1(1:b1,1);
32 bias1
33 null_bias1=zeros([(Freq(length(Freq))-Freq(1))/(Delta_Freq),1]);
34
35 for i=1:(((Freq(length(Freq))-Freq(1))/(Delta_Freq))+1)
36 [minimum,index]= min(AMP1(a1:b1));
37 null_bias1(i)=bias1(index+3);
38 a1=b1+total1-aux1+4;
39 b1=a1+aux1-3;
40 end
41
42 null_bias1
43
44 %----- Amplitude minimums
-----
45 AMP2=monRFsweepv2(:,2);
46
47 aux2=(Volth2_F-Volth2_I)/Bias_Resolution;
48 total2 = (Volth2_F-Volth1_I)/Bias_Resolution;
49 a2=total2-aux2+4;
50 b2=total2+1; % Number of steps of the bias sweep
51
14/02/10 11:24 C:\MATLAB7\work\mon_RF_sweep.m 2 of 2
52 bias2=monRFsweepv2(total2-aux2+1:b2,1);
53 bias2

```

```

54 null_bias2=zeros([(Freq(length(Freq))-Freq(1))/(Delta_Freq),1]);
55
56 for i=1:(((Freq(length(Freq))-Freq(1))/(Delta_Freq))+1)
57 [minimum,index]= min(AMP2(a2:b2));
58 null_bias2(i)=bias2(index+3);
59 a2=b2+total2-aux2+4;
60 b2=a2+aux2-3;
61 end
62
63 null_bias2
64
65
66
67 %----- Dispersion in ps/nm
-----
68
69 c=3e8;
70 Wlength = c/Freq_Laser;
71
72 dispersion=zeros([(Freq(length(Freq))-Freq(1))/(Delta_Freq),1]);
73
74 for i=1:(((Freq(length(Freq))-Freq(1))/(Delta_Freq))+1)
75 dispersion(i)=(1/2-(null_bias2(i)-null_bias1(i))/Vpi)*(c/(3*Wlength*Wlength*Freq
(i)*Freq(i)));
76
77 end
78
79 dispersion
80
81 figure
82
83 plot(Freq,null_bias2-null_bias1)
84 title('Delta Null Bias vs RF Frequency');
85 figure
86
87 plot(Freq,dispersion)
88 title('Dispersion vs RF Frequency');

```

- **Matlab Program to obtain the Null Amplitude Bias Difference vs RF amplitude and Dispersion vs RF amplitude graphics in section 4.2.2.2**

```

1 clc
2 clear all
3 close all
4
5 %----- The files are loaded
-----
6 load ampv1.txt
7 load ampv2.txt
8
9 %----- Simulation data
-----
10 Freq_Laser=192.4e12;
11 Bias_Resolution=0.01;
12 Volth1_I=-3.5;
13 Volth1_F=0;
14 Volth2_I=-1.75;
15 Volth2_F=1.75;
16 Vpi=3.5;
17
18
19 %----- Frequency Resolution
-----
20 Amp=(0.12:0.16:4.12);
21 Delta_Amp=0.16;
22
23
24 %----- Amplitude minimums
-----
25 AMP1=ampv1(:,1);
26 a1=4;
27 aux1=(Volth1_F-Volth1_I)/Bias_Resolution;
28 total1 = (Volth2_F-Volth1_I)/Bias_Resolution;
29 b1=aux1+1; % Number of steps of the bias sweep
30
31 bias1=ampv1(1:b1,2);
32 bias1
33 null_bias1=zeros([(Amp(length(Amp))-Amp(1))/(Delta_Amp),1]);
34
35 for i=1:([(Amp(length(Amp))-Amp(1))/(Delta_Amp))+1)
36 [minimum,index]= min(AMP1(a1:b1));
37 null_bias1(i)=bias1(index+3);
38 a1=b1+total1-aux1+4;
39 b1=a1+aux1-3;
40 end
41
42 null_bias1
43
44 %----- Amplitude minimums
-----
45 AMP2=ampv2(:,1);
46
47 aux2=(Volth2_F-Volth2_I)/Bias_Resolution;
48 total2 = (Volth2_F-Volth1_I)/Bias_Resolution;
49 a2=total2-aux2+4;
50 b2=total2+1; % Number of steps of the bias sweep
51
14/02/10 11:22 C:\MATLAB7\work\mon_Ampsweep.m 2 of 2
52 bias2=ampv2(total2-aux2+1:b2,2);
53 bias2

```

```

54 null_bias2=zeros([(Amp(length(Amp))-Amp(1))/(Delta_Amp),1]);
55
56 for i=1:(((Amp(length(Amp))-Amp(1))/(Delta_Amp))+1)
57 [minimum,index]= min(AMP2(a2:b2));
58 null_bias2(i)=bias2(index+3);
59 a2=b2+total2-aux2+4;
60 b2=a2+aux2-3;
61 end
62
63 null_bias2
64
65
66
67 %----- Dispersion in ps/nm
-----
68
69 c=3e8;
70 Wlength = c/Freq_Laser;
71 Rffreq = 2e9;
72
73 dispersion=zeros([(Amp(length(Amp))-Amp(1))/(Delta_Amp),1]);
74
75 for i=1:(((Amp(length(Amp))-Amp(1))/(Delta_Amp))+1)
76 dispersion(i)=(1/2-(null_bias2(i)-null_bias1(i))/Vpi)*(c/
(3*Wlength*Wlength*Rffreq*Rffreq));
77
78 end
79
80 dispersion
81
82 figure
83
84 plot(Amp,null_bias2-null_bias1)
85 title('Delta Null Bias vs RF Amplitude');
86 figure
87
88 plot(Amp,dispersion)
89 title('Dispersion vs RF Amplitude');

```

- **Matlab Program to obtain the Null Amplitude Bias Difference vs Nominal dispersion and Dispersion vs Nominal Dispersion graphics in section 4.2.2.3**

```

1 clc
2 clear all
3 close all
4
5 %----- The files are loaded
-----
6 load monDsweepv1.txt
7 load monDsweepv2.txt
8
9 %----- Simulation data
-----
10 Freq_Laser=192.4e12;
11 Bias_Resolution=0.01;
12 Volth1_I=-3.5;
13 Volth1_F=0;
14 Volth2_I=-1.75;
15 Volth2_F=1.75;
16 Vpi=3.5;
17
18
19 %----- Frequency Resolution
-----
20 L=(0:5000:160000);
21 Delta_L=5000;
22 Dnom=L*17e-6;
23 Delta_D=Delta_L*17e-6;
24
25
26 %----- Amplitude minimums
-----
27 AMP1=monDsweepv1(:,2);
28 a1=4;
29 aux1=(Volth1_F-Volth1_I)/Bias_Resolution;
30 total1 = (Volth2_F-Volth1_I)/Bias_Resolution;
31 b1=aux1+1; % Number of steps of the bias sweep
32
33 bias1=monDsweepv1(1:b1,1);
34 bias1
35 null_bias1=zeros([(Dnom(length(Dnom))-Dnom(1))/(Delta_D),1]);
36
37 for i=1:(((Dnom(length(Dnom))-Dnom(1))/(Delta_D))+1)
38 [minimum,index]= min(AMP1(a1:b1));
39 null_bias1(i)=bias1(index+3);
40 a1=b1+total1-aux1+4;
41 b1=a1+aux1-3;
42 end
43
44 null_bias1
45
46 %----- Amplitude minimums
-----
47 AMP2=monDsweepv2(:,2);
48
49 aux2=(Volth2_F-Volth2_I)/Bias_Resolution;
50 total2 = (Volth2_F-Volth1_I)/Bias_Resolution;
51 a2=total2-aux2+4;
14/02/10 11:23 C:\MATLAB7\work\mon_Dsweep.m 2 of 2
52 b2=total2+1; % Number of steps of the bias sweep
53

```

```

54 bias2=monDsweepv2(total2-aux2+1:b2,1);
55 bias2
56 null_bias2=zeros([(Dnom(length(Dnom))-Dnom(1))/(Delta_D),1]);
57
58 for i=1:(((Dnom(length(Dnom))-Dnom(1))/(Delta_D))+1)
59 [minimum,index]= min(AMP2(a2:b2));
60 null_bias2(i)=bias2(index+3);
61 a2=b2+total2-aux2+4;
62 b2=a2+aux2-3;
63 end
64
65 null_bias2
66
67
68
69 %----- Dispersion in ps/nm
-----
70
71 c=3e8;
72 Wlength = c/Freq_Laser;
73 Rffreq = 2e9;
74
75 dispersion=zeros([(Dnom(length(Dnom))-Dnom(1))/(Delta_D),1]);
76
77 for i=1:(((Dnom(length(Dnom))-Dnom(1))/(Delta_D))+1)
78 dispersion(i)=(1/2-(null_bias2(i)-null_bias1(i))/Vpi)*(c/
(3*Wlength*Wlength*Rffreq*Rffreq));
79
80 end
81
82 dispersion
83
84 figure
85
86 plot(Dnom,null_bias2-null_bias1)
87 title('Delta Null Bias vs Nominal D');
88 figure
89
90 plot(Dnom,dispersion)
91 title('Dispersion vs Nominal D');

```

- **Matlab Program to obtain the Null Amplitude Bias Difference vs Coupling factor and Dispersion vs Coupling Factor graphics in section 4.2.2.4**

```

1 clc
2 clear all
3 close all
4
5 %----- The files are loaded
-----
6 load monAlphasweepv1.txt
7 load monAlphasweepv2.txt
8
9 %----- Simulation data
-----
10 Freq_Laser=192.4e12;
11 Bias_Resolution=0.01;
12 Volth1_I=-3.5;
13 Volth1_F=0;
14 Volth2_I=-1.75;
15 Volth2_F=1.75;
16 Vpi=3.5;
17
18
19 %----- Frequency Resolution
-----
20 Alpha=(0.51:0.02:0.99);
21 Delta_Alpha=0.02;
22
23
24 %----- Amplitude minimums
-----
25 AMP1=monAlphasweepv1(:,2);
26 a1=4;
27 aux1=(Volth1_F-Volth1_I)/Bias_Resolution;
28 total1 = (Volth2_F-Volth1_I)/Bias_Resolution;
29 b1=aux1+1; % Number of steps of the bias sweep
30
31 bias1=monAlphasweepv1(1:b1,1);
32 bias1
33 null_bias1=zeros([(Alpha(length(Alpha))-Alpha(1))/(Delta_Alpha),1]);
34
35 for i=1:(((Alpha(length(Alpha))-Alpha(1))/(Delta_Alpha))+1)
36 [minimum,index]= min(AMP1(a1:b1));
37 null_bias1(i)=bias1(index+3);
38 a1=b1+total1-aux1+4;
39 b1=a1+aux1-3;
40 end
41
42 null_bias1
43
44 %----- Amplitude minimums
-----
45 AMP2=monAlphasweepv2(:,2);
46
47 aux2=(Volth2_F-Volth2_I)/Bias_Resolution;
48 total2 = (Volth2_F-Volth1_I)/Bias_Resolution;
49 a2=total2-aux2+4;
50 b2=total2+1; % Number of steps of the bias sweep
51
14/02/10 11:22 C:\MATLAB7\work\mon_Alphasweep.m 2 of 2

```

```

52 bias2=monAlphasweepv2(total2-aux2+1:b2,1);
53 bias2
54 null_bias2=zeros([(Alpha(length(Alpha))-Alpha(1))/(Delta_Alpha),1]);
55
56 for i=1:(((Alpha(length(Alpha))-Alpha(1))/(Delta_Alpha))+1)
57 [minimum,index]= min(AMP2(a2:b2));
58 null_bias2(i)=bias2(index+3);
59 a2=b2+total2-aux2+4;
60 b2=a2+aux2-3;
61 end
62
63 null_bias2
64
65
66
67 %----- Dispersion in ps/nm
-----
68
69 c=3e8;
70 Wlength = c/Freq_Laser;
71 Rffreq = 2e9;
72
73 dispersion=zeros([(Alpha(length(Alpha))-Alpha(1))/(Delta_Alpha),1]);
74
75 for i=1:(((Alpha(length(Alpha))-Alpha(1))/(Delta_Alpha))+1)
76 dispersion(i)=(1/2-(null_bias2(i)-null_bias1(i))/Vpi)*(c/
(3*Wlength*Wlength*Rffreq*Rffreq));
77
78 end
79
80 dispersion
81
82 figure
83
84 plot(Alpha,null_bias2-null_bias1)
85 title('Delta Null Bias vs Alpha');
86 figure
87
88 plot(Alpha,dispersion)
89 title('Dispersion vs Alpha' );

```

Matlab Program to obtain the Transfer Function of a Modulator:

7. INDEX OF TABLES

<i>Table 3.1. NEW FOCUS 6427 Features.</i>	49
<i>Table 3.2. FUJITSU FTM7921ER/052 H74M-5208-062 features.</i>	51
<i>Table 3.3. AGERE Systems 2860E features</i>	53
<i>Table 3.4. CDC-04074 features</i>	54
<i>Table 3.5. Dispersion Compensating Fiber features</i>	55
<i>Table 3.6. HP 8753D measurer features</i>	56
<i>Table 3.7. HP 8753D signal generator features</i>	56
<i>Table 3.8. HP 8153A features.</i>	57
<i>Table 3.9 FUJITSU Experimental features</i>	60
<i>Table 3.10 Optical Power values</i>	63
<i>Table 3.11 Measured Dispersion vs Nominal Dispersion for FBG</i>	65
<i>Table 3.12 Measured Dispersion vs Nominal Dispersion for DCF</i>	66
<i>Table 4.1 HP 83424A Laser features</i>	89
<i>Table 4.2 Measured Dispersion vs Nominal Dispersion for FBG</i>	95

8. INDEX OF FIGURES

<i>Figure 2.1 Chromatic dispersion basic schema</i>	9
<i>Figure 2.2 Block composed by MZM, DUT and Detector</i>	12
<i>Figure 2.3 Schematic of Mach-Zehnder Modulator</i>	13
<i>Figure 2.4 Mach-Zehnder's Transfer Function</i>	14
<i>Figure 2.5 MPSM basic setup</i>	21
<i>Figure 2.6. Optical phase shifts inserted by the DUT</i>	22
<i>Figure 2.7 Fiber Bragg Grating operating principle</i>	25
<i>Figure 2.9 VPI simulation setup for measuring the transfer function of a MZM in Asymmetric Configuration</i>	29
<i>Figure 2.10 Configured Global Parameters</i>	30
<i>Figure 2.11 General Parameters</i>	30
<i>Figure 2.12 Physical parameters of the Laser</i>	30
<i>Figure 2.13 Physical parameters of the RF Source</i>	31
<i>Figure 2.14 Modulator physical parameters</i>	31
<i>Figure 2.15 Bias sweep configuration</i>	32
<i>Figure 2.16. Transfer Function of an Asymmetric MZ Modulator</i>	32
<i>Figure 3.1 ABCM basic setup</i>	33
<i>Figure 3.2 VPI setup for ABCM: 1- Optical source 2- Sine function generator 3- MZM 4- Fiber section 5- DC source 6- Photodetector 7- Phase and Magnitude detector 8- 2D Analyzer</i>	36
<i>Figure 3.3 Amplitude-vs-Bias graphics for: a. null dispersion (top) b. Positive dispersion (center) c. Negative dispersion (bottom). Fixed zeros in blue, moving zeros in red</i>	38
<i>Figure 3.4 Amplitude-vs-Bias graphic for Positive Dispersion inputting Bias and RF tone through different branches. Fixed zeros in blue, moving zeros in red</i>	40
<i>Figure 3.5 Amplitude-vs-Bias graphic for a 1360 ps/nm nominal dispersion with a 6GHz RF frequency. Fixed zeros in blue, moving zeros in red</i>	40
<i>Figure 3.6 VPI setup for ABCM (Second stage). Highlighted with discontinuous line: Vi Text module</i>	41
<i>Figure 3.7 Zero-Amplitude Bias-vs-RF Frequency Curve</i>	43
<i>Figure 3.8. Chromatic Dispersion-vs-RF Frequency Curve</i>	43
<i>Figure 3.9. Zero-Amplitude Bias-vs-RF Amplitude Curve</i>	45
<i>Figure 3.10. Chromatic Dispersion-vs-RF Amplitude Curve</i>	46
<i>Figure 3.11 Zero-Amplitude Bias-vs-Nominal Dispersion Curve</i>	47
<i>Figure 3.12 Chromatic Dispersion-vs-Nominal Dispersion Curve</i>	47

Figure 3.13 Laser New Focus 6427	48
Figure 3.14 FA-851	49
Figure 3.15 FUJITSU FTM7921ER/052 H74M-5208-062	50
Figure 3.16. Polarization Controller	51
Figure 3.17. Bias tee	52
Figure 3.18. AGERE Systems 2860E	53
Figure 3.19. PIRELLI CDC-04074	54
Figure 3.20 Chromatic Dispersion Compensating Fiber	55
Figure 3.21 HP 8753D.....	56
Figure 3.22 HP 8153A	57
Figure 3.23 Experimental Transfer Function setup	58
Figure 3.24 FUJITSU FTM7921ER/052 H74M-5208-062.....	59
Figure 3.25 ABCM Experimental Setup	60
Figure 3.26 Moving Zeros Displacement. Blue: without the DUT. Red: with the DUT.	61
Figure 3.27 ABCM measures obtained for FBG	65
Figure 3.28 ABCM measures obtained for DCF	66
Figure 4.1 General schematic for Dispersion Monitoring System	67
Figure 4.2 Bessel Functions: order 0 (red), order 1 (green) and order 2 (blue)	69
Figure 4.3 VPI schematic for phase modulation with carrier suppression	72
Figure 4.4 Spectrum of the phase modulated optical signal.....	73
Figure 4.5 Zoom on Figure 4.4 highlighting main sidebands and suppressed carrier.....	73
Figure 4.6 VPI schematic for ABCM - SC: 1- Optical source 2- Sine generator 3- Input coupler 4- DC source 5- MZM 6- Output coupler 7- Fiber section 8-Power meter 9- Photo detector 10- 1st harmonic amplitude and phase detector 11- 2nd harmonic amplitude and phase detector 12- 1st harmonic XY visualizer 13- 2nd harmonic XY visualizer	74
Figure 4.7 Amplitude-vs-Bias graphics for: 1st harmonic (top) 2nd harmonic (bottom)	76
Figure 4.8 VPI setup for ABCM - SC (Second stage). Highlighted with discontinuous line: Vi Text module.....	78
Figure 4.9 Zero-Amplitude Bias Delta-vs-RF frequency Curve	79
Figure 4.10 Chromatic Dispersion-vs-RF frequency Curve.....	80
Figure 4.11 Spectrums of the phase modulated optical signal obtained with RF amplitude equal to: a) 2.60 V b) 2.65 V c) 2.70 V d) 2.75 V e) 2.80 V f) 2.85 V	82
Figure 4.12 Zero-amplitude Bias Delta-vs-RF amplitude curve	83
Figure 4.13 Chromatic Dispersion-vs-RF amplitude curve.....	84
Figure 4.14 Zero-amplitude Bias Delta-vs-Nominal Dispersion Curve.....	85

<i>Figure 4.15 Chromatic Dispersion-vs-Nominal Dispersion Curve</i>	85
<i>Figure 4.16 Zero-amplitude Bias Delta-vs-Alpha Curve</i>	86
<i>Figure 4.17 Chromatic Dispersion-vs-Alpha Curve</i>	87
<i>Figure 4.18 Optical Coupler</i>	88
<i>Figure 4.19 HP 83424A</i>	88
<i>Figure 4.20 HP Agilent Spectrum Analyzer</i>	89
<i>Figure 4.21. Setup for the Carrier cancellation Procedure</i>	92
<i>Figure 4.22 Spectrum analyzer capture corresponding to the heterodyning of the phase modulated signal with 20 dBm RF amplitude.</i>	93
<i>Figure 4.23 Setup for ABCM –SC Experiment</i>	94
<i>Figure 4.24 Spectrum analyzer capture of the output of the dual-drive modulator with zero phase modulator DC voltage</i>	94
<i>Figure 4.25 a) Spectrum analyzer capture of the output of the dual-drive modulator with zero phase modulator DC voltage b) Spectrum analyzer capture of the output of the DCF with a 2.2 V. phase modulator DC voltage c) same as b) but for a 4.05 V. DC voltage.</i>	95
<i>Figure 4.26 Optimun ABCM –SC Setup (not implemented)</i>	96

9. BIBLIOGRAPHIC REFERENCES

- [1] María C. Santos – “Real Time Chromatic Dispersion Measurement and Monitoring Technique based on Phase control and Zeros Detection”, technical patent, 2009.
- [2] María C. Santos, José A. Ibarra, Fernando Moral, Cristhian Obando, Edurne García-Villar, Cristóbal Romero, Xavier Ferrer - “On-line chromatic dispersion monitoring technique based on zero detection”, proposal paper TSC, 2009.
- [3] S. Ryu, Y. Horiuchi, and K. Mochizuki, “Novel chromatic dispersion measurement method over continuous gigahertz tuning range”, J. Lightwave Technol., vol. 7, pp 1177 – 1180, Aug. 1989.
- [4] C. Peucheret, F. Liu and R.J.S. Pedersen, “Measurement of small dispersion values in optical components”, Electronics Letters, Vol. 35, No. 5, pp. 409 – 411, January 1999.
- [5] P. Hernday, “Measuring the group delay characteristics of narrow – band devices by the modulation phase shift method”, Agilent Technologies, 2002.
- [6] VPI Transmission Marker - VPI Component Marker, “User’s Manual”.
- [7] S. P. De Bernardo Rodi, M. A. Mitre Gutiérrez “Group delay measures at optical frequencies: Standard Modulation Phase – Shift Method and New Bias – controlled Amplitude Zero-Shift Method” PFC - ETSETB, 2007.
- [8] Aleix Carnero T. and Arnau Martí S. - “Chromatic Dispersion Measures at optical frequencies with second harmonic detection” PFC - ETSETB, 2009.
- [9] Edurne Garcia V. and Cristóbal Romero V. – “Advanced Chromatic Dispersion Measurement Techniques at Optical Frequencies” TFC - EPSC, 2009.
- [10] Fernando Moral C. and Xavier Ferrer P. – “Design and Deployment of a Dispersion Measurement Testing at Optical Frequencies” TFC - EPSC, 2009.